1-1-1964

A kinetic study of tin dissolution.

Alex W. K. Lui
University of Windsor

Recommended Citation

Lui, Alex W. K., "A kinetic study of tin dissolution." (1964). *Electronic Theses and Dissertations*. 6036.
https://scholar.uwindsor.ca/etd/6036

A KINETIC STUDY OF TIN DISSOLUTION

BY

ALEX W.K. LUI

A Dissertation
Submitted to the Faculty of Graduate Studies Through the
Department of Chemical Engineering in Partial Fulfilment
of the Requirements for the Degree of
Doctor of Philosophy at the
University of Windsor

Windsor, Ontario
1964

ProQuest Information and Learning Company
789 East Eisenhower Parkway
P.O. Box 1346
Ann Arbor, MI 48106-1346

ABX 6104

APPROVED BY: Alex Guyf

Robert A. Stayer

Roger J. Thibert

L. Krause.

S. J. Pine

ABSTRACT

A kinetic study of the dissolution of tin has been made by rotating cylindrical specimens in oxygenated hydrochloric acid solutions.

It has been shown that over a wide range of conditions, the dissolution proceeds in two autocatalytic stages with the rate during each stage being dependent on the square root of the stannic ion concentration in the corroding solution. The transition from one stage to the other is determined by the formation and subsequent decomposition of hydrogen peroxide and is not associated with any change in the surface properties of the samples.

The rate of dissolution during the second stage, when peroxide concentrations have become negligible, may be represented by the rate equation:

$$\frac{d}{dt}\left[Sn^{++++}\right] = 9.16 \times 10^{-2} \left[Sn^{++++}\right]^{1/2} \frac{A^{1/2}}{V} \; P_{O_2}^{\;1/2} \; e^{-\frac{4700}{RT}} \; (rpm.)^{0.92}$$

for rotational speeds above 11,000 rpm.

Activation energies, oxygen, acid and ammonium chloride dependence data seem to indicate that control of the heterogeneous corrosion process by the homogeneous oxidation of stannous species at the metal-solution interface is highly improbable.

Diffusion of stannic species from the metal-solution interface appears to be the most reasonable controlling step.

ACKNOWLEDGMENTS

The author wishes to express his sincere appreciation to Dr. A.W. Gnyp for his valuable advice and constructive criticisms.

Thanks are expressed to Prof. R.G. Billinghurst for his willingness to do X-ray diffraction analyses.

The author is also indebted to Mr. Otto Brudy for suggestions and assistance in setting up the apparatus.

The financial assistance offered by the National Research Council during the period 1962-1964 has been greatly appreciated.

TABLE OF CONTENTS

LIST OF TABLES

Table Page

LIST OF FIGURES

Figure Page

Figure Page

CHAPTER I

INTRODUCTION

Corrosion is still a very important industrial consideration but very little has been accomplished on the clarification of the kinetics and mechanism by which metals are destroyed. The usual corrosion data based, generally, on short term studies extrapolated to longer periods of time[33] provide qualitatively comparative information.

Copper is the only metal that has been subjected to a fundamental investigation.[25,48,49] It has been shown that, over a wide range of condition, the dissolution of copper in air saturated solutions is an autocatalytic process.

It is of considerable interest and practical importance to determine whether other metals capable of existing in two or more oxidation states will corrode by some similar autocatalytic mechanism.

Tin was chosen for this study because it bears strong resemblance to copper with respect to complex formation in chloride solutions. Both metals have two oxidation states. It was felt that the dissolution of tin by simple hydrogen displacement in air-free acid solutions would provide a simple yet interesting complication to the more important corrosion by dissolved oxygen. The object of this thesis is to provide more understanding of the mechanism by which tin and metals in general corrode in aerated acid solutions.

CHAPTER II

LITERATURE REVIEW

I. Metal Corrosion

Considerable effort has been devoted to the study of the corrosion of copper, but little is known about tin. It will be helpful to review the results of studies on copper before considering the relatively unknown tin behavior.

A. Copper Dissolution

Lu and Graydon[48,49] are perhaps the earliest investigators to undertake a systematic study of metal dissolution kinetics. Using rotating metal cylinders, they studied the rate of copper dissolution in aqueous ammonium hydroxide and aqueous sulfuric acid solutions as a function of temperature, oxygen concentration, rotational speed, sample area and corroding solution volume. Over a wide range of conditions, they found that the reaction rate is autocatalytic and is well represented by a half-order rate equation. The authors explained the behavior in terms of a mechanism based on the following assumptions:

(1) the cupric ion concentration in the bulk of the solution is the same as the cupric ion concentration at the copper solution interface,

(2) the cuprous ion, cupric ion equilibrium

$$Cu + Cu^{++} \rightleftharpoons 2Cu^{+}$$

is assumed to be established at the interface,

(3) the rate of dissolution of copper is controlled by the removal of cuprous ion from the interface by a process which is first

order with respect to cuprous ions

$$-\frac{d}{dt}\left[Cu^+\right]_i = K\left[Cu^+\right]_i$$

Their work was extended by Gnyp[25] to hydrochloric acid solutions. He modified the qualitative method of Schales[73] to detect quantitively hydrogen peroxide formation during the course of dissolution. Gnyp's work on the homogeneous oxidation of cuprous ion supported the assumption of the previous investigators that the rate of oxidation of cuprous copper at the metal-solution interface could be the controlling step in the dissolution process.

Hill[26] developed a procedure based on the technique of Campbell and Thomas[14] to study the films of corrosion products formed on copper surfaces corroding in 1M KCl solutions. Basically, his apparatus consisted of an electronic voltmeter measuring the potential of the cell formed by the copper and its corrosion film as one electrode and a silver-silver chloride reference electrode. On the assumption that the film was essentially cuprous oxide, he proposed the following mechanism for the initial corrosion of copper in potassium chloride solutions:

$$2Cu + O_2 + H^+ \longrightarrow 2Cu^+ + HO_2^-$$

$$2Cu^+ + HO_2^- + 2Cu \longrightarrow 2Cu_2O + H^+$$

Weeks and Hill[82] extended this study to dilute hydrochloric acid solutions by using a radioactive tracer technique. Cobalt 60 was used to make a solid solution alloy with copper. Since cobalt is considerably electropositive with respect to copper, a homogeneous alloy of this type would be expected to corrode at approximately the same rate as pure copper.

They proposed a double adsorption mechanism as an explanation for their observations. The kinetic steps have been assumed to be:

$$2Cu + O_2 \rightleftharpoons Cu_2O_2 \text{ (adsorbed)}$$

$$\text{(adsorbed) } Cu_2O_2 + H^+ + Cl^- \rightleftharpoons Cu_2O_2 + HCl \text{ (adsorbed)}$$

$$\text{(adsorbed) } Cu_2O_2 + H^+ \rightleftharpoons 2Cu^+ + HO_2^-$$

To account for the fact that hydrogen peroxide could not be detected in the corroding solution, the authors further assumed the following step:

$$2Cu^+ + HO_2^- + 3H^+ \rightleftharpoons 2Cu^{++} + 2H_2O$$

This is a modification of the theory of the catalytic decomposition of hydrogen peroxide as suggested by Haber and Weiss[27] and Evans, Baxendale and Park[20].

B. Tin Dissolution

The chemistry of tin in acidic media has been studied by Henry[34], Ditto[19] and Berzelius.[5,6] In the absence of oxygen, they found that tin dissolves in hydrochloric and sulfuric acid solutions in the stannous form with the evolution of hydrogen gas. Dilute sulfuric acid, however, does not act on tin in the cold, but increasing the concentration to $H_2SO_4 \cdot 6H_2O$, initiates action. In general, hydrogen gas is given off in dilute sulfuric acid solution, but SO_2, H_2S and S are formed with concentrated acid solutions. When a solution of tin in concentrated sulfuric acid is diluted with water, the tin is precipitated as stannic acid.

Concentrated nitric acid does not act on tin metal, but if water is added, the tin will dissolve. If the solution is heated, the tin will be oxidized to hydrated stannic oxide. The above studies provided general knowledge about the metal, but very little was done with respect to the determination of corrosion rates.

Hole and Foster[33] are perhaps the earliest pioneers in the study of the corrosion of tin. Their experimental method was rather simple. Metal sheets were immersed for 7 or 28 days in half a litre of corroding acid solution which was renewed daily. The rate of dissolution was recorded as total weight loss of metal per unit of exposed surface area per day. In hydrochloric acid solutions the metal dissolved at a rate of 0.11 gm/sq.cm.per day, in sulfuric acid, 0.045 gm/sq.cm.per day and in nitric acid, 0.007gm/sq.cm.per day.

A more advanced study was carried out by Whitman and Russel[80] who studied the effect of oxygen on tin dissolution in various acidic media. The oxygen concentration was controlled by mixing hydrogen with air or pure oxygen. Their results showed that the presence of dissolved oxygen increased the corrosion rate of the metal. Since tin evolves hydrogen gas in acids, the oxygen effect is more important in weaker acids where hydrogen evolution increases at a much more rapid rate than does corrosion by oxygen. The corrosion rate in hydrochloric acid was considerably higher than in sulfuric, nitric, and acetic acids.

Khitrov and Shatalova[37,38] studied the effect of temperature on the corrosion resistance of metals in acidic media. Tin, steel, aluminum and lead were corroded in non-oxidizing acids at different temperatures. The rate of tin corrosion in 1-7 M solutions of HCl and H_2SO_4 was observed to increase with increasing temperature. In the 0-80°C. range, the rate obeyed the Van't Hoff and Arrhenius Laws. The rate of diffusion also increased with increase in temperature but not as rapidly as did the corrosion rate. As a result, diffusion control at high temperatures must be expected. In general, a corrosion process occurring at low temperatures is accelerated at higher temperatures. This acceleration is associated with a fall in hydrogen overvoltage, decrease in polarization, decrease in viscosity of the solution and destruction of protective films.

The extensive use of tin as a protective coating for iron and copper has prompted investigators to focus their attention on the corrosion of tin-plate. Ireland[35] studied the corrosion of tin-plated iron under normal conditions and in sealed cans. He observed that iron was attacked when the tin-iron couple was exposed to a corrosive agent under normal conditions, but was not affected in a sealed can. The author explained that the mechanism of tin corrosion within a can is quite different from that of the process of corrosion of tin plate in air. Tin is considerably below iron in the electromotive series. When the tin-iron couple is exposed to a corrosive agent under normal conditions, the tin is unaffected while the iron is attacked. Inside a food can, conditions are different when the supply of oxygen is limited. It was observed that in the first superficial attack on the tin plate, tin became anodic and acted as an anticorrosion agent. It not only protected the steel by covering it but also exerted a potential which prevented direct attack on the exposed steel.

The corrosion of tin plate and its inhibition by chromate-containing solutions was studied by Kerr.[44,45] He found that when tin-plate is immersed in an alkaline phosphate-chromate solution, it acquires an invisible film which protects it against blackening by S-containing food and also greatly retards rusting in moist air. The effect of variation in coating thickness on the resistance to corrosion of electro-tinplate was also investigated. Tests made by corroding tin-plate in humidity chambers and by salt spray revealed that the resistance to corrosion decreases as the thickness of the tin deposit diminishes.

A more fundamental explanation was advanced by Wade[84] in his recent study on the corrosion of tin-plate in citric acid. The author assumed that the corrosion process could be divided into 3 periods: In the first period, the steel base is completely covered with a film of SnO-SnO_2. Because of its high hydrogen overvoltage, tin protects the steel in the can. In the second period, after the tin has corroded, the steel base is partly exposed and alloy layers begin to be affected. Because the electrode potential of Fe becomes nobler than that of Sn, contrary to the usual ionization tendency, the corrosion of the steel base does not accelerate. In the third period, after the tin is completely dissolved, the alloy layer and steel base are completely exposed. The electrode potential of the alloy layer in citric acid solution was nobler than that of steel or tin, thus allowing the steel to dissolve. The author concluded that the thickness of the tin coating and cracks or exposed portions of steel are important factors affecting corrosion resistance of tin-plate.

Local corrosion of tin in dilute chloride solutions was studied by Briton and Michael[9] by means of electrode potential measurements. The results of their work revealed that local corrosion cannot be prevented indefinitely by special physical or chemical preparation of the metal surface, nor by the addition of alloying metal to the tin. However, they showed that the time elapsing before local corrosion begins is affected by surface conditions. Local corrosion is initiated and accelerated by crevices resulting from surface defects or by contact of the metal with another solid surface.

The inhibition of tin corrosion was studied by Ammar and Riad[2] in 8 different acid, alkaline and neutral solutions. The authors reported that sodium pyrophosphate decreases the corrosion rate in acidic media. Because of the amphoteric character of tin, the rate of corrosion of the metal in acid and alkaline solutions is greater than that in neutral ones. Since the addition of sodium pyrophosphate to acid solutions will increase the pH to the neutral range, it is expected that tin will not go into solution as readily in this pH range as it does in the acid.

Considerable effort has been devoted to the study of the electrochemical corrosion of metals. Shah and Davies[74] investigated the anodic corrosion of tin in alkaline solutions. They found that when an oxide-free tin surface is anodically polarized in deaerated alkaline solutions, only half the current is used for tin dissolution, the remaining half being used for oxide formation.

Hagymas and Quintin[31,32] studied the electrochemical corrosion of tin in sulfuric acid. In 0.1 to 1.0 M solutions the hydrogen overvoltage on the Sn electrode did not vary with acid concentration. The reactions

$$Sn \longrightarrow Sn^{++} + 2e^-$$

and

$$2H^+ + 2e^- \longrightarrow H_2$$

control the kinetics of corrosion of the Sn electrode in the acid media.

The author[89] made preliminary investigations on the dissolution of tin in hydrochloric acid solutions. Over a wide range of conditions, the reaction appeared to be zero-order with respect to stannic ion in the solution for approximately 40 minutes with transition to an autocatalytic half-order rate at higher stannic ion concentrations. The autocatalytic half-order rate was also directly proportional to the square root of A/V (where A is the area of sample surface, and V is the volume of corroding solution), and to the square root of oxygen concentration. He interpreted the results in terms of film formation on the sample surface, but no explanation was given for the complex rate dependence on rotational speed.

II. Homogeneous Oxidation

Because the homogeneous oxidation of cuprous ions was found to be a possible controlling step in the dissolution of copper[25], it was important to determine whether the homogeneous oxidation of stannous ions is important to the heterogeneous corrosion process of tin.

Extensive studies on the oxidation of stannous chloride have been carried out by various workers, yet disagreements are found in the results of their work. It is necessary to review some of their techniques and experimental conditions for complete understanding of these discrepancies. Essentially, they all used the same apparatus to follow the course of reaction. A gas burette was connected to the reaction vessel and the change in gas volume was interpreted in terms of stannous chloride oxidized at any time.

A. Stannous Oxidation

Young[87] was the first to study the oxidation of stannous chloride. He reported that the rate of autoxidation was dependent on the acidity of the solution and that the presence of foreign material could accelerate or inhibit the reaction. On the basis of electrical conductance measurements, he inferred that stannous chloride existed as hydrotrichlorostannous acid ($HSnCl_3$) and hydrotetrachlorostannous acid (H_2SnCl_4) in hydrochloric acid solution.

Larsen and Walton[50] studied the role of activated carbon in oxidation-reduction reactions. They concluded that activated carbon catalysed the autoxidation of stannous chloride solutions.

Miyamoto[59,60,61] showed that the rate of oxidation was dependent on the method of aeration of the stannous solutions. He suggested his results were applicable to a mixed reaction occurring partly in solution and partly in the liquid-gas interface.

On the other hand, Filson and Walton[21] reported that the autoxidation of stannous chloride occurs in solution. As evidence, they showed a high temperature coefficient and a negligible increase in rate with increase in the liquid-gas interface. They also found that, within certain limits, the rate of oxidation of stannous chloride increased directly with increasing acid concentration. The authors considered this to be unusual as the general tendency is for compounds to become more stable toward oxygen with increasing acid concentration.[51] They explained that the increase in reactivity was due to catalysis by hydrogen ions. They also investigated the catalytic effect of a number of salts finding cuprous chloride to be a very powerful catalyst.

Haring and Walton[28,29,30] investigated a number of factors that affect this autoxidation. They reported the rate to be zero order with respect to stannous chloride. Increasing temperatures increased the rate of oxidation. They implied that the true temperature coefficient was masked by changes in the solubility of oxygen and changes in the complex equilibria exisiting in solution. To account for the great influence of some added materials on oxidation rate, and also for the reaction being exothermic, they suggested that the reaction is of the chain type. By means of titanium sulfate, they detected a peroxide in fresh, partially oxidized, samples of stannous chloride, but this peroxide disappeared by reaction with remaining stannous chloride.[56] They also found that visible light had no effect on the reaction, but ultra-violet was absorbed and accelerated the process. These observations are presented as further evidence to support their assumption that the reaction is a chain process. In non-aqueous solutions, they found a direct linear relationship between the rate of oxidation and hydrochloric acid concentration.

No fundamental explanations were advanced until Lochman and Tompkins[52] published their work. They considered the possible equilibria between stannous and chloride ions to be:

(a) $Sn^{++} + H_2O \rightleftharpoons Sn(OH)^{+} + H^{+}$

(b) $Sn^{++} + Cl^{-} \rightleftharpoons SnCl^{+}$

(c) $SnCl^{+} + Cl^{-} \rightleftharpoons SnCl_2$

(d) $SnCl_2 + Cl^{-} \rightleftharpoons SnCl_3^{-}$

(e) $SnCl_3^{-} + Cl^{-} \rightleftharpoons SnCl_4^{=}$

(f) $SnCl_3^{-} + H^{+} \rightleftharpoons HSnCl_3$

(g) $SnCl_4^{=} + H^{+} \rightleftharpoons HSnCl_4^{-}$

(h) $HSnCl_4^{-} + H^{+} \rightleftharpoons H_2SnCl_4$

They were unable to identify any particular species as the material undergoing oxidation. Their experimental data conformed to the rate equation:

$$r = \frac{k_1 \left[\mathrm{SnCl_2}\right]}{1 + k_2\left[\mathrm{SnCl_2}\right]}$$

This would explain why previous workers[21,28,50,57,87] did not agree on their order of reaction with respect to stannous chloride. At low stannous ion concentrations, the equation reduces to

$$r = k_1 \left[\mathrm{SnCl_2}\right]$$

to show first order dependence on stannous chloride. At high stannous ion concentrations, it is of the form of

$$r = k_1/k_2$$

and is zero order with respect to stannous chloride. They also found that the rate of autoxidation was proportional to the square root of the concentration of $HSnCl_3$ complex although the oxidation of other species could not be necessarily excluded.

Naumann[62], studying the oxidation of the salt in nitric acid solutions, found that, in the presence of hydrochloric acid solution, nitric acid was reduced to ammonia. In the absence of hydrochloric acid, the reduction was to nitric oxide.

According to Dhar[18], oxidation of stannous ion is retarded by easily oxidizable substances such as sugar and glycerol.

B. Oxidation of Other Solutions

As part of the general corrosion programme it is important to discuss the oxidation of other metallic ions in aqueous solutions.

Russell[71] was the first to study the stability of titanous solutions. He reported that resistance to oxidation in 4M sulfuric acid was considerably higher than in the corresponding chloride solutions. Mackenzie and Tompkins [57] studied the autoxidation of titanous chloride in aqueous solutions by an absorption method. They found the rate to be a linear function of the oxygen partial pressure and inversely proportional to the concentration of the free HCl in solution. They suggested that the rate was largely controlled by hydrolysis and complex formation.

A potentiometric technique which can be used to follow a rapid reaction continuously was devised by Gnyp[25] in his study of the rate of oxidation of cuprous ion. A platinum electrode was immersed in a cuprous-cupric solution, and changes in potential at the electrode gave the amount of cuprous ion oxidized. Over the temperature range 0-35°C., he found that the oxidation rate was proportional to the cuprous concentration, oxygen partial pressure and the square root of hydrogen ion, but inversely proportional to the square root of chloride ion concentration.

Baskerville and Stevenson[3] were the earliest investigators to consider the oxidation of ferrous iron. They found that the oxidation rate was very slow in acid and neutral solutions. Pound [63,64] found that at room temperature ferrous ions oxidize in alcoholic media much more rapidly than in aqueous solutions.

According to Lamb and Elder [51], the small change in ferrous sulfate concentration in sulfuric acid due to oxidation would satisfy a first-order or second-order ferrous ion dependence. The addition of copper sulfate catalyzed the reaction.

Posner[65] investigated the kinetics of the oxidation of ferrous ions in concentrated hydrochloric acid solutions (4-8N). He found the reaction to be first order with respect to ferrous ion and oxygen concentrations, but a more complex function of hydrochloric acid. On the basis of a Haber-Weiss[27] formulation, he proposed that the oxidation occurs via a complex formed between associated HCl and ferrous ions.

George[23] extended the studies to various aqueous solutions using a colorimetric method to follow the concentration changes. He confirmed a first order dependence on ferrous ion in bicarbonate, but not in sulfate or nitrate solutions.

In phosphoric acid solutions, Cher and Davidson[13] found that the oxidation of ferrous ion was first order in ferrous ion. Cupric ions had a marked catalytic effect at concentrations lower than 10^{-3}M.

III. Hydrogen Peroxide Formation

The formation of hydrogen peroxide during the dissolution of metals in acidic media has been observed by many investigators. Churchill[12] made use of a photographic technique to detect hydrogen peroxide produced by corrosion reactions. His method consisted of supporting a small rectangular metal sheet over the emulsion of a photographic plate. The plate was known to be highly sensitive to the action of hydrogen peroxide. Action on the plate by corroding metal was compared to that by substances known to produce hydrogen peroxide.

Kramer[39,40,41] and Louw and Naude[47] used modified Geiger-Müller counters to pick up electron emission from freshly abraded surfaces by cutting metal under water containing dissolved oxygen. Hydrogen peroxide was detected in the case of zinc, aluminium, magnesium and nickel, but not copper. Bailey[4] and Dawden and Reynolds[17] suggested that copper decomposes the hydrogen peroxide by a surface reaction. However, Weeks and Hill[82] believed this to be a catalytic decomposition process.

By means of a radioactive tracer technique, Abramova, Gankina and Doklady[1] confirmed the formation of hydrogen peroxide during the dissolution of metals. They corroded tin in an acid solution containing ordinary hydrogen peroxide solution under an atmosphere of synthetic air containing the O^{19} isotope instead of ordinary oxygen. At the end of the experiment, some hydrogen peroxide in the solution was found to be radioactive. This suggested that intermediate peroxide was formed during the course of corrosion.

IV. Analysis of Tin

The polarography of tin has been well studied by Lingane.[53,54,55] The reduction of stannous tin to the metal produces excellently defined waves from 1M HCl, with a half-wave potential of -0.47v vs S.C.E. when 0.01 per cent gelatin is present as a maximum suppressor. Chlorostannate complex ion also produces a well developed doublet wave. The first wave results from the reduction of the chlorostannate ion to chlorostannite ion, and the second corresponds to complete reduction to the metal. The author found that the most suitable supporting electrolyte was 4M ammonium chloride and 1M HCl solution containing 0.01 per cent gelatin. This provides the high chloride ion concentration essential to full development of the chlorostannate wave, and a small enough hydrogen ion concentration so that the diffusion current plateau is well developed before the final current rise due to reduction of hydrogen ion begins. The half-wave potential of the first wave is -0.25v and that of the second is -0.52v vs S.C.E. In this supporting electrolyte, the first diffusion current is not fully developed before the second stage of reduction begins. Measurement of the second wave for routine analysis is recommended by Lingane.

Phillips and Morgan[66,67] have outlined procedures for the polarographic determination of tin in an alloy, using the supporting electrolyte suggested by Lingane.[53,54,55]

Snell and Snell[75] have made a complete study of colorimetric determinations of metals. Stafford[76] used ammonium molybdate, in the presence of phosphate, as reagent to give moylbdenum blue with $SnCl_2$. Unfortunately, at high acidity, the blue colour is not formed and at low acidity inconsistent results are obtained. Oxidation-reduction agents must be completely eliminated.

Clark[15,16] and Stone[77] used 1-methyl-3,4-dimercaptobenzene as a reagent to measure the quantity of tin present in the range of 1.5-6 ppm. This reagent reacts to give a red precipitate, more quickly with Sn^{++} than with Sn^{++++}. The acidity of the sample and standard solution must be matched before this reagent can be used.

CHAPTER IV
KINETIC STUDIES

I. Tin Dissolution

A. Introduction

Some preliminary work has been carried out by the author[89] on the corrosion of tin in hydrochloric acid solutions. He suggested that film formation was responsible for the rate dependence on $(A/V)^{1/2}$, but no further investigation was made on the nature of the film and its effect on the corrosion rate. Furthermore, it was not possible at that time to provide an explanation for the rate dependence on rotational speed.

In view of this limitation, it was decided to extend this study in order to try to provide interpretations for those results which could not be explained previously.

B. Experimental Details

1. Materials

Analar grade tin bar supplied by the British Drug Houses Ltd. was machined into cylinders of 0.360 inches in diameter with a concentric hole to fit onto a rotating shaft. The analysis according to the manufacturer is given on p. 19.

FIGURE 1

ARRANGEMENT OF APPARATUS

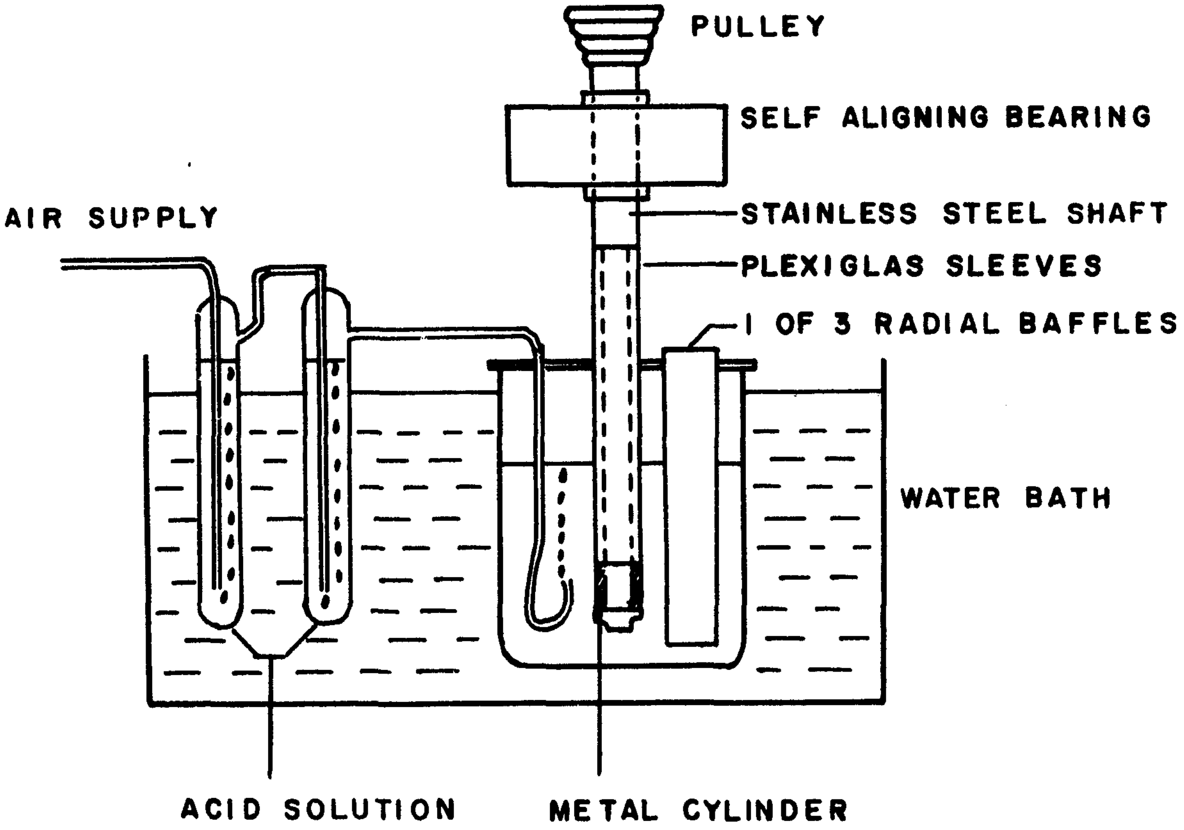

TABLE 1

Tin Analysis

Lead	0.01 per cent
Copper	0.0025
Bismuth	0.002
Iron	0.002
Total Foreign Material	0.04
Arsenic	0.0001
Antimony	0.025

All reagents used were of analytical grade, and redistilled water was used for all solutions.

2. Apparatus

The cylindrical tin samples were rotated on a stainless steel shaft. Plexiglas sleeves and a cap screwed tightly at the end protected the ends of the tin sample and the steel shaft from corrosion. The shaft was rotated by means of a Type 7HM Hoover vacuum motor at speeds ranging from 1,000 to 15,000 rpm. Figure 1 is a schematic representation of the experimental apparatus.

The reaction vessel consisted of a pyrex beaker fitted with a plexiglas cover holding three plexiglas baffle plates mounted radially.

3. Procedure

A measured volume of hydrochloric acid solution in the reaction vessel was flushed with air for approximately 20 minutes before each corrosion run. Initially, the air passed through a series of wash bottles containing hydrochloric acid of the same concentration as in the reaction beaker.

Freshly machined specimens were manually polished to 3/0 emery paper smoothness. The polished cylinders were cleaned with distilled water and dried with filter paper. Grease stains were removed before each run with absolute alcohol. After each run, the metal samples were washed and dried, carebeing taken to prevent any damage to the surface film that might possibly form. A check on the material balance was maintained by weighing the clean,dry specimens before and after each run.

Samples of the corroding solutions were withdrawn for analysis at convenient intervals of time. The concentration of tin was determined by a polarographic technique described in Appendix I. For every sample of solution withdrawn for analysis an equal volume of fresh acid was added to the reaction vessel to eliminate excessive volume change during the corrosion process.

The surface roughness of the sample was measured before and after each run by means of a Profilometer supplied by Micrometrical Manufacturing Company of Ann Arbor, Michigan.

C. Discussion of Results

1. Rate Dependence on Stannic Ion Concentration

The first point is to establish the order of the dissolution reaction. As shown in Figure 2, the data obtained in this research from solutions containing dissolved oxygen gave curved plots of $\left[Sn^{++++}\right]$ vs time. This is essentially evidence of an autocatalytic process. A plot of $\left[Sn^{++++}\right]^{1/2}$ vs time shows two linear sections according to Figure 3. This is indicative that there must be some half-order dependence on $\left[Sn^{++++}\right]$ during the corrosion. The data are most successfully correlated by considering the dissolution to occur in two successive half-order stages with transition from one to the other occurring about 40 minutes after initiation of corrosion.

Essentially, the dissolution of tin can be considered in terms of two parallel autocatalytic reactions that may be represented by the equation:

$$\frac{d}{dt}\left[Sn^{++++}\right] = (k_1^* + k_2^*)\left[Sn^{++++}\right]^{1/2}$$

where $\left[Sn^{++++}\right]$ represents the concentration of the complex stannic ion in solution and k_1^* and k_2^* are velocity constants showing different dependence on experimental variables. Changes in the relative values of the two rate constants during the course of dissolution can alter the net rate of corrosion to produce the observed two stages.

The study of the dissolution of tin is a determination of the factors affecting the magnitudes of k_1^* and k_2^*. These half-order rate constants have been evaluated as functions of temperature, rotational speed, acid concentration, oxygen concentration, solution volume and specimen area.

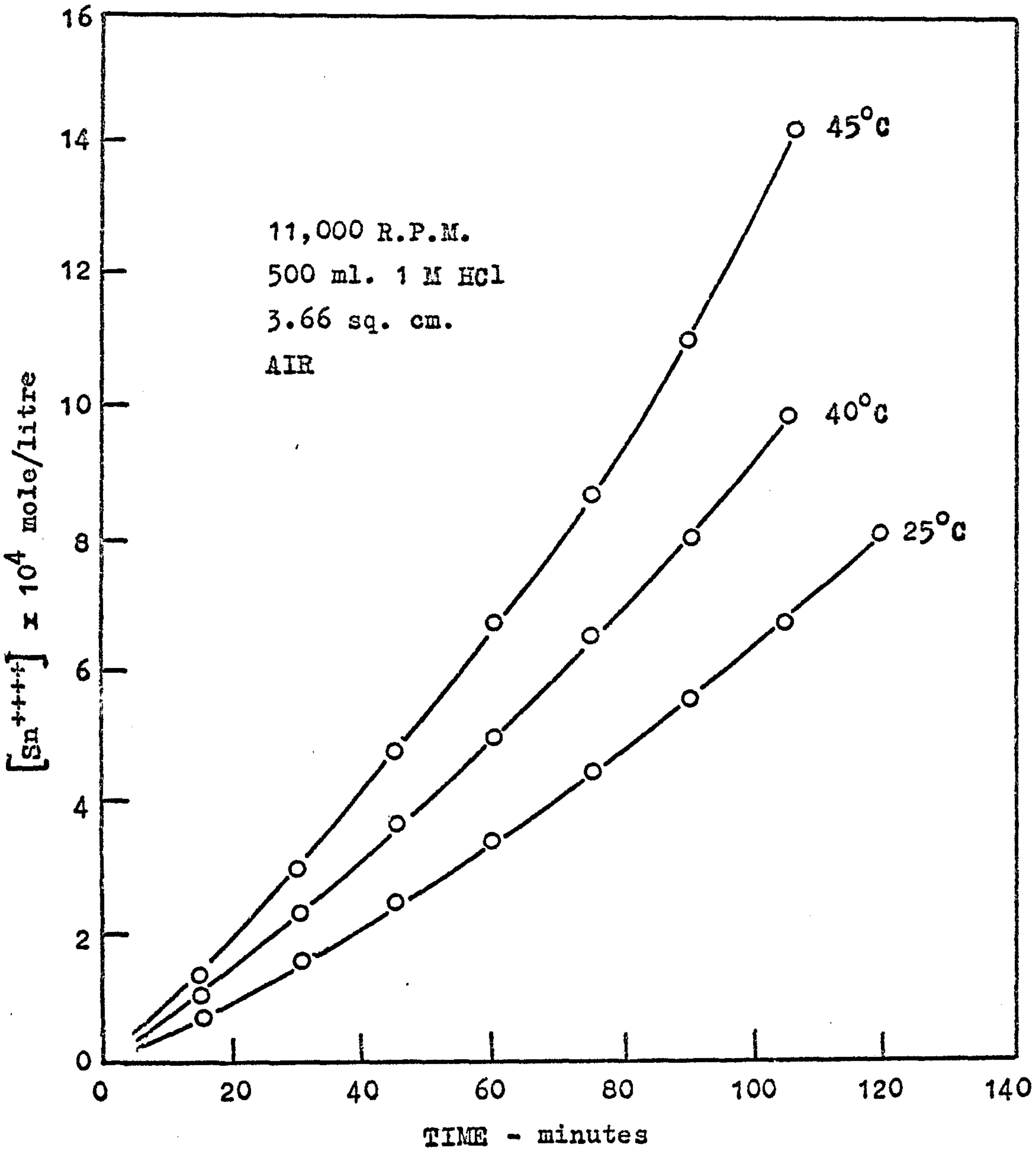

FIGURE 2 RATE OF DISSOLUTION OF TIN

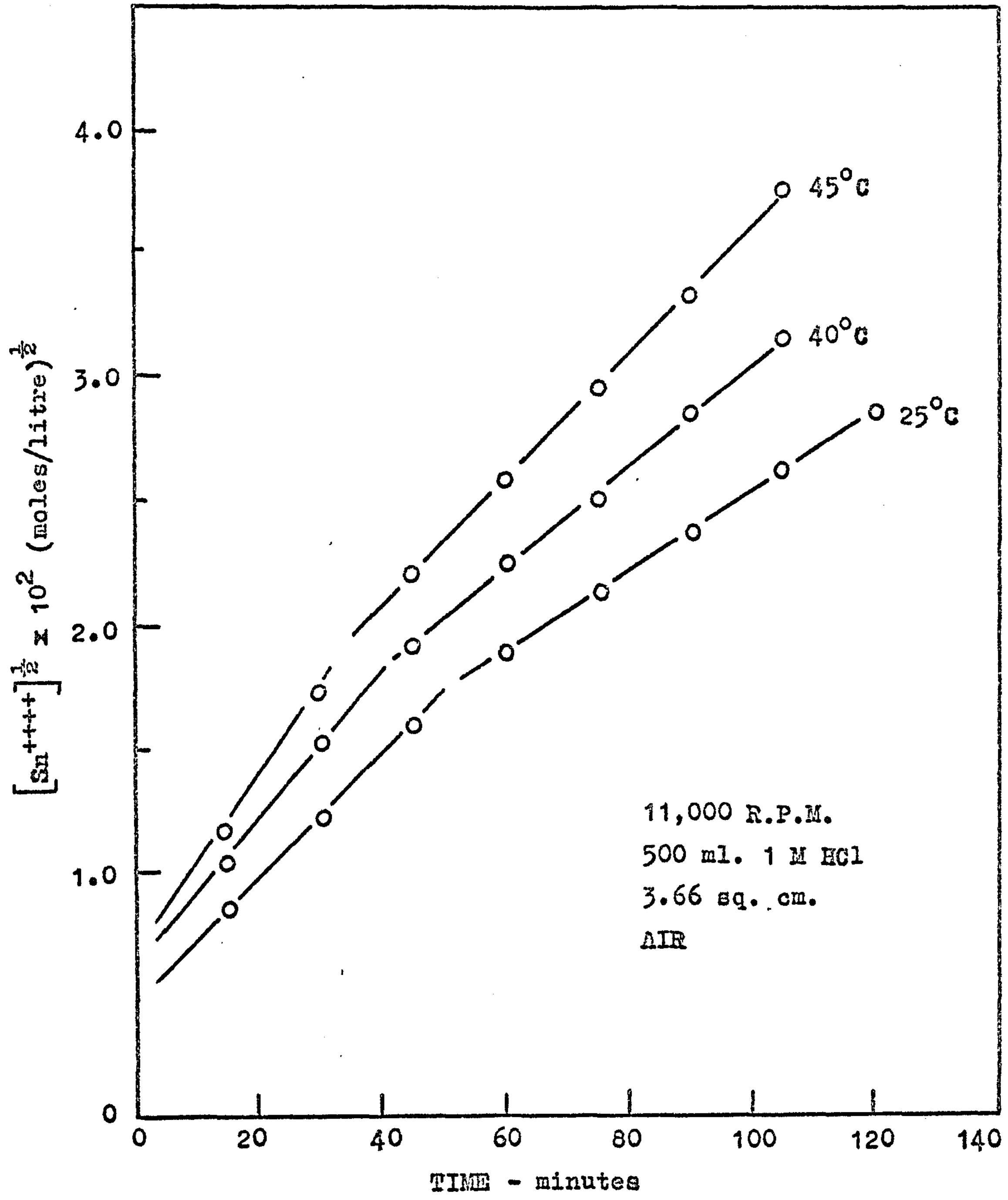

FIGURE 3 HALF-ORDER DISSOLUTION OF TIN

2. Rate Dependence on Temperature and Rotational Speed

The half-order rate dependence on temperature has been studied over a wide range of rotational speeds. The temperature coefficient evaluated as an Arrhenius activation energy from Figure 4 for the second stage of reaction is a linear function of rotational speed up to 11,000 rpm . Figure 5 shows that above this speed the apparent activation energy is essentially constant at 4.7 kcal/gm.mol. At 11,000 rpm., the activation energy for the first stage is only 2.5 kcal/gm.mol, as shown in Figure 6.

The effect of rotational speed has been investigated over the range 1,000-15,000 rpm. Figure 7 illustrating the variation of, the stage II rate with rotational speed, shows three distinct regions.

It is not readily apparent why this behaviour occurs. An attempt has been made to explain this complex dependence of dissolution rate on rotational speed in terms of optical observations made on corroding tin surfaces.

It has been shown by various investigators that tin evolves hydrogen gas from acids but it was impossible to detect any gas bubbles on the metal surface in 1 M HCl. By corroding specimens in 6 M HCl it was easy to observe gas bubble formation.

Stationary samples were covered with large gas bubbles readily seen with the naked eye.

Rotation of the sample at speeds up to 3,000 rpm. did not remove all of the large visible bubbles.

Over the range 3,000-11,000 rpm. the large bubbles were removed from the surface quite readily but very small ones were still attached to the sample surface.

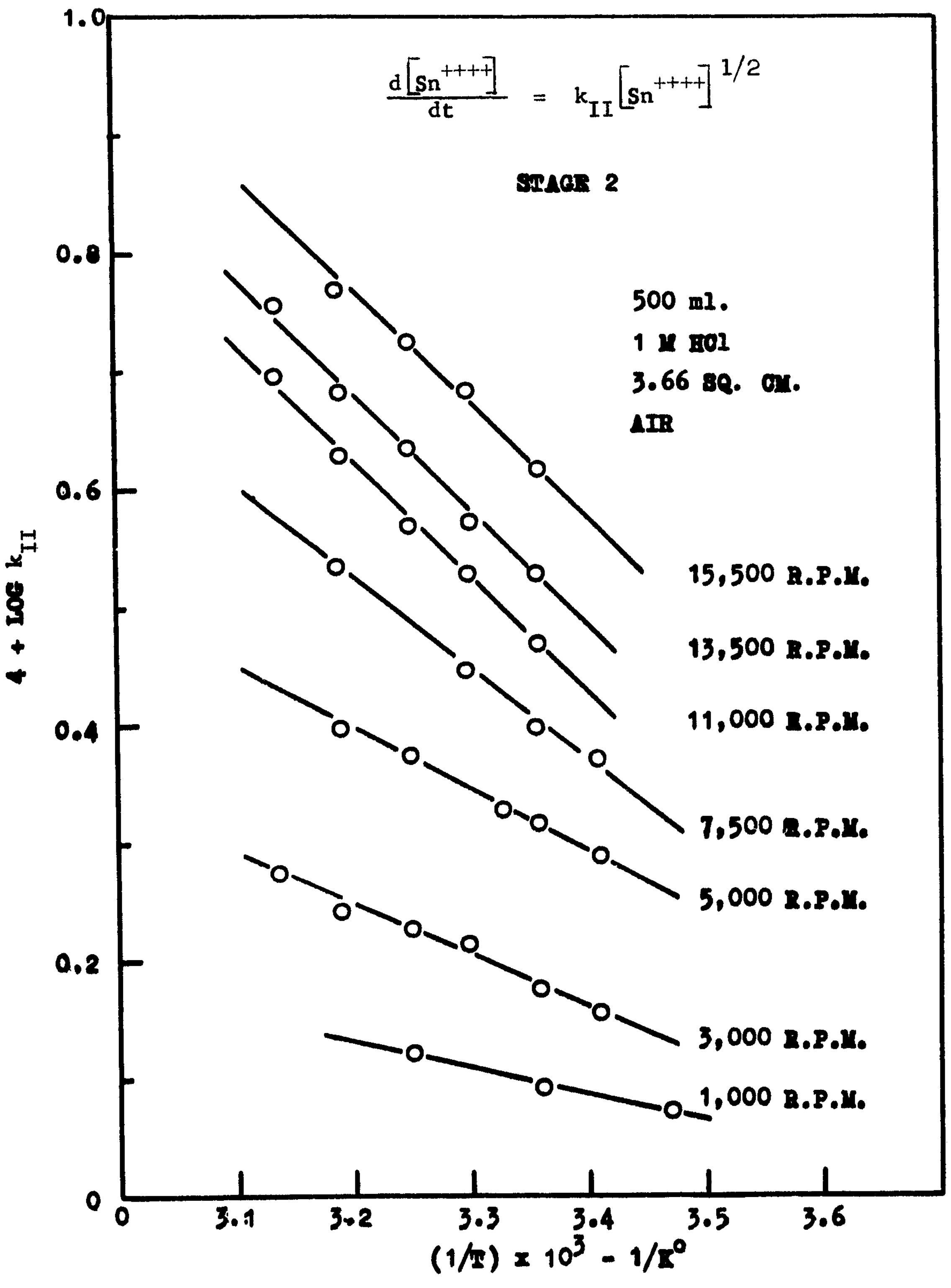

FIGURE 4 DISSOLUTION AS FUNCTION OF TEMPERATURE

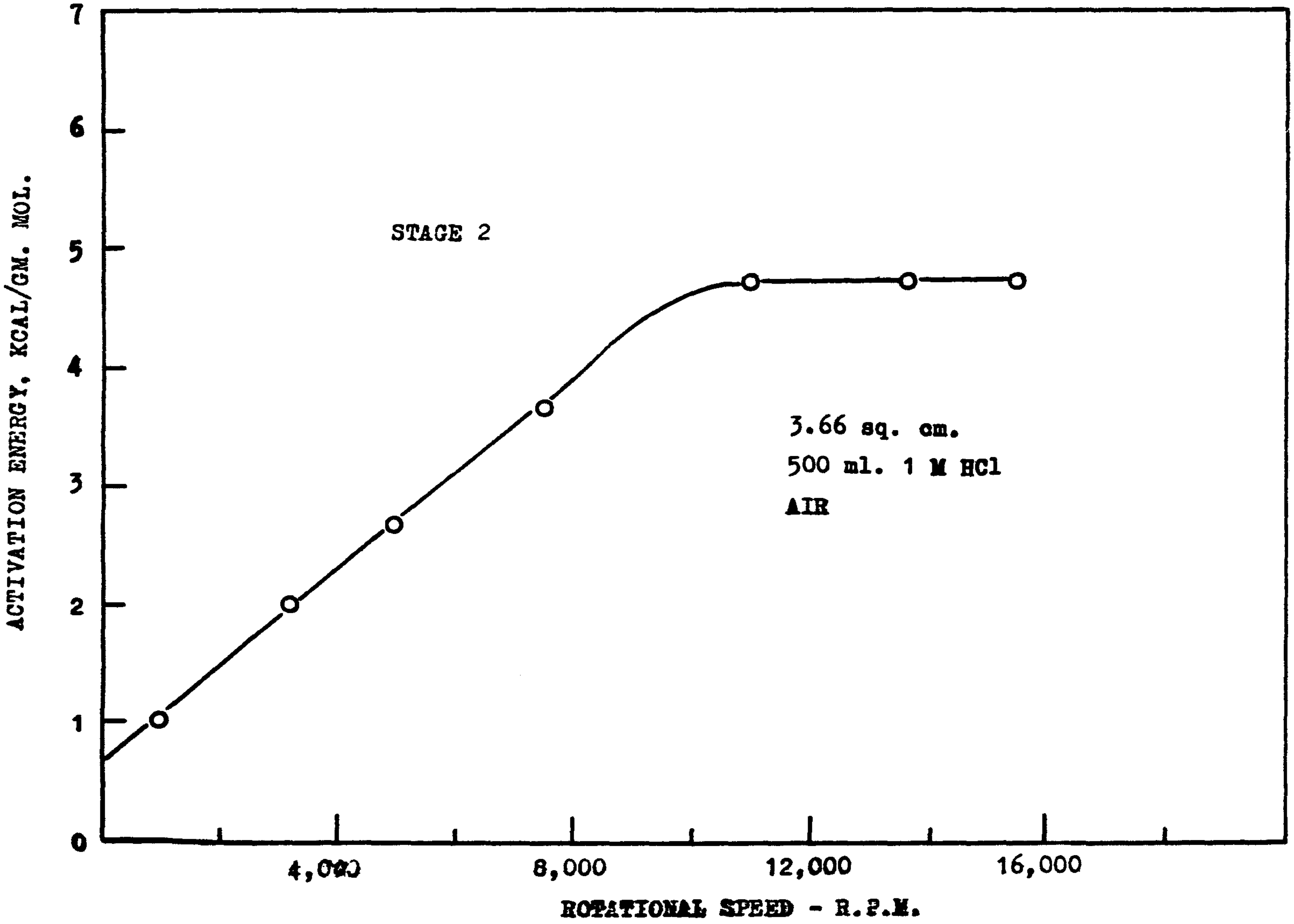

FIGURE 5 ACTIVATION ENERGY AS FUNCTION OF ROTATIONAL SPEED

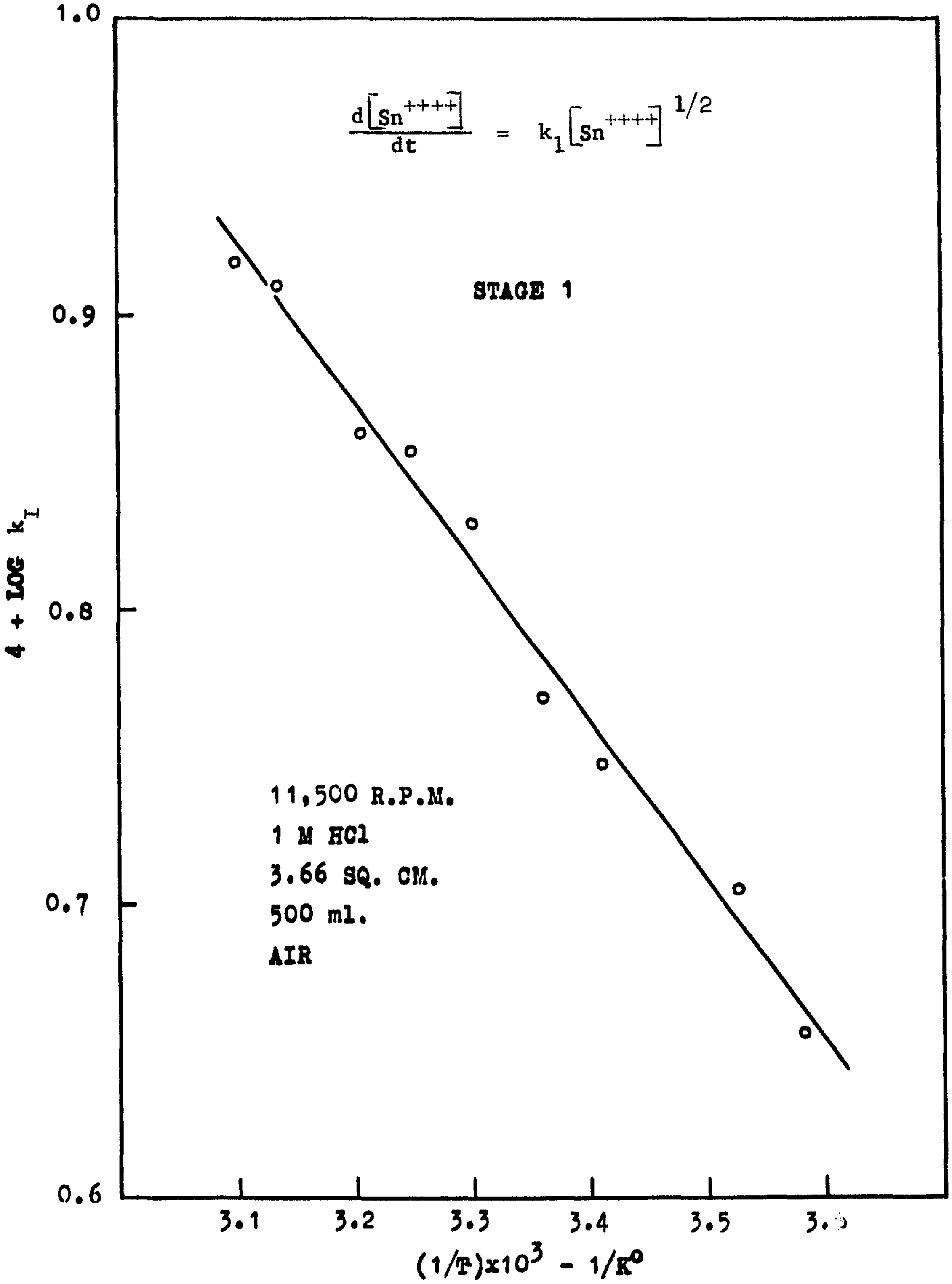

FIGURE 6 DISSOLUTION AS FUNCTION OF TEMPERATURE

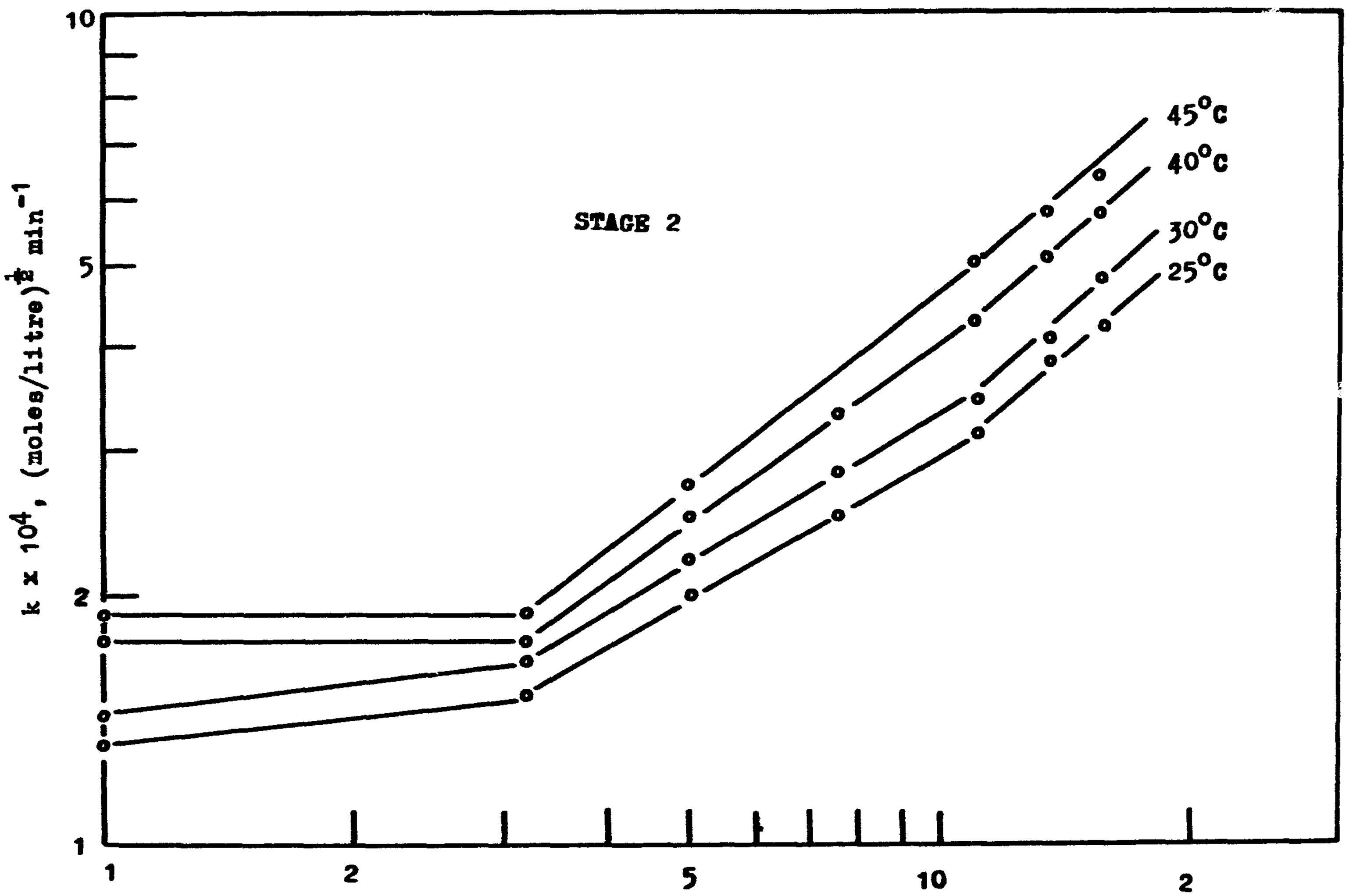

FIGURE 7 DISSOLUTION AS FUNCTION OF ROTATIONAL SPEED

TABLE 2

Dissolution Rate as a Function of Rotational Speed (Stage 2)

1,000-3,000 rpm.	
25-30°C.	$k \propto (rpm.)^{0.12}$
40-45°C.	$k \propto (rpm.)^{0}$
3,000-11,000 rpm.	
20°C.	$k \propto (rpm.)^{0.54}$
25°C.	$k \propto (rpm.)^{0.56}$
30°C.	$k \propto (rpm.)^{0.61}$
35°C.	$k \propto (rpm.)^{0.71}$
40°C.	$k \propto (rpm.)^{0.76}$
11,000-15,000 rpm.	
25-45°C.	$k \propto (rpm.)^{0.92}$

Above 11,000 rpm.it was not possible to detect any bubbles on the metal..

Although such behaviour cannot be observed in 1 M HCl solutions it is not unreasonable to expect some comparable elimination of hydrogen gas from corroding specimens.

The relative independence of rate on rotational speed and the low Arrhenius activation energy below 3,000 rpm. suggest diffusional control by a relatively stable barrier. At the low speeds, the corroding metal surface is protected predominantly by the molecular hydrogen gas bubbles.

Over the range, 3,000-11,000 rpm. the influence of rotational speed is quite markedly dependent on temperature. This dependence may be a measure of the tendency of gas bubbles to leave the corroding surface at different temperatures. In this region, corrosion rates are still determined by diffusion through a protective gas film.

Above 11,000 rpm. when the surfaces are essentially clean of gas bubbles, the activation energy approaches a constant value of 4.7 kcal/gm mole. The low value of activation energy and relatively constant effect of rpm are indicative of diffusional control but now at a liquid-metal interface.

Table 2 provides a convenient summary of the experimental data.

Because the Arrhenius activation energy and effect of rotational speed on corrosion rate were essentially constant above 11,000 rpm, all subsequent studies were carried out at 11,000 rpm.

3. Effect of Surface Roughness and Film Formation

In order to eliminate the possibility that film formation or changes in surface properties may be responsible for the transition from one stage to the other, three different sets of experiments were carried out.

(1) Manually polished samples having an arithmetic average surface roughness of 20 microinches were corroded for two hours until the crystalline structure, beneath the black surface film, was well developed with an arithmetic average roughness of the order of 55-65 microinches. The samples were re-run in a fresh solution for two hours. At the end of this time, the average roughness would be in the range of 50-100 microinches.

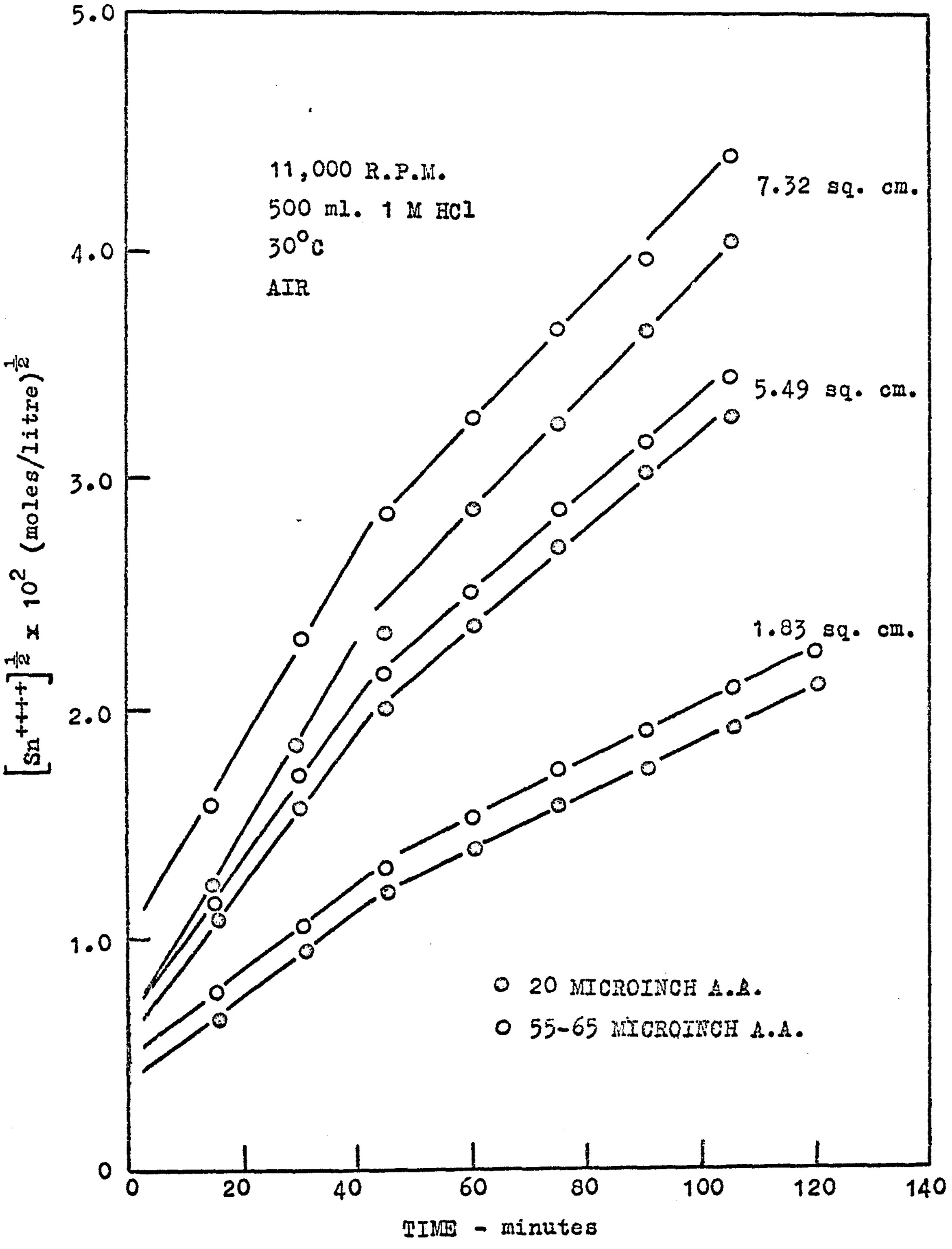

FIGURE 8 EFFECT OF SURFACE ROUGHNESS

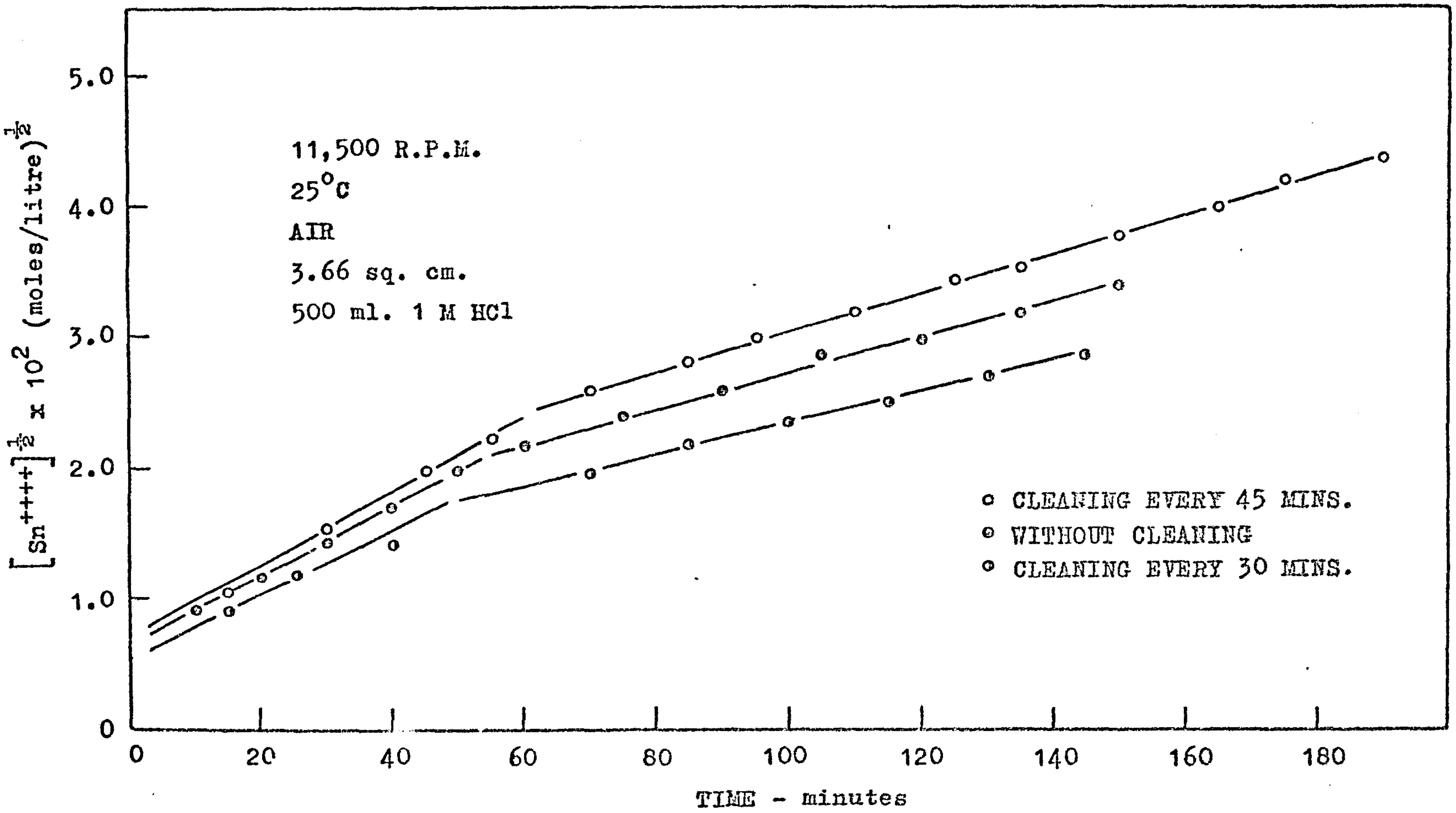

FIGURE 9 EFFECT OF CLEANING SAMPLE SURFACE

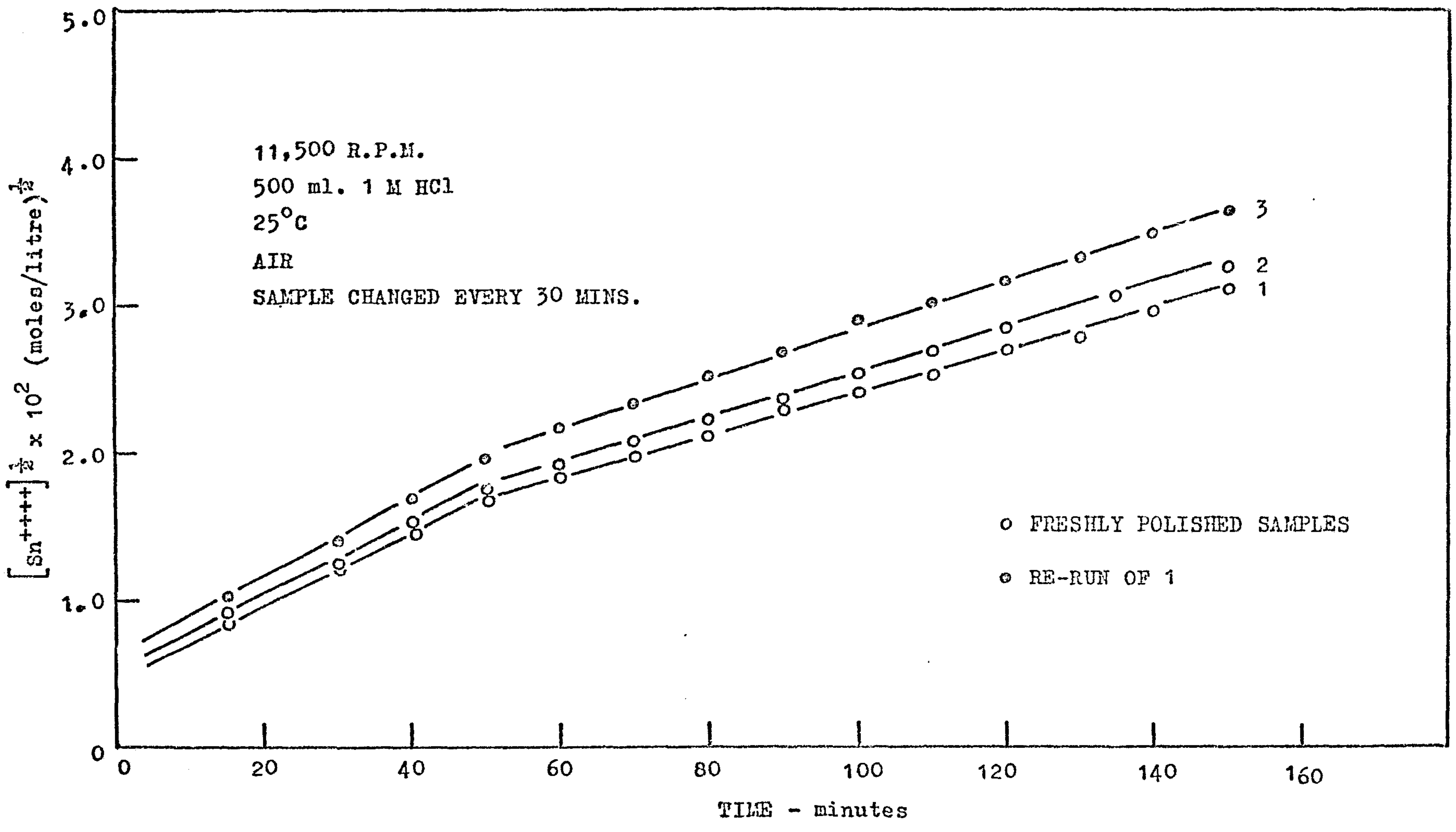

FIGURE 10 EFFECT OF REPLACEMENT OF SAMPLE

Figure 8 shows that the effect of surface roughness on the two half-order autocatalytic processes is insignificant.

(2) Corroding specimens were removed from the solution and the surfaces were cleaned free of any deposit several times during a two hour run. According to Figure 9, cleaning the samples at different intervals had no effect on the two half- order rates.

(3) Substitution of freshly polished specimens into the original corroding solution every 30 minutes showed essentially the same two stages as in Figure 10.

Results of these experiments suggest that the transition from Stage 1 to Stage 2 is not dependent on surface roughness or surface film formation.

4. Rate Dependence on Sample Area and Corroding Solution Volume

Although there is no half-order dependence on actual surface area, Figure 8 suggests that there must be some relationship between the rate of dissolution of tin and the apparent surface area of the specimen.

Figure 11 shows that both autocatalytic rates are directly proportional to the square root of the sample area.

Over the range of volume studied the autocatalytic rates are inversely proportional to the solution volume. Figure 12 illustrates the linear dependence of rate on the $A^{1/2}/V$ ratio.

A critical examination of the autocatalytic rates obtained by corroding samples of different areas, (Figure 8), revealed that the transition from Stage 1 to Stage 2 occurring when the ratio of concentration of Sn^{++++} in the solution to the area of the metal was of the order 0.4-0.8 X 10^{-4} mole per lit. per sq. cm.

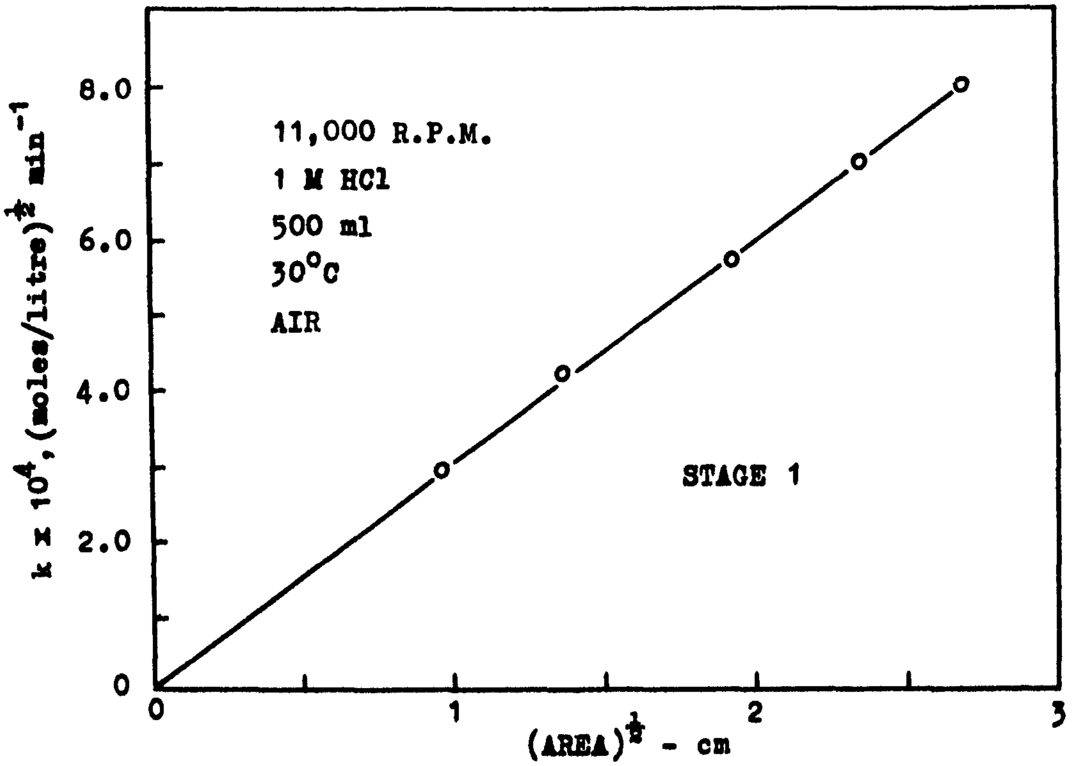

FIGURE 11A DISSOLUTION AS FUNCTION OF AREA

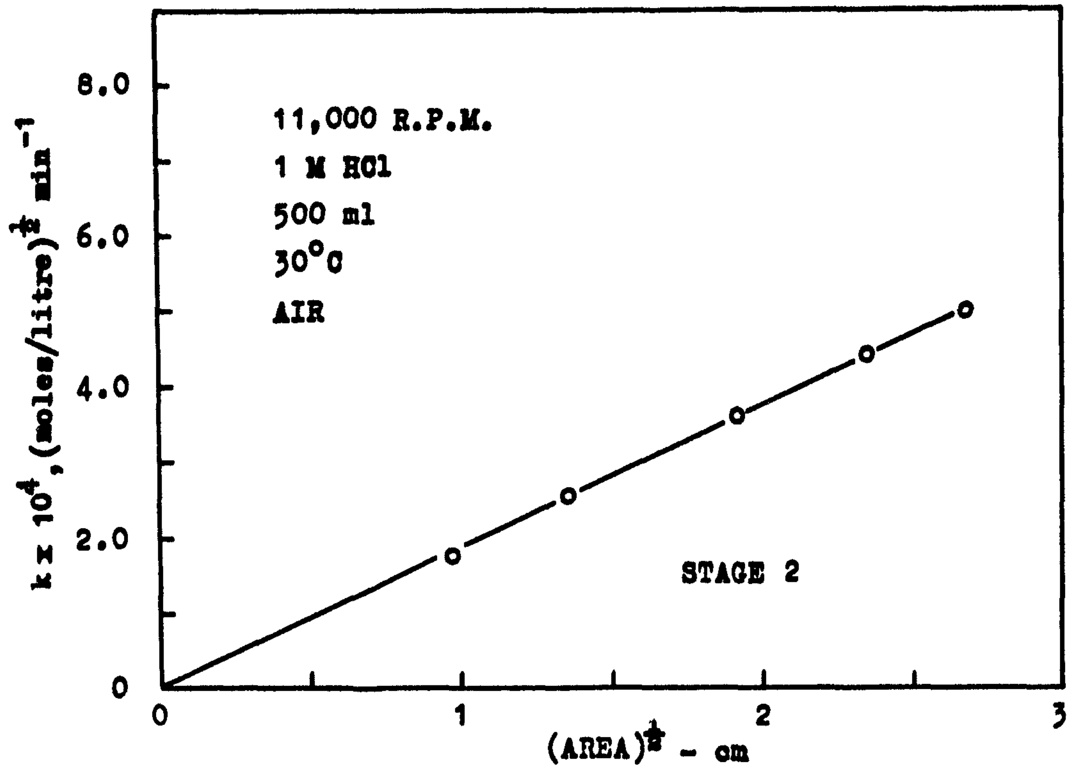

FIGURE 11B DISSOLUTION AS FUNCTION OF AREA

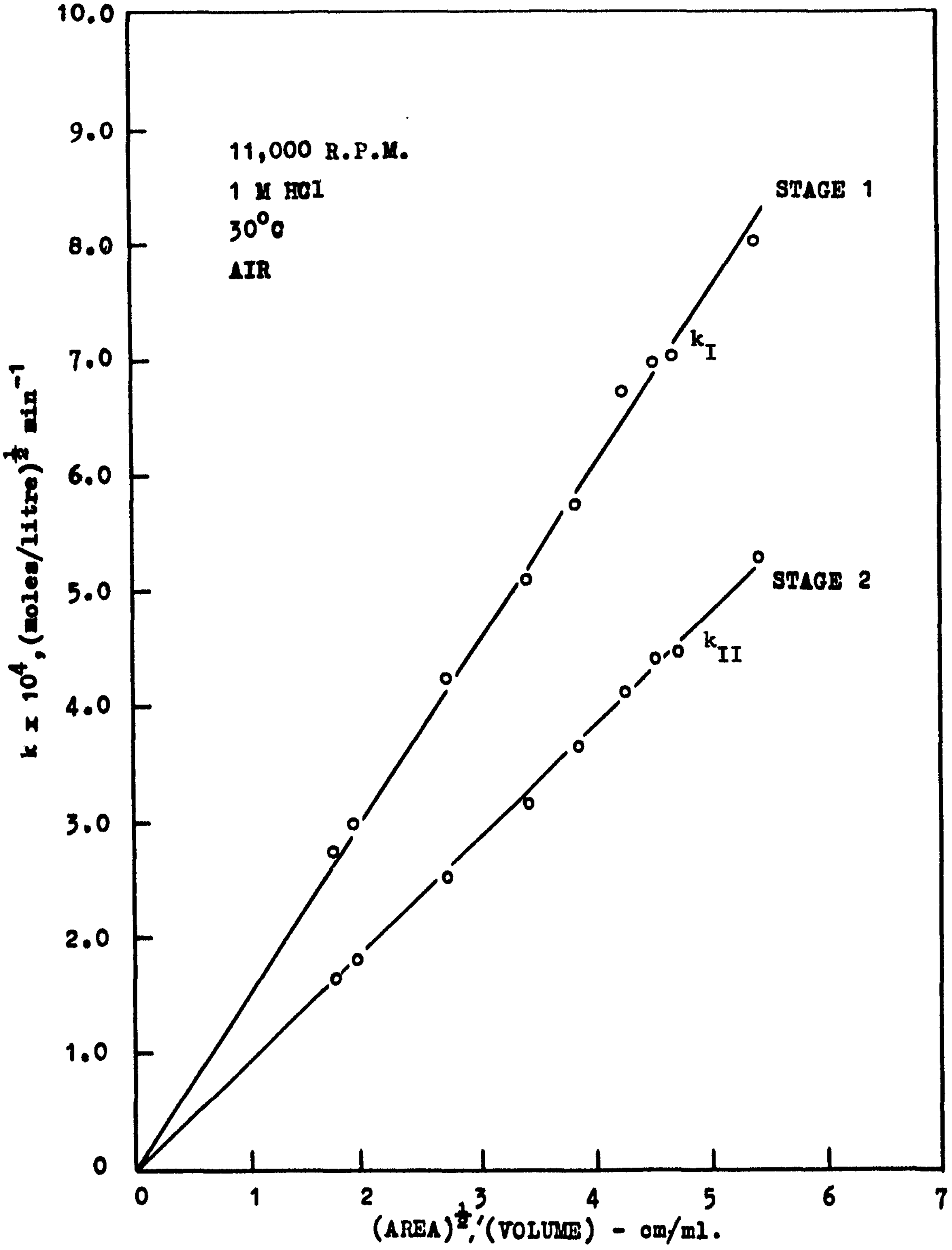

FIGURE 12 DISSOLUTION AS FUNCTION OF A/V

Because the break in the half-order plot was not associated with the surface condition of the sample but seemed to depend on the corroding solution concentration and apparent surface area, it was felt that some mechanism dependent on solution composition must be responsible for this behaviour.

The presence of reaction intermediates could play a major role in determining the rate of dissolution.

5. Identification of Reaction Intermediates

A preliminary test with Schales reagent (details described in Appendix II) revealed the presence of hydrogen peroxide in the solution during the first stage of corrosion. It was impossible to detect any after transition to the second stage. The high acidity used in this study prevented quantitative estimation of peroxide concentrations by this analytical procedure.

Reliable quantitative measures of hydrogen peroxide concentrations in corroding solutions could be obtained polarographically only in 0.1 M HCl using 1 M sodium acetate as supporting electrolyte (details discussed in Appendix III). At high acid concentrations even standard peroxide solutions failed to give meaningful results.

The data in Table 3 show that hydrogen peroxide was produced during the corrosion process. The concentration increased during the first 50 to 60 minutes, but decreased very rapidly after a maximum concentration of about 4.0×10^{-4} mol/lit.

TABLE 3

Formation of Hydrogen Peroxide During Dissolution of Tin in 0.1 M HCl Solution at 25°C.

	Run 1	Run 2	$[Sn^{++++}]$ in 0.15 M HCl
Time (min.)	$[H_2O_2]$ (mol./l.) X 10^{-4}	$[H_2O_2]$ (mol./l.) X 10^{-4}	(mol./l.) X 10^{-4}
0	0	0	0
10	0	2.0	0.6
20	2.0	2.0	1.0
30	4.0	4.0	2.2
40	4.0	4.0	3.2
50	4.0	4.0	4.0
60	4.0	2.0	4.9
70	2.0	0	6.0
80	2.0	0	7.1
90	0	0	8.3

The concentration of Sn^{++++} could not be obtained in 0.1 M HCl because below 0.15 M HCl, hydrolysis occurs causing analytical errors as high as 28% (based on material balance between weight of metal lost and stannic ions found in the solution).Estimation of $[Sn^{++++}]$ is possible from dissolution data in 0.15 M HCl.

6. Effect of Hydrogen Peroxide and Stannic Ions Addition

To study the role of the intermediate hydrogen peroxide and product Sn^{++++} during the corrosion process, two series of investigations were undertaken.

Since the transition from one stage to the other occurred when the stannic ion concentration in the solution was of the order 1.5-3.0 X 10^{-4} (generally 2.0 X 10^{-4}) mol./l. when a half-inch sample was used, it was felt that a determination of the effect of adding Sn^{++++} would be in order. Addition of stannic ion corresponding to an initial concentration higher

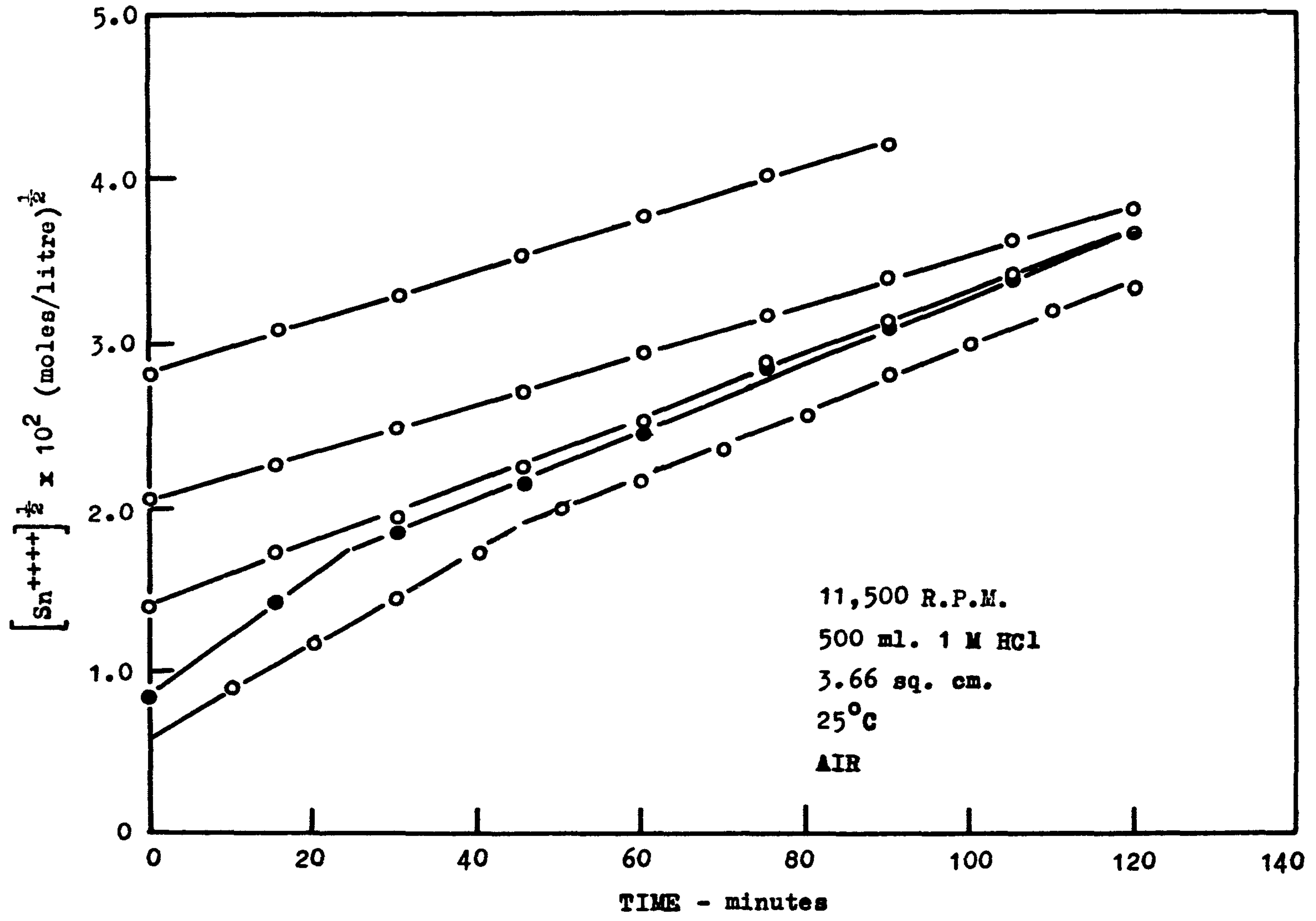

FIGURE 13 EFFECT OF INITIAL TIN CONCENTRATION

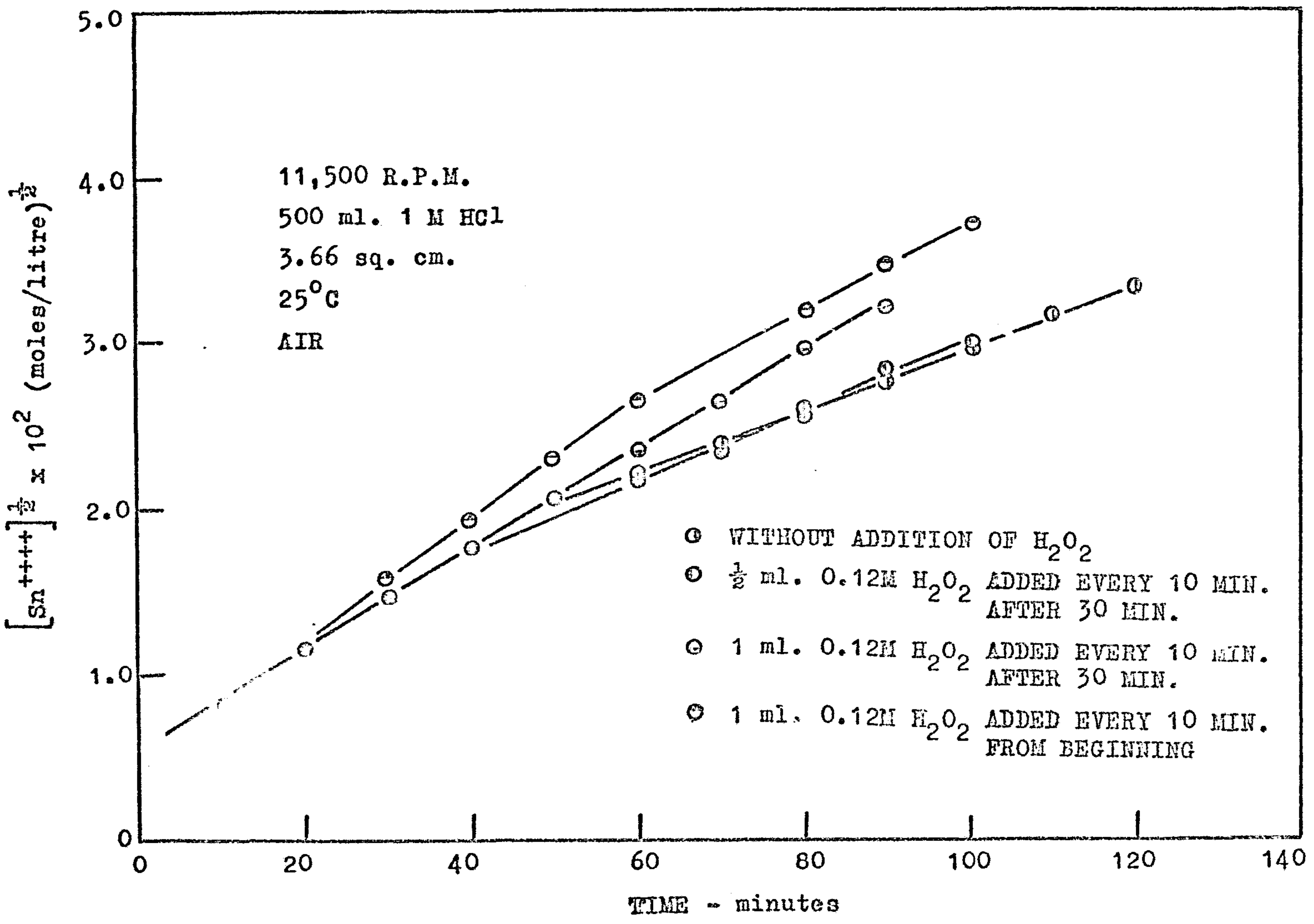

FIGURE 14 EFFECT OF HYDROGEN PEROXIDE

than 2.25×10^{-4} mol/l. eliminated the first stage as shown in Figure 13. However, with the initial addition of stannic ion a slight decrease in Stage 2 rate was always observed. (A rate constant of 3.0×10^{-4}(mol/l.)$^{1/2}$ min^{-1} with initial concentration of 4.3×10^{-4} mol/l. compared with 3.3×10^{-4}(mol/l.)$^{1/2}$ min^{-1} for an ordinary run.)

The effect of peroxide was studied by adding hydrogen peroxide solution periodically to a 1 M HCl corroding medium. It was possible to eliminate the second stage of corrosion by making additions that would raise the peroxide to at least 2.5×10^{-4} mol/l. every 10 minutes. Resulting concentrations below this level had no effect on the transition. Higher concentrations increased both half-order rates. Figure 14 illustrates the results of this investigation.

It would appear that the first stage is the result of accelerated corrosion due to the presence of hydrogen peroxide produced as an intermediate product. Increasing stannic ion concentrations tend to promote the decomposition of peroxide and lower the rate of dissolution.

7. Effect of Hydrochloric Acid Concentration

Because peroxide formation during corrosion could be studied successfully only in 0.1 M HCl solutions, it was important to see whether changes in acid concentration could alter the initial corrosion rate by affecting the formation and decomposition of peroxide.

Table 4 shows that over the range 0.15-4.0 M HCl the Stage 1 and Stage 2 dissolution rates are essentially independent of acid concentration.

TABLE 4

Effect of Hydrochloric Acid
(Dissolution under air)

[HCl]	k(1/2-order), $(\text{mol./l.})^{1/2}\text{min.}^{-1}$ (1st stage)	k (1/2-order) (2nd stage) $(\text{mol./l.})^{1/2}\text{min.}^{-1}$
	25°C - 11,400 rpm	
0.146M	6.4×10^{-4}	3.6×10^{-4}
0.250	6.2	-
0.499	6.4	-
0.998	6.3	3.35
2.000	-	3.40
2.030	6.5	-
2.875	6.3	3.30
4.030	6.2	3.40
	30°C - 11,000 rpm	
0.323	6.6×10^{-4}	3.4×10^{-4}
0.401	6.5	3.5
0.546	6.7	4.14
0.802	6.3	3.70
1.014	6.3	3.60

According to Figure 15 and Table 5 corrosion in nitrogen - saturated acid solutions is a zero order process also independent of acid concentration.

TABLE 5

Effect of Hydrochloric Acid
(Dissolution Under Nitrogen)

[HCl]	k(zero-order), $(\text{mol./l.})\text{min.}^{-1}$
0.495 M	0.75×10^{-6}
1.004	0.80
2.120	0.80
2.800	0.79

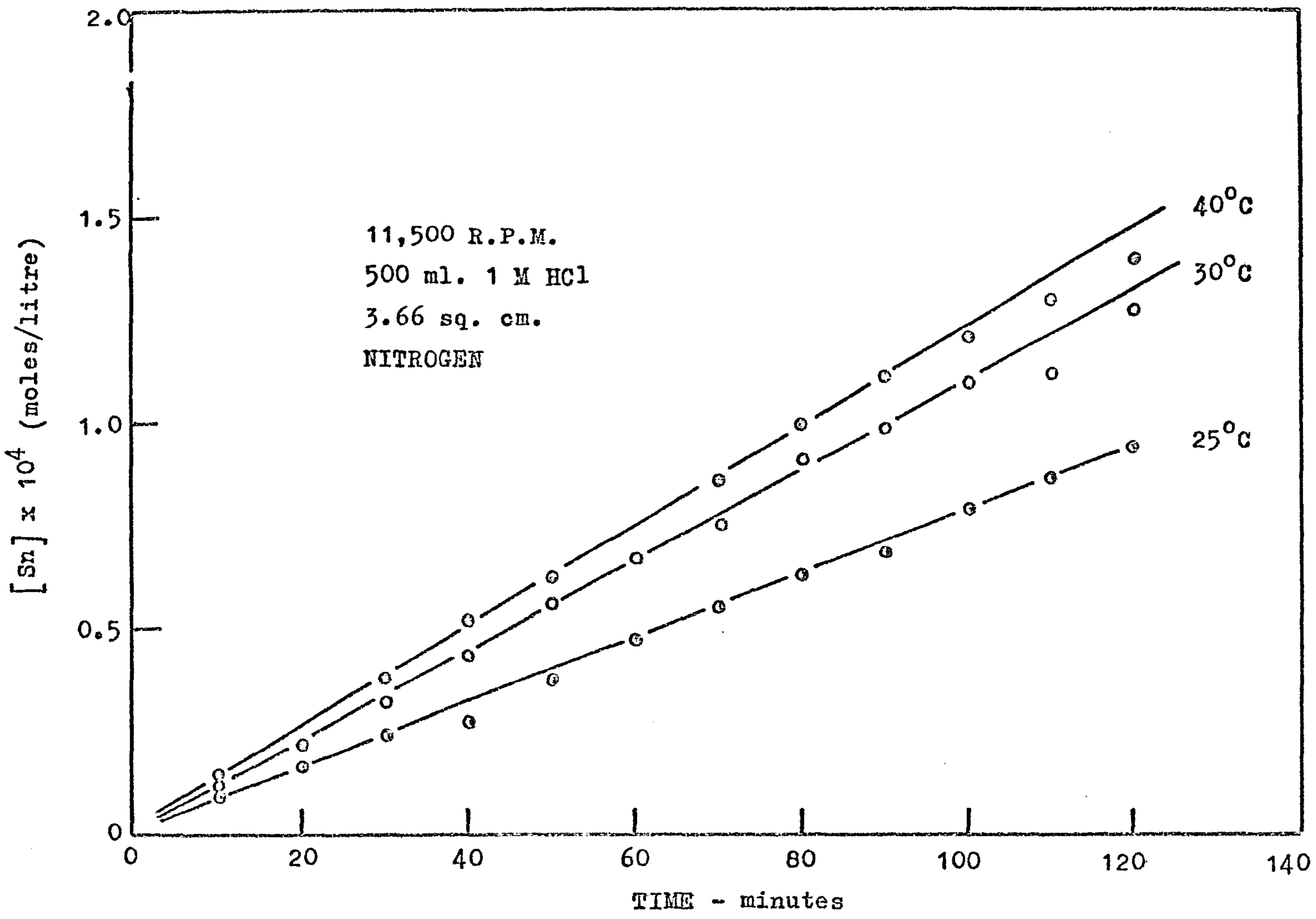

FIGURE 15 ZERO ORDER DISSOLUTION OF TIN

Dissolution rates independent of acid concentration are not uncommon. Lu[49] working on the dissolution of copper and Bumbulis[11] on the dissolution of brass, found that above 0.1 M H_2SO_4 the dissolution rates were independent of acid concentration. Their findings conform to Thomas' assumption[78] that adsorption of hydrogen atoms on metal surfaces follows a Langmuir type adsorption isotherm.

This behaviour suggests that adsorption of hydrogen ions or atoms on the metal surface could play a prominent role in the corrosion process.

8. Effect of Chloride Ions

The effect of chloride ion was studied by adding ammonium chloride to a 1.0 M HCl solution. Table 6 shows that the rates are slightly inhibited by the addition of ammonium chloride.

TABLE 6

Effect of NH_4Cl
in 1 M HCl

$[NH_4Cl]$	1st stage k, $(mol./l.)^{1/2}min.^{-1}$	2nd stage k, $(mol/l.)^{1/2}min.^{-1}$
0.1 M	6.2×10^{-4}	3.5×10^{-4}
0.4	6.0	3.3
0.8	5.6	3.2
1.0	5.5	3.15

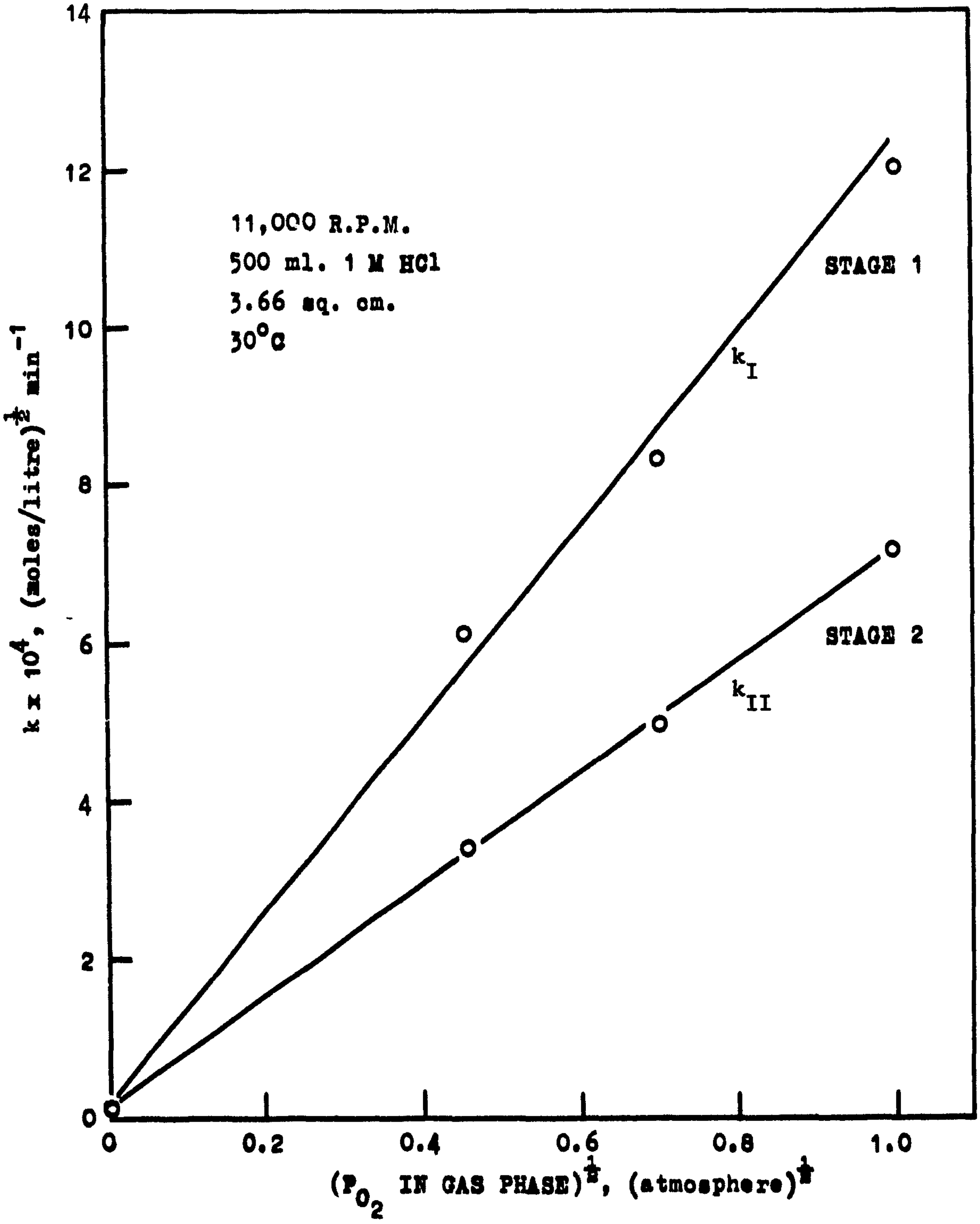

FIGURE 16 EFFECT OF OXYGEN CONCENTRATION

The decrease in rate associated with increase in ammonium chloride concentration may be partly due to the increase in viscosity of the corroding solution and partly due to blocking by adsorption of the activated sites on the metal surface by ammonium ions.

9. Rate Dependence on Oxygen Concentration

The effect of oxygen on the two half-order rates was determined by passing different mixtures of oxygen-nitrogen gas through the corroding solution. Figure 16 indicates that the rates of dissolution are most effectively correlated in terms of the square root of the oxygen partial pressure in the gas phase with which the solution is equilibrated.

II. Homogeneous Oxidation

A. Introduction

Because homogeneous oxidation of stannous chloride could be a significant step in the dissolution process, it was decided to examine this oxidation reaction under conditions comparable to those in the metal dissolution studies. The controversial conclusions recorded by previous investigators[21,28,52,87] following the course of reaction in terms of volume changes in a gas burette suggested an entirely different approach to this study.

B. Experimental Details

1. Apparatus

Because the gas-volume-measurement method of following the course of the reaction is not sensitive enough for the low concentration range of stannous ion used in this investigation, it was decided to adopt a colo-

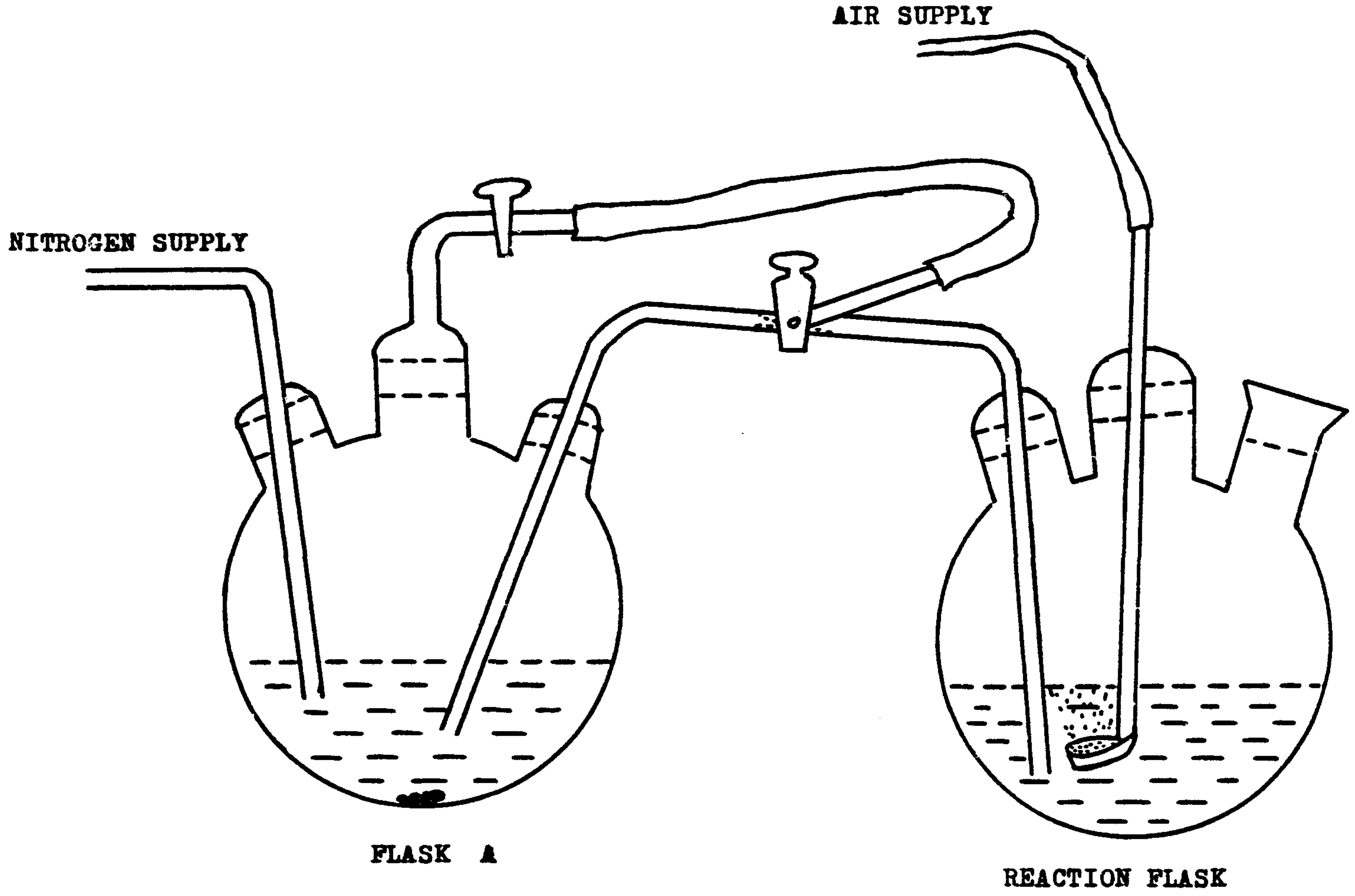

FIGURE 17 REACTION CELLS

rimetric method utilizing a Bausch and Lomb Spectronic 20 colorimeter. The reaction cells consisted essentially of the glassware shown in Figure 17.

2. Procedure

Flask A, containing a 300-ml. volume of hydrochloric acid solution, was flushed with nitrogen for a period of 4-5 hours until complete deaeration (as measured with a model 777 Oxygen Analyzer supplied by the Beckman Instruments Inc., Fullerton, California) was achieved. Stannous chloride ($SnCl_2 \cdot 2H_2O$) supplied by the British Drug Houses Limited was dissolved in the deaerated acid solution. A volume of 200 ml. of the homogeneous solution was transferred under nitrogen pressure from cell A to the reaction flask.

To start the stannous oxidation, a stream of compressed air or nitrogen-oxygen mixture was introduced into the solution. At the same time, a calculated volume of oxygen-saturated hydrochloric acid solution, of the same concentration, was poured quickly into the reaction flask to make up an initial concentration of oxygen corresponding to saturation by the gas stream passing through the solution.

Samples were taken at five-minute intervals for colorimetric analysis (details described in Appendix 4). From the degree of decolorization of a standardized potassium permanganate solution, it was possible to determine the concentration of stannous chloride at any time. All runs were carried out in a constant temperature bath regulated to ± 0.1 degree of the desired temperature.

The gas rate, 1.5 l./min, was high enough to eliminate rate dependence on gas flow rate.

C. Discussion of Results

1. Stannous Ion Dependence

The rate dependence on stannous ion had stirred up some disagreement among earlier investigators. Under the conditions of this research, the results are best represented by a first order behavior. As shown in Figure 18, a plot of log $[Sn^{++}]$ vs time produces a linear relationship. At each temperature, a 2-3 fold change in initial stannous ion concentration has no effect on the slope as shown in Figure 19.

A plot of $1/[Sn^{++}]$ vs time also produces a linear relationship, but the slopes change with variation of initial stannous concentration. This behavior would eliminate the possibility that the reaction rate is of the second order with respect to stannous ion as might be suggested by the linear relationship of Figure 20.

The first-order dependence on stannous ion may be summarized by the rate law

$$-\frac{d}{dt}[Sn^{++}] = k'[Sn^{++}]$$

where k' is calculated from the slopes in Figure 18 and is independent of initial stannous ion concentrations, but depends on oxygen and hydrochloric acid concentrations, and temperature variations.

The concentration range in this research is of the order $3\text{-}8 \times 10^{-3}$ mol/l. and is considered within the low range when compared to that used by Filson and Walton[21], and Lochman and Tompkins[52] who worked with solution of the order of 7×10^{-1} mol/l. The first-order dependence on stannous ion found in this research conforms to their rate equation for dilute solution of stannous ion.

$$r = k[SnCl_2]$$

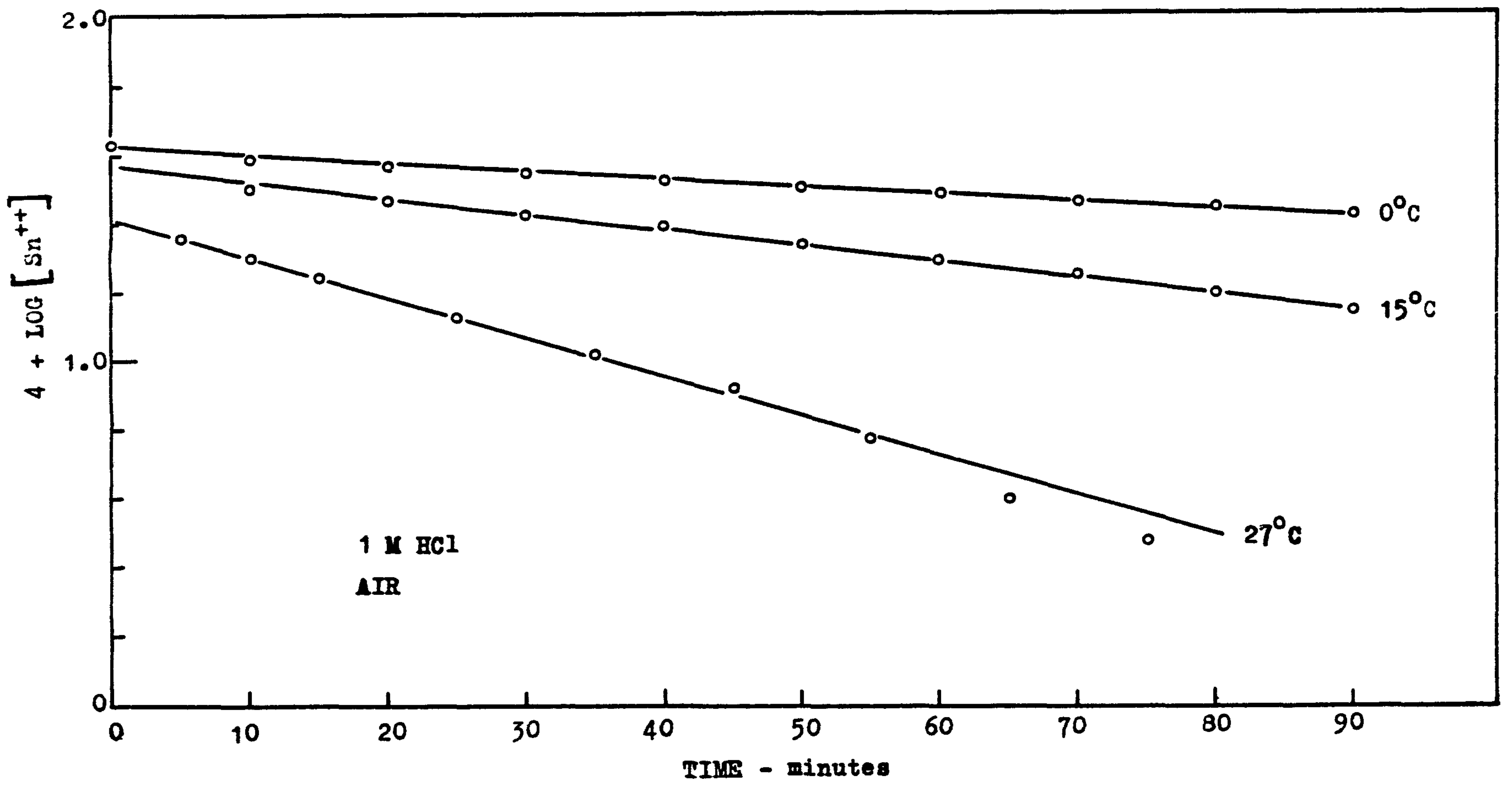

FIGURE 18 FIRST-ORDER REACTION OF STANNOUS CHLORIDE

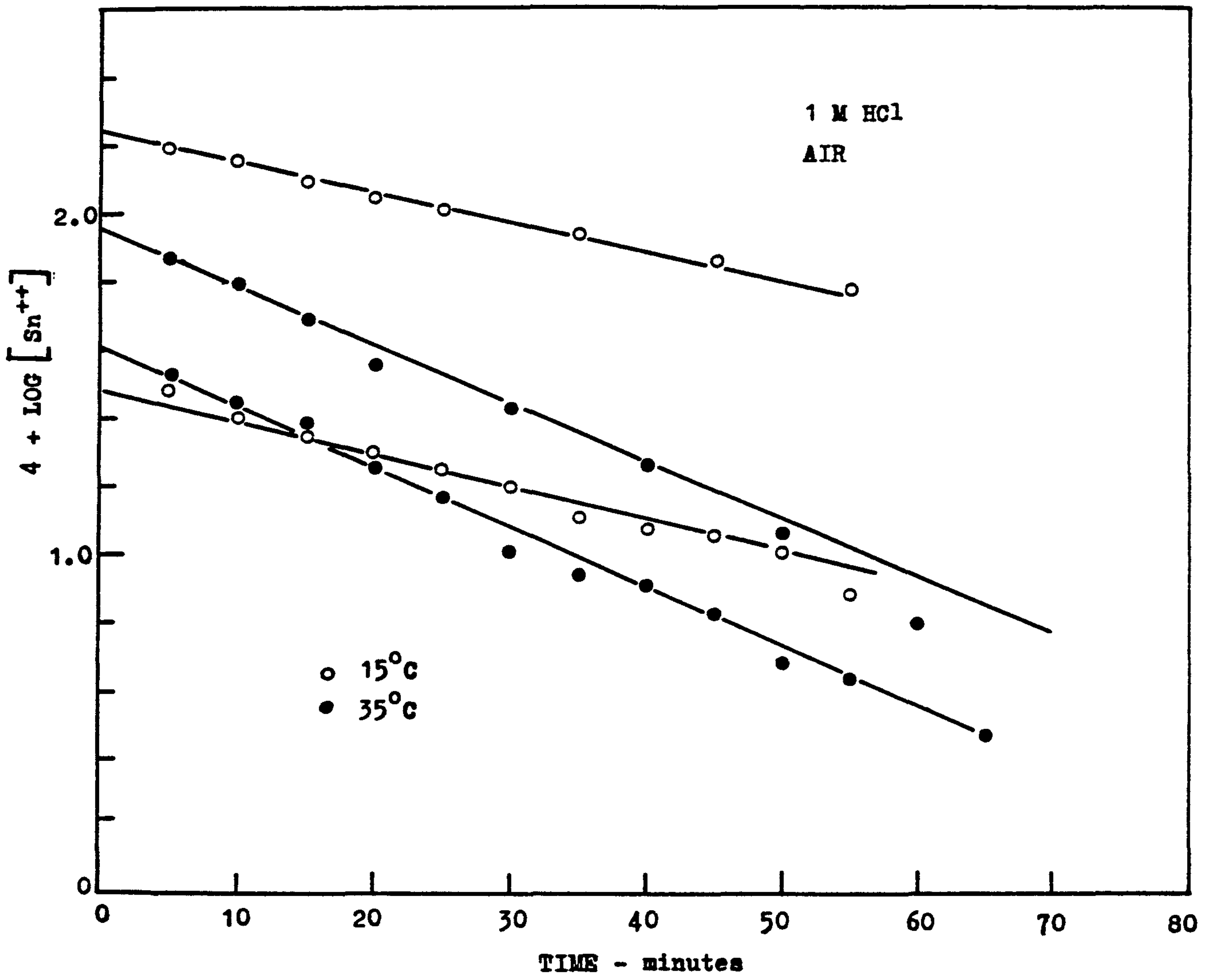

FIGURE 19 FIRST-ORDER REACTION OF STANNOUS CHLORIDE

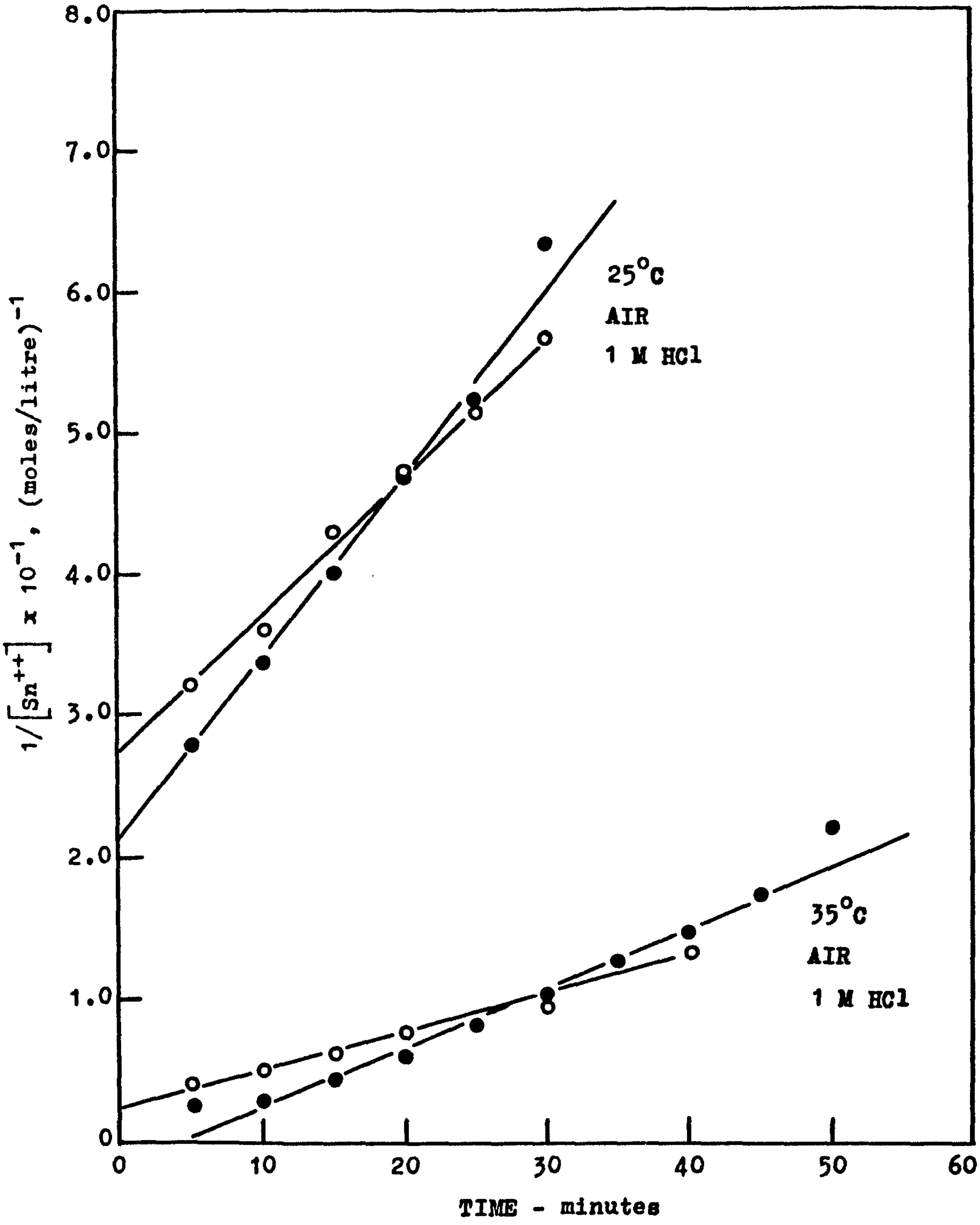

FIGURE 20 SECOND-ORDER REACTION OF STANNOUS CHLORIDE

2. Oxygen Dependence

In the absence of oxygen there is virtually no oxidation of stannous solutions. The effect of oxygen was determined by blowing air ($P_{O_2} = 0.21$ atm) and synthetic oxygen-nitrogen gas through the system. Figure 21 shows the linear relationship between k and oxygen partial pressure.

Because it was impossible to add large amounts of oxygen-saturated solution into the reaction flask to create initial oxygen saturation corresponding to the high oxygen content in the gas stream, it was impractical to attempt experiments in which the oxygen pressures were greater than 0.6 atm.

For partial pressures of oxygen below 0.6 atm, the kinetics of the reaction can be represented by the rate law:

$$-\frac{d}{dt}\left[Sn^{++}\right] = k''\left[Sn^{++}\right]\left[O_2\right]$$

where k'' is a function of temperature and hydrochloric acid concentration.

3. Temperature Dependence

The first-order rate dependence on temperature has been studied in 1 M HCl solutions over the range 0°-40°C. Figure 18 shows the linear relationship between log $\left[Sn^{++}\right]$ vs time at various temperatures with no correction made for the changing solubility of oxygen. Figure 22 shows the variation of solubility of oxygen in different acid concentrations at different temperatures. The k values calculated from the slopes of curves in Figure 18 were corrected for the same oxygen concentration in solution on the basis of the previously determined first-order dependence on oxygen with data from Figure 22. The corrected values are listed in Table 7.

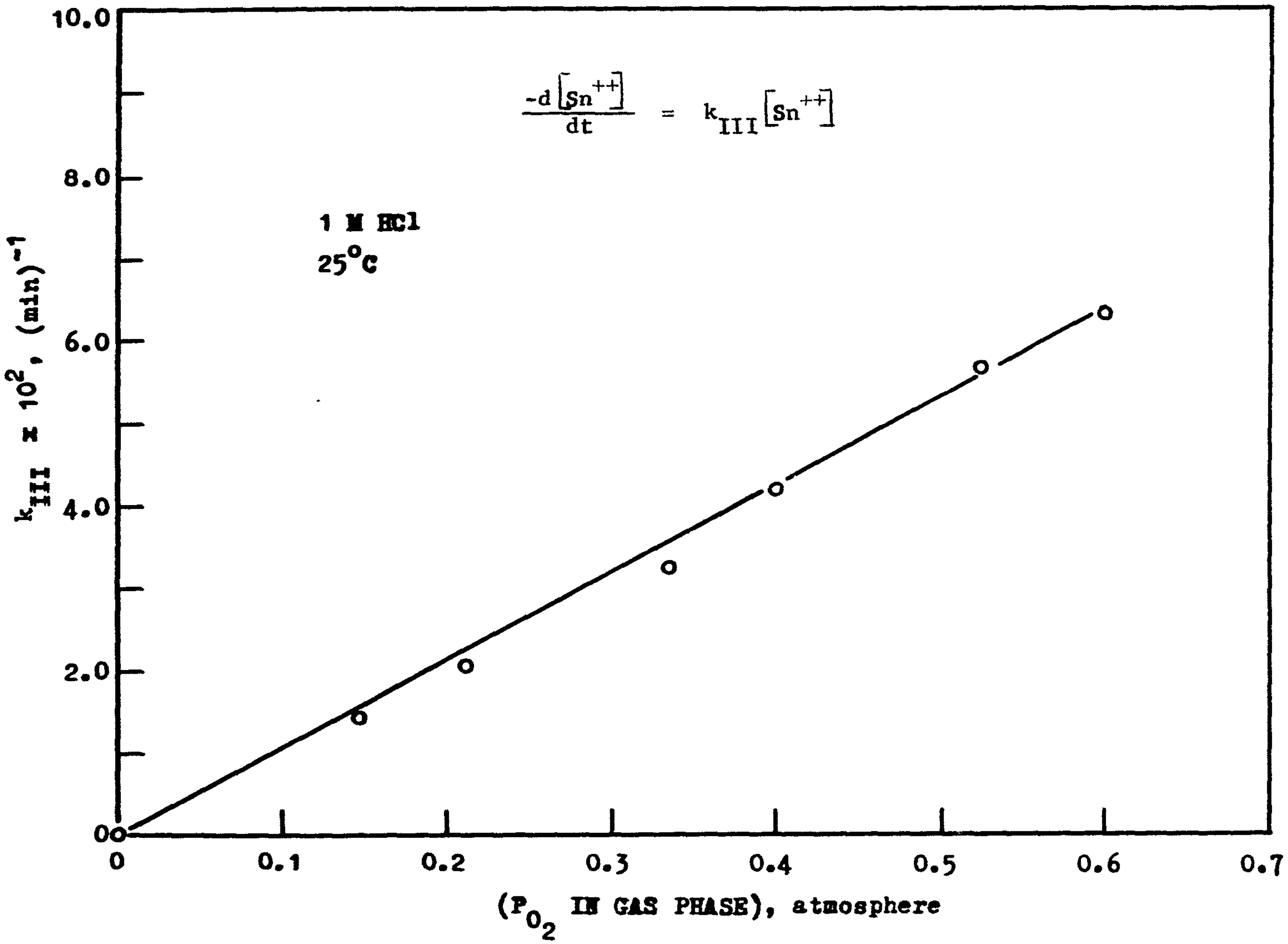

FIGURE 21 EFFECT OF OXYGEN CONCENTRATION

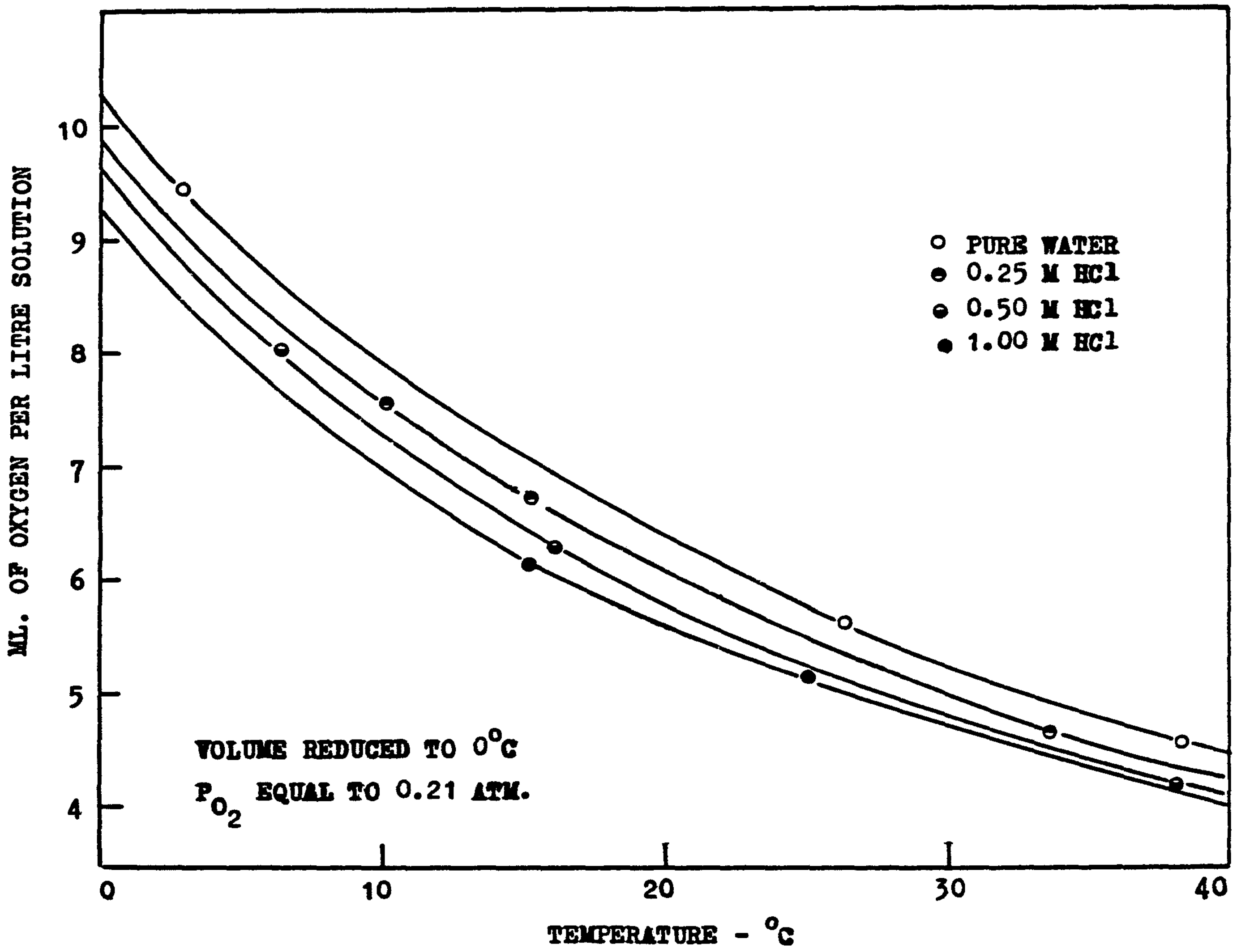

FIGURE 22 SOLUBILITY OF OXYGEN

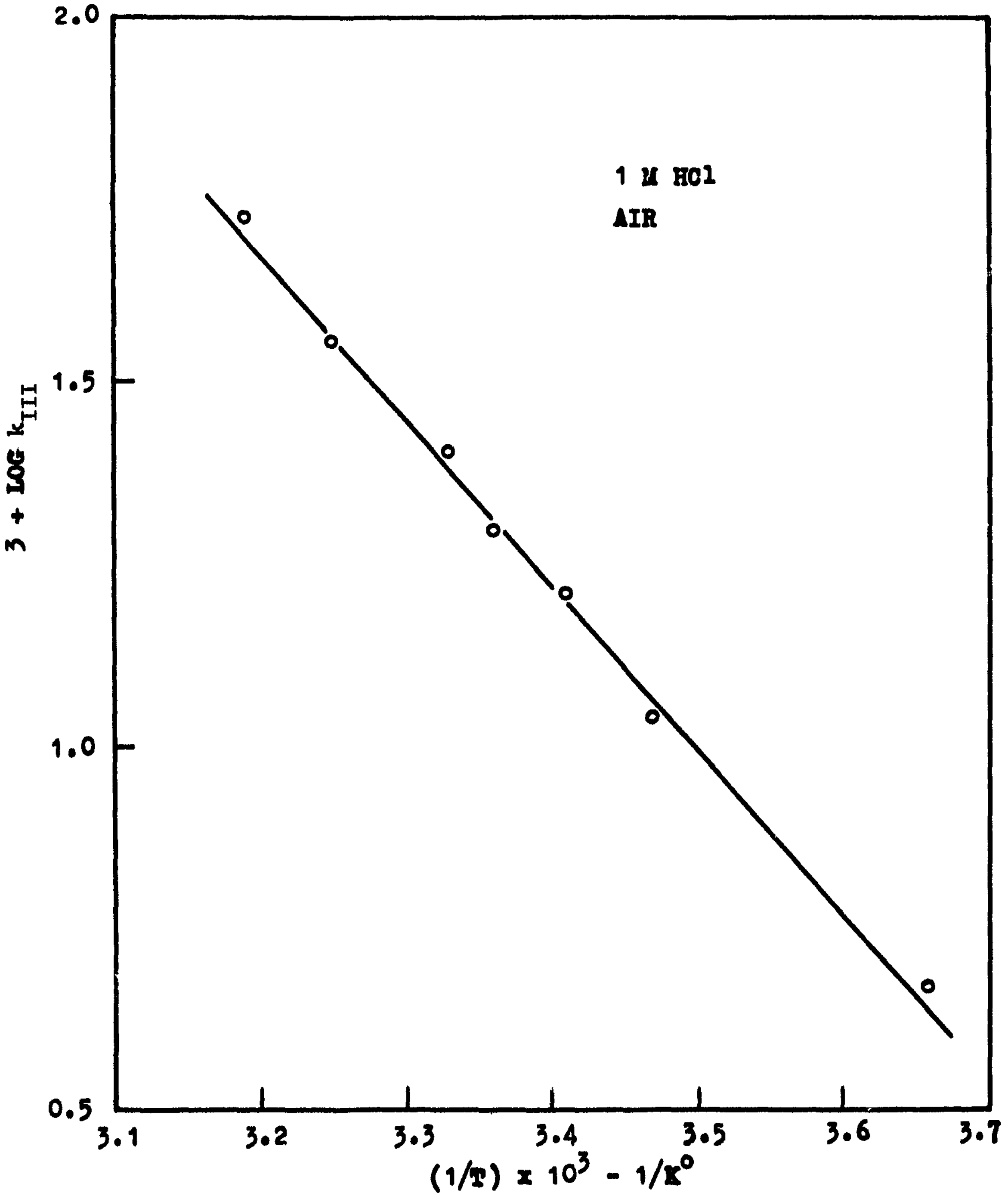

FIGURE 23 OXIDATION AS FUNCTION OF TEMPERATURE

The linear dependence of log k on 1/T is shown in Figure 23. The apparent activation energy calculated from the slope is of the order of 10.5 kcal/gm.mol.

TABLE 7

Corrected for Solubility of Oxygen at Different Temperature

Temperatures	k' X O_2 Concentration		
0°C.	$4.86 \times 10^{-3} \times 5.25/9.5$	=	2.68×10^{-3}
15°C.	$1.08 \times 10^{-2} \times 5.25/6.20$	=	9.15×10^{-3}
20°C.	$1.63 \times 10^{-2} \times 5.25/5.70$	=	1.5×10^{-2}
25°C.	$1.98 \times 10^{-2} \times 5.25/5.25$	=	1.98×10^{-2}
27°C.	$2.55 \times 10^{-2} \times 5.25/4.95$	=	2.71×10^{-2}
35°C.	$3.73 \times 10^{-2} \times 5.25/4.5$	=	4.35×10^{-2}
40°C.	$5.38 \times 10^{-2} \times 5.25/4.25$	=	6.65×10^{-2}

4. Hydrochloric Acid Dependence

The oxidation rate of stannous chloride increased with increasing concentrations of hydrochloric acid. From Figure 24 the rate may be shown to depend on the first power of acid concentration over the concentration range 0.25-0.75 M HCl.

The above behavior may be discussed in terms of the following equilibria suggested by Young:[87]

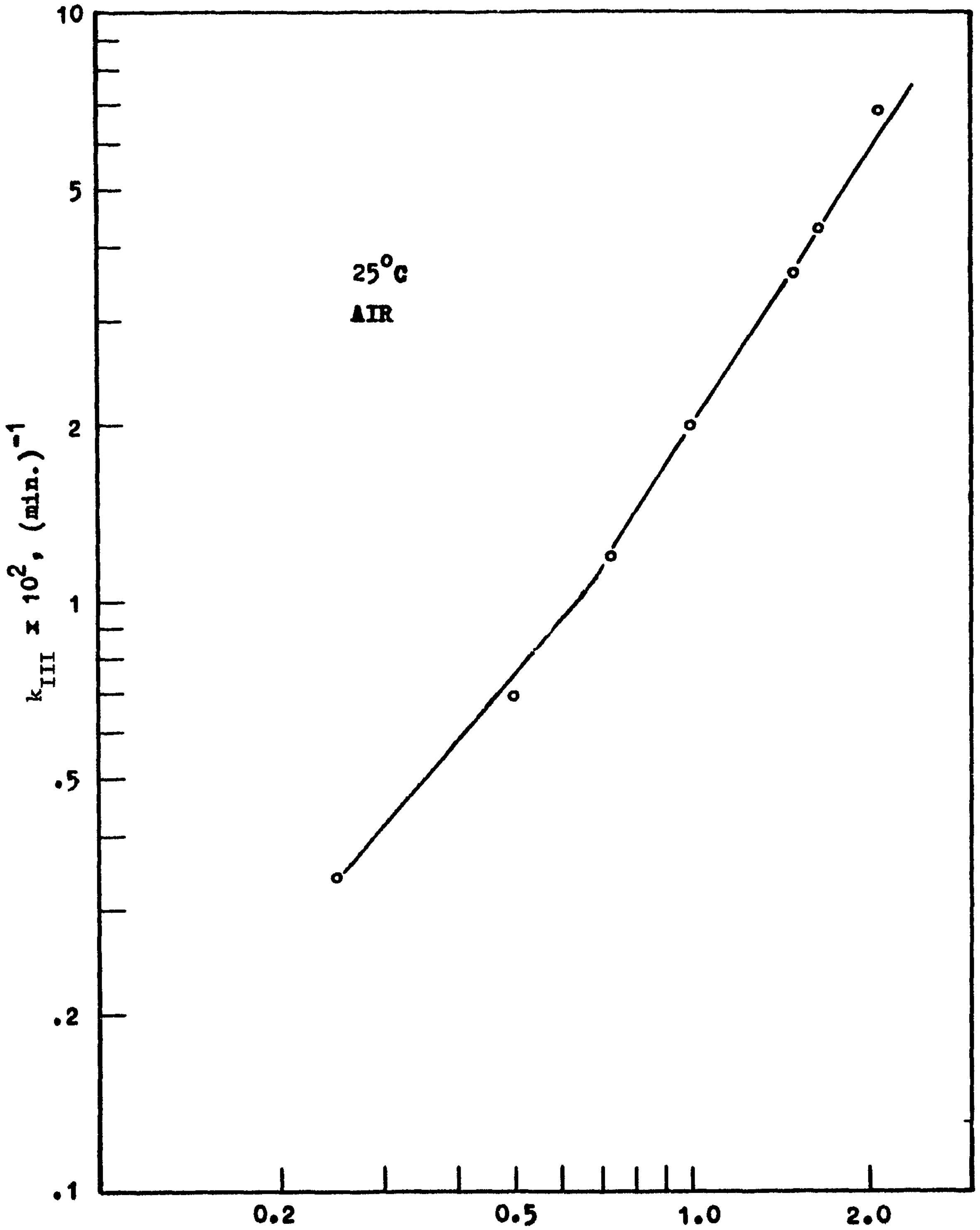

FIGURE 24 EFFECT OF HYDROCHLORIC ACID

$$HCl + SnCl_2 \rightleftharpoons HSnCl_3$$

$$HCl + HSnCl_3 \rightleftharpoons H_2SnCl_4$$

Assuming that only complex species are oxidized, it is possible to write the following series of elementary reactions based on Posner's[65] previously suggested treatment.

$$HSnCl_3 + O_2 \xrightarrow{k_1} HO_2^- + SnCl_3^+$$

$$H_2SnCl_4 + O_2 \xrightarrow{k_2} 2OH + SnCl_4$$

$$HO_2^- + H^+ \rightleftharpoons H_2O_2$$

$$HSnCl_3 + H_2O_2 \xrightarrow{k_3} SnCl_3 + OH + H_2O$$

$$H_2SnCl_4 + H_2O_2 \xrightarrow{k_4} SnCl_4 + 2H_2O$$

$$SnCl_3 + OH \xrightarrow{k_5} SnCl_3^+ + OH^-$$

where (OH) and ($SnCl_3$) are intermediate free radicals. From the above series of reactions, the following rate equations may be written:

$$\frac{d}{dt}\left[SnCl_3^+\right] = k_1\left[HSnCl_3\right]\left[O_2\right] + k_5\left[SnCl_3\right]\left[OH\right]$$

$$\frac{d}{dt}\left[SnCl_4\right] = k_2\left[H_2SnCl_4\right]\left[O_2\right] + k_4\left[H_2SnCl_4\right]\left[H_2O_2\right]$$

The net rate of formation of quadrivalent tin is then

$$\frac{d}{dt}\left[Sn^{++++}\right] = k_1\left[HSnCl_3\right]\left[O_2\right] + k_5\left[SnCl_3\right]\left[OH\right] + k_2\left[H_2SnCl_4\right]\left[O_2\right] + k_4\left[H_2SnCl_4\right]\left[H_2O_2\right]$$

By applying steady state approximations for $[OH]$, it is possible to write

$$\frac{d}{dt}[OH] = 2k_2[H_2SnCl_4][O_2] + k_3[HSnCl_3][H_2O_2] - k_5[SnCl_3][OH]$$
$$= 0$$

from which $$[OH] = \frac{2k_2[H_2SnCl_4][O_2] + k_3[HSnCl_3][H_2O_2]}{k_5[SnCl_3]}$$

By appropriate substitution the rate equation becomes:

$$\frac{d}{dt}[Sn^{++++}] = k_1[HSnCl_3][O_2] + k_3[HSnCl_3][H_2O_2] + 3k_2[H_2SnCl_4][O_2]$$
$$+ k_4[H_2SnCl_4][H_2O_2]$$

By means of titanium sulfate, it was possible to show the presence of peroxide during the course of oxidation.when the concentration of stannous chloride was of the order 7 - 10 X 10^{-2} M. However, in the concentration range of stannous chloride (3.- 8 X 10^{-3}) used, the concentration of peroxide was insignificant. By neglecting the terms involving $[H_2O_2]$, the above rate equation becomes:

$$\frac{d}{dt}[Sn^{++++}] = k_1[HSnCl_3][O_2] + 3k_2[H_2SnCl_4][O_2]$$

It follows that the oxidation rate is proportional to the first power of oxygen concentration. The above rate equation also conforms to Lochman and Tompkin's[52] suggestion that the main species oxidized in the stannous solution are two complex molecules of the form $HSnCl_3$ and H_2SnCl_4.

Young[87] showed that for the concentration range 0.25 - 7.7 M HCl, the equilibrium

$$SnCl_2 + HCl \rightleftharpoons HSnCl_3$$

is significant at low acid concentrations, while at high concentrations the equilibrium

$$HSnCl_3 + HCl \rightleftharpoons H_2SnCl_4$$

becomes more important. At low acid concentrations when the second equilibrium is insignificant and the concentration of H_2SnCl_4 may be considered to be negligible the rate equation may be reduced to the form:

$$\frac{d}{dt}\left[Sn^{++++}\right] = k_1\left[HSnCl_3\right]\left[O_2\right]$$

$$= k_1'\left[HCl\right]\left[SnCl_2\right]\left[O_2\right]$$

with the rate being proportional to the first power of hydrochloric acid concentration. At high concentrations, the rate equation could reduce to

$$\frac{d}{dt}\left[Sn^{++++}\right] = 3k_2\left[H_2SnCl_4\right]\left[O_2\right]$$

$$= k_2'\left[HCl\right]^2\left[SnCl_2\right]\left[O_2\right]$$

with the rate being proportional to the second power of hydrochloric acid concentration. The constants k_1', and k_2' arise from use of the above two equilibria in the appropriate form of the rate equation.

The results of this research showed that between 0.25 M to 0.75 M, the oxidation rate was proportional to the first power of hydrochloric acid concentration. Between 0.75 M to 2.0 M HCl, the rate was proportional to 1.5th power. At low acid concentrations (0.25 - 0.75 M) the equilibrium

$$HCl + SnCl_2 \rightleftharpoons HSnCl_3$$

is significant in determining solution composition. At higher concentrations (0.75 M - 2.0 M) a transition from one equilibrium to another should take place. As a result the rate of stannous chloride oxidation should

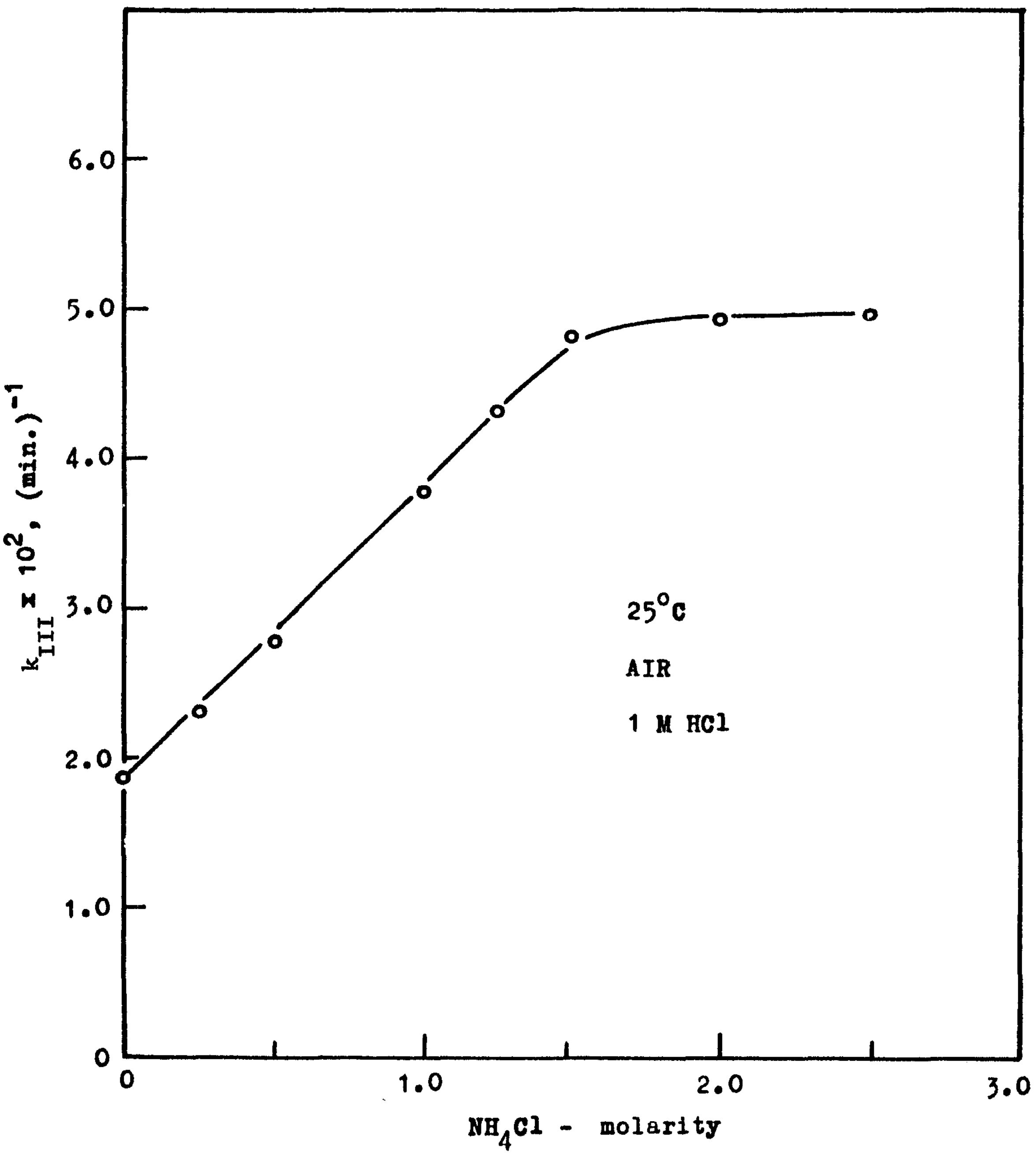

FIGURE 25 EFFECT OF AMMONIUM CHLORIDE

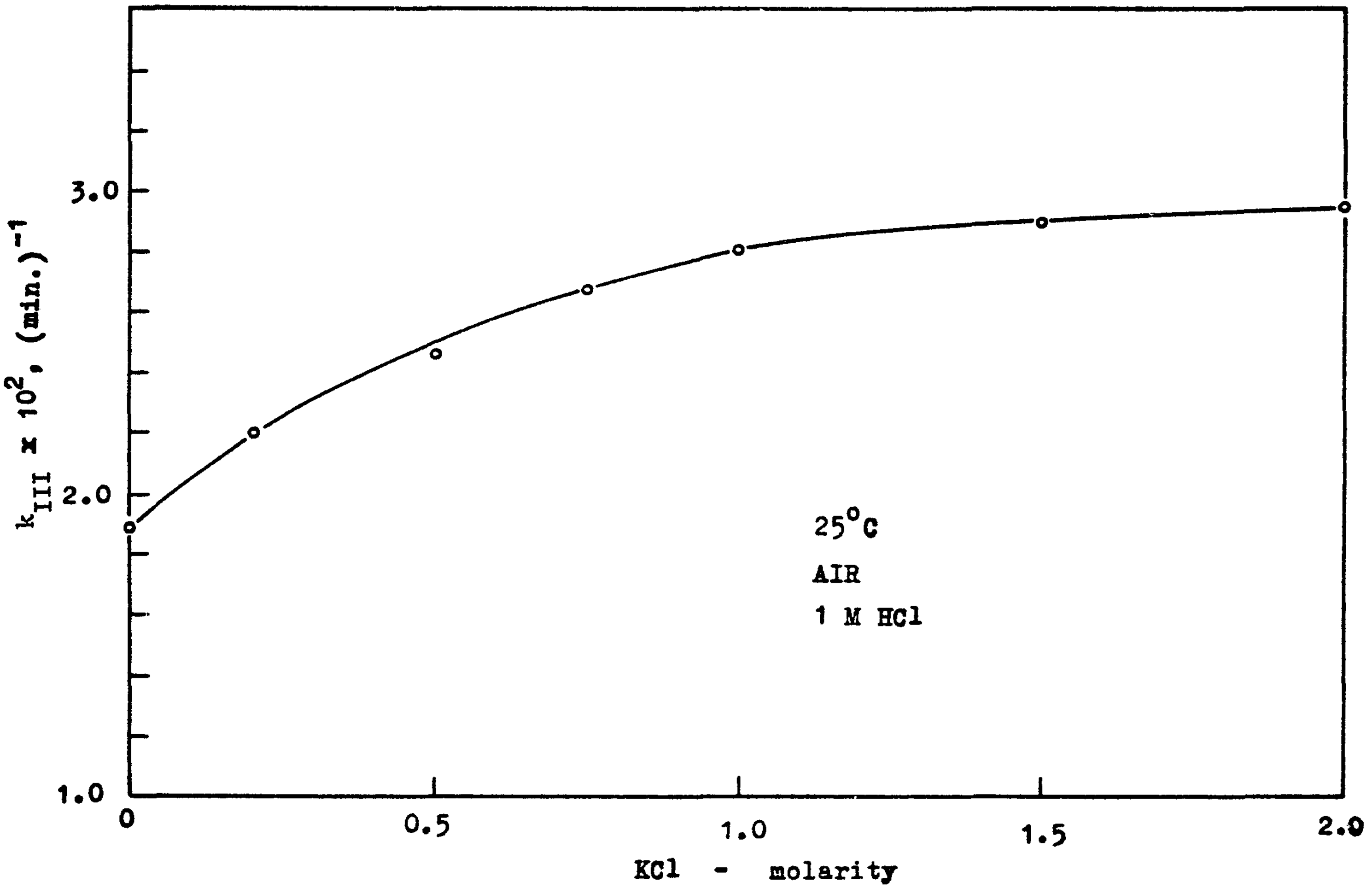

FIGURE 26 EFFECT OF POTASSIUM CHLORIDE

show some dependence on HCl concentration between one and two.

5. Chloride Ion Dependence

The rate dependence on chloride ion was studied by adding ammonium chloride or potassium chloride to 1 M HCl solutions. In both cases, the oxidation rate increased towards limiting values with increasing concentrations of chloride ion. With ammonium chloride, the maximum rate was obtained at concentrations of chloride ion above 2.5 gm.ion/l. as shown in Figure 25. In the case of potassium chloride, a lower maximum rate was obtained when the chloride ion concentration exceed 2.0 gm.ion/l. as shown in Figure 26.

This behavior can be explained by the fact that the main species undergoing oxidation in solution are complex molecules[70], of the type NH_4SnCl_3 or K_2SnCl_4. The added salts simply tie up the stannous ions in the solution to form the above complex species. As a result the oxidation rate increased as the concentration of the complex increased. With sufficiently high additions of KCl or NH_4Cl when all the stannous chloride has been complexed, further addition will have no effect and the solution should oxidize at a constant rate.

Because it is well known[70] that the stabilities of the two complexes are quite different, the oxidation rates need not be the same.

6. Hydrogen-Ion Dependence

The effect of hydrogen ion was studied by varying the concentration of sulfuric acid at a constant ammonium chloride concentration. The results are shown in Figure 27. Below 1 M H_2SO_4 there is a linear dependence on hydrogen ion (no correction applied for variable oxygen

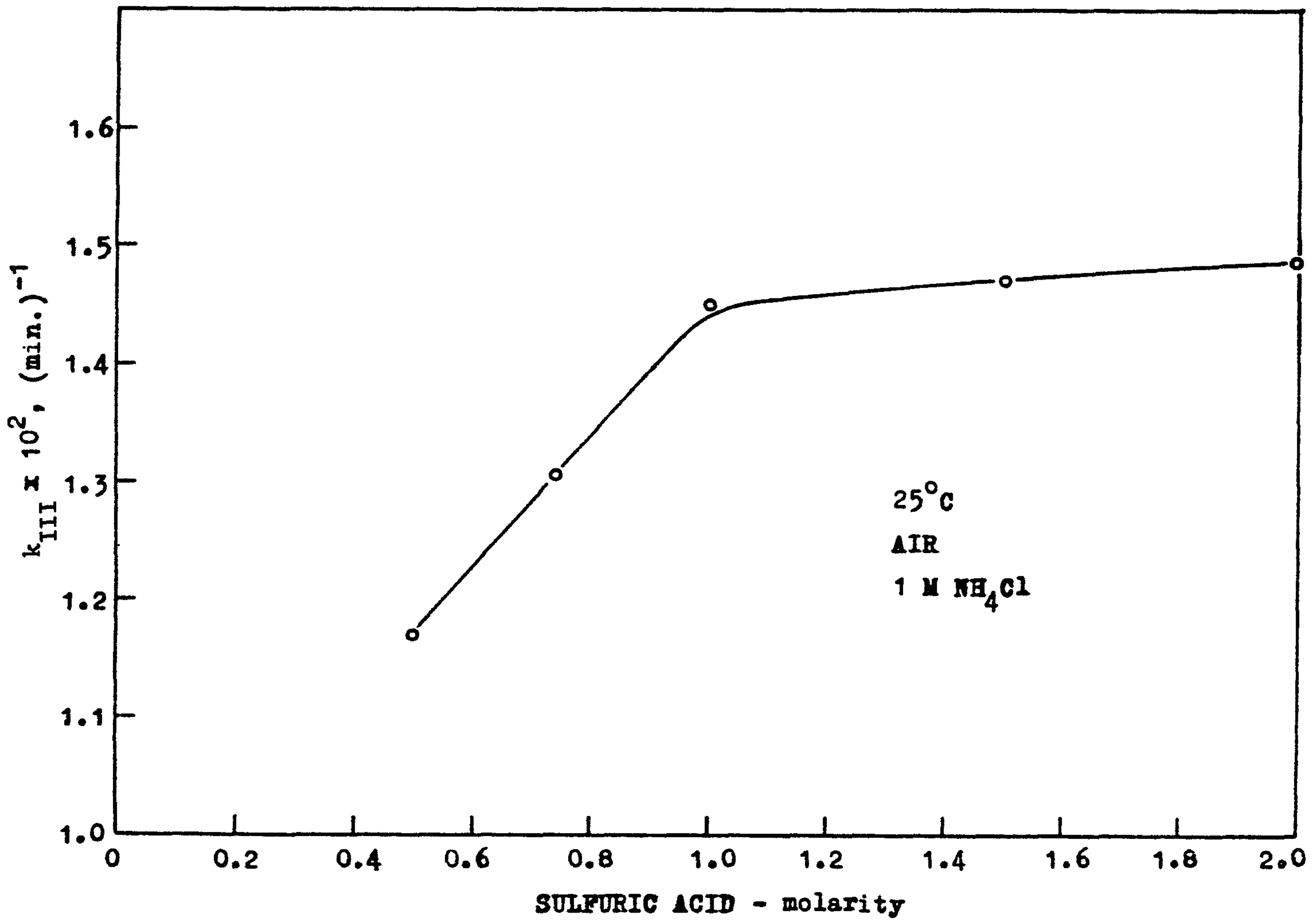

FIGURE 27 EFFECT OF SULFURIC ACID

solubility). Above 1 M H_2SO_4 the rates are essentially constant. A possible explanation for this behavior is that the sulfuric acid provides hydrogen ions, and the ammonium chloride provides chloride ions for $SnCl_2$ to form the complexes $HSnCl_3$ and H_2SnCl_4, in addition to NH_4SnCl_3. Initially, when the proportion of the $HSnCl_3$, H_2SnCl_4 complexes can increase with respect to the NH_4SnCl_3 with increasing hydrogen ion concentration, there should be a corresponding increase in oxidation rate. Since chloride ion concentration is constant, there must be a limit to the amount of the more reactive complex species that can form. As a result the rate should be essentially constant.

7. Surface Area Effect

The surface area inside the reaction flask was increased by the addition of inert teflon strips. There was no change in oxidation rate when the surface area was increased by a factor of three. This suggests that the data obtained in this research are applicable to the homogeneous oxidation of stannous chloride solution.

D. Oxidation Summary

Oxidation may be summarized by the relationship:

$$-\frac{d}{dt}\left[Sn^{++}\right] = k\left[Sn^{++}\right]\left[P_{O_2}\right]\left[HCl\right]^n \, e^{-\frac{10450}{RT}}$$

where n = 1.0 for acid concentrations between 0.25-0.75 M

n = 1.5 for acid concentrations between 0.75-2.0 M.

The magnitude of k has been evaluated from the integrated form of the rate equation

$$k = \ln \frac{[Sn^{++}]_{t_1}}{[Sn^{++}]_{t_2}} \frac{e^{\frac{10450}{RT}}}{[P_{O_2}][HCl]^n}$$

Tables 8A and 8B show that the value of k is essentially independent of all variables giving a mean value of 3.03×10^6 for the low acid range (0.25-0.75 M) and 4.27×10^6 for higher acid concentration range (0.75-2.0 M) with an average deviation of ± 7%.

TABLE 8A

Evaluation of rate Constant
(homogeneous oxidation)

$-\frac{d}{dt} \ln [Sn^{++}]$	T	P_{O_2}	[HCl]	k
3.45×10^{-3}	25°C	0.21	0.25	2.9×10^6
6.90			0.50	2.89
11.80			0.74	3.3

mean value of k = 3.03×10^6

TABLE 8B

Evaluation of rate Constant
(homogeneous oxidation)

$-\frac{d}{dt}\ln[Sn^{++}]$	T	P_{O_2}	[HCl]	k
1.18×10^{-2}	25°C	0.21	0.74	3.30×10^{6}
1.98			1.00	4.15
3.59			1.50	4.07
4.27			1.67	4.15
6.80			2.2	4.35
0.486	0	0.21	1.00	4.58
1.08	15			3.92
1.63	20			4.37
1.98	25			4.15
2.55	27			4.38
3.73	35			4.30
5.38	40			4.50
3.13	25	0.33	1.00	4.15
5.60		0.55		4.48
6.20		0.60		4.55
4.10		0.40		4.50

mean value of $k = 4.27 \times 10^{6}$

III Mechanism of Tin Dissolution

Table 9 provides a comparison between the heterogeneous and homogeneous reactions.

TABLE 9

Comparison of Heterogeneous Disssolution
and
Homogeneous Oxidation

	Heterogeneous Reaction	Homogeneous Reaction
Activation Energy	2.5 Kcal (1st Stage) 4.7 Kcal (2nd Stage)	10.5 Kcal
HCl Dependence	Independent	1st power between 0.25-0.75M 3/2th power between 0.75-2.00M
Oxygen Dependence	1/2 power	1st power
NH_4Cl	inhibits the reaction	accelerates the reaction
Under Nitrogen	zero-order reaction with respect to tin concentration	no reaction

On the basis of the above behaviour it is reasonable to conclude that the homogeneous reaction cannot be a controlling step in the heterogeneous dissolution process.

The established experimental facts may be discussed in terms of the following mechanism:

1. Hydrogen ions are adsorbed[8,78] on active sites on the surface of the metal with evolution of hydrogen gas and formation of stannous ions according to a series of steps similar to

$$Sn^{o} + H^{+} \rightleftharpoons SnH_{s}^{+}$$

$$2(SnH^{+})_{s} \xrightarrow{\text{very slow}} (Sn^{++})_{i} + (Sn\text{-}H_{2})_{s}$$

where SnH_{s}^{+} represents a transitory surface state, and $(Sn\text{-}H_{2})_{s}$ represents hydrogen gas attached to the metal surface. The discharge of hydrogen gas from the surface need not occur at the point of formation.

Adsorption of hydrogen ions is suggested by the fact that in many cases the dependence of dissolution rate on hydrogen ion concentration conforms to a Langmuir adsorption isotherm.

2. The stannous species, stannic species equilibrium[7]

$$Sn^{o} + (Sn^{++++})_{i} \overset{\text{fast}}{\rightleftharpoons} 2(Sn^{++})_{i}$$

is assumed to be established at all times at the metal-solution interface. As a result

$$\left[Sn^{++}\right]_{i} = K_{1}'' (Sn^{++++})_{i}^{1/2}$$

Bakier and Basinski[7] studying the equilibrium found that metallic tin dissolved in a solution of acidic stannic chloride or aqueous stannic chloride containing ammonium chloride quite readily in the absence of oxygen. The above mechanism has been tested in our laboratory by corroding the metal in hydrochloric acid solutions under nitrogen. Stannous ions which cannot be detected under air-saturation are found in large amounts in the air-free solutions. This behavior indicates that metallic tin dissolves in the form of Sn^{++} ion. The Sn^{++++} species found in air-free solution, are produced according to the above equilibrium, with the simultaneous formation of a redeposited tin film.

3. Stannous species are oxidized to stannic species[1] by dissolved oxygen at the metal-solution interface with the formation of peroxide intermediate according to

$$(SnH^+)_s + (Sn^{++})_i + O_i \xrightarrow[\text{slow}]{k_2''} (SnOH^-)_s + (Sn^{++++})_i$$

$$SnOH^-{}_s + O_i \xrightarrow[\text{fast}]{k_3''} Sn^o_s + (HO_2^-)_i$$

$$(HO_2^-)_i + H^+ \overset{\text{fast}}{\rightleftharpoons} (H_2O_2)_i$$

The formation of O_i is accomplished through adsorption and dissociation of oxygen molecules at the metal surface according to

$$2Sn^o + (O_2)_i \rightleftharpoons 2(SnO)_s \rightleftharpoons 2Sn + 2O_i$$

As a result

$$[O_i] = K' [O_2]_i^{1/2}$$

The fraction of the metal surface in the SnO_s state must be negligibly small because even with pure oxygen only questionable traces of any oxide structure were detected in the surface film by X-ray diffraction analysis.

By assuming that the Sn^{++++} ions diffuse into the bulk of the solution from a region of higher concentration at the metal-solution interface, it is possible to approximate the relationship between the two concentrations by writing

$$[Sn^{++++}]_i = k' [Sn^{++++}]_b$$

where k' could be a complex function of rpm. that essentially is independent of concentration.

$[Sn^{++++}]_i$ is the concentration of stannic species in the metal solution interface and $[Sn^{++++}]_b$ is the concentration in the bulk of the solution.

The formation of stannic species by oxygen oxidation is then given by

$$\frac{d}{dt}[Sn^{++++}]_i = k'' [Sn^{++}{}_i][O_i][SnH_s^+]$$

$$\frac{d}{dt}[Sn^{++++}]_i = k''' [Sn^{++++}]_i^{1/2} [O]_i$$

if the fraction of the surface covered with adsorbed hydrogen ion remains essentially constant. As a result,

$$\frac{d}{dt}[Sn^{++++}]_b = k_{O_2} [Sn^{++++}]_b^{1/2} [O_2]^{1/2}$$

where k_{O_2} represent the rate constant determining corrosion rate by oxygen.

4. Stannous species could also be oxidized by the peroxide intermediates[69] according to

$$(SnH^+)_s + (Sn^{++})_i + (H_2O_2)_i \xrightarrow[slow]{k_4''} (Sn^{++++})_i + (SnOH^-)_s + H_2O$$

The step is assumed on the basis of the elimination of stage 2 by the addition of hydrogen peroxide. The formation of stannic species by peroxide oxidation is given by

$$\frac{d}{dt}\left[Sn^{++++}\right]_i = k'\left[Sn^{++}\right]_i \left[H_2O_2\right]$$

or

$$\frac{d}{dt}\left[Sn^{++++}\right]_b = k_{H_2O_2}\left[Sn^{++++}\right]_b^{1/2} \left[H_2O_2\right]$$

where $k_{H_2O_2}$ represents the rate constant determining corrosion rate by hydrogen peroxide.

Since the above half-order rates occur simultaneously, it would appear that a simple linear relationship should be obtained from a plot of $(Sn^{++++})^{1/2}$ vs time. However, the transition from stage 1 to stage 2 suggests some additional process that removes hydrogen peroxide from the solution.

5. The formation and decomposition of all intermediates[56] occurring at the interface during the course of dissolution can be summed up by the following equations:

$$Sn^{++++} + 2HO_2^- \xrightarrow[\text{fast}]{k_5''} Sn^{++} + 2HO_2$$

$$HO_2 + H_2O_2 \xrightarrow[\text{fast}]{k_6''} OH^- + OH + O_2 + H^+$$

$$2OH + Sn^{o} \xrightarrow[\text{fast}]{k_7''} Sn^{++} + 2OH^-$$

Experiments in our laboratory have show that stannic ions accelerate the decomposition of hydrogen peroxide.

It would appear that as dissolution progresses metallic tin will be plated back and the intermediate peroxide will be decomposed at higher stannic concentration. This mechanism is suggested by the detection of hydrogen peroxide during the initial stage of corrosion

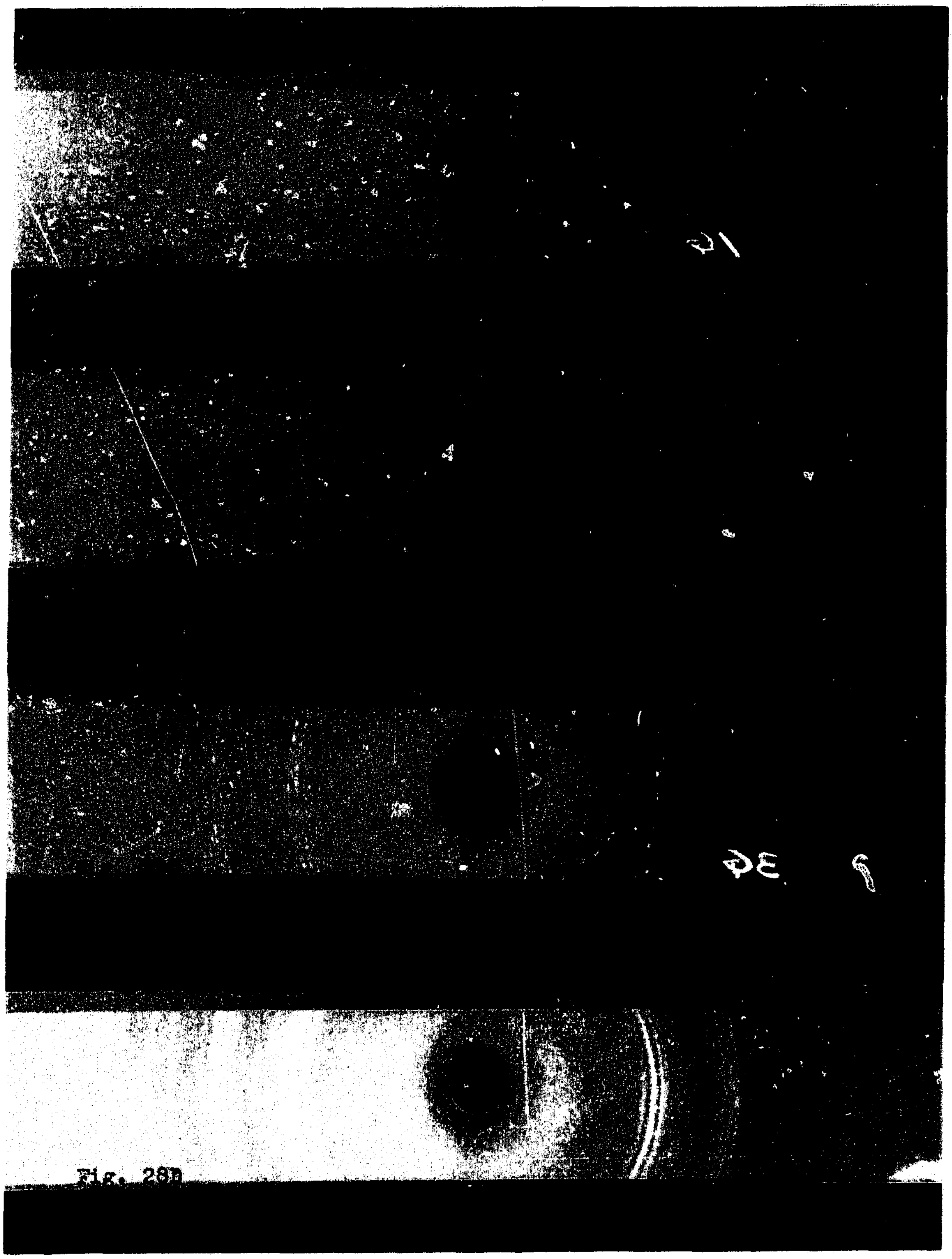

FIGURE 28 X-RAY DIFFRACTION ANALYSIS OF SURFACE FILM. FORMATION UNDER (A) 1 N HCl, O_2, (B) 2 N HCl, AIR, (C) 4 M NH_4Cl + 1 N HCl, AIR, (D) $SnCl_4$ + 1 N HCl, AIR.

but not during the second stage. An X-ray diffraction analysis of the surface film showed redeposited β-tin according to Figure 28. Although traces of SnO-SnO_2 may be present in the surface film when samples are corroded under pure oxygen as shown in Figure 28A, the predominant material however, is β-tin. The effect of Sn^{++++} on H_2O_2 is consistent with the theory proposed by various investigators [27,56,83,85,86] for the decomposition of hydrogen peroxide by metal ions.

It seems reasonable to conclude that the hydrogen peroxide concentration will increase initially, but decomposition will become more rapid with increasing stannic concentrations. Essentially, the dissolution rate before the transition from stage 1 to stage 2 is the resultant of an oxygen effect and a peroxide effect. When the stannic concentrations are high enough, the peroxide effect is insignificant and the dissolution rate is determined solely by the role of oxygen.

An explanation for the square root dependence on sample area cannot be given in terms of measurements of bulk corroding solution properties, however, the same dependence on area has been observed for samples corroding under nitrogen. Figure 29 shows the zero-order dissolution rate to be a linear function of the square root of sample area.

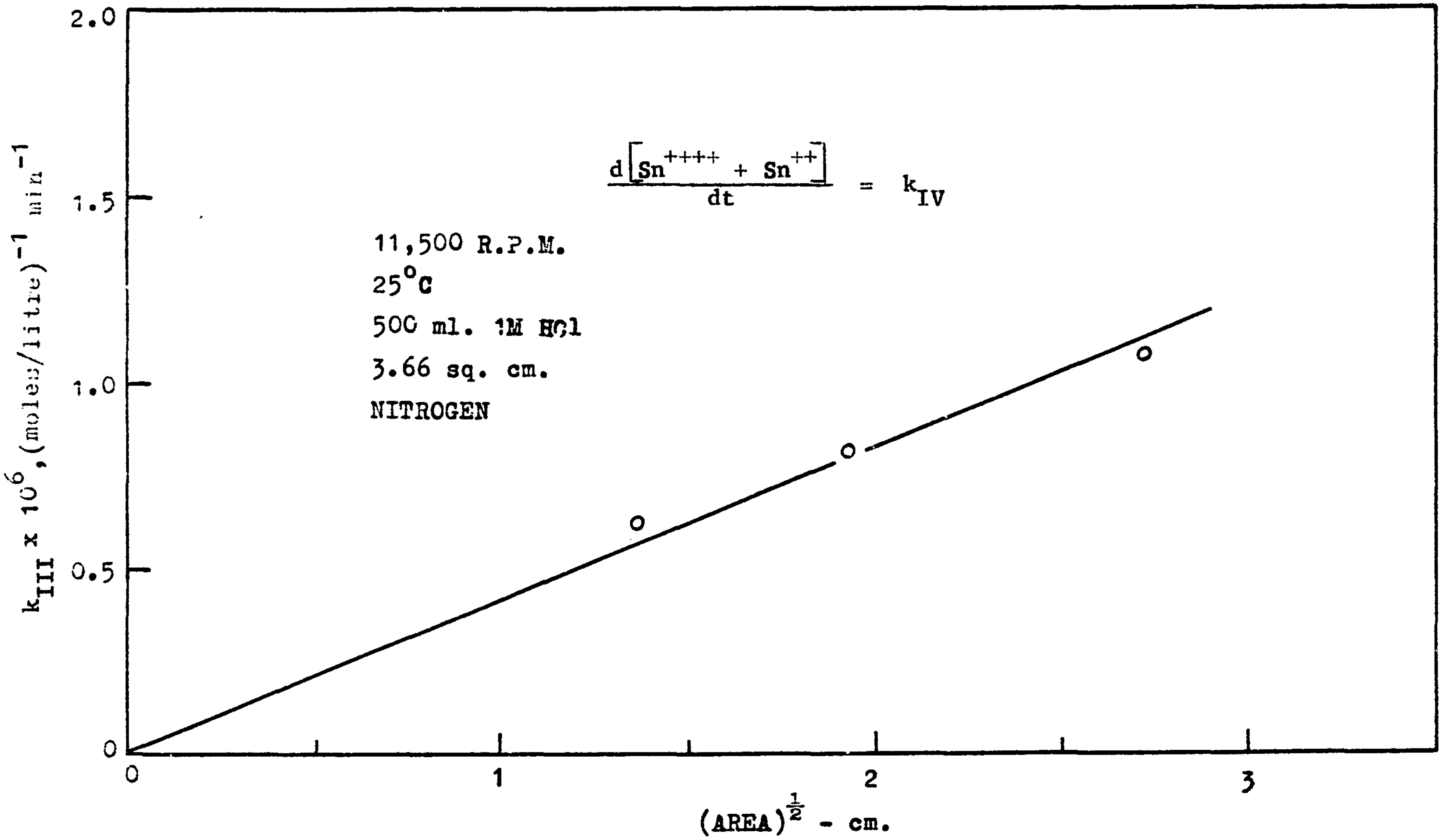

FIGURE 29 DISSOLUTION AS FUNCTION OF AREA

IV. Empirical Equation for Tin Dissolution

The dissolution rate of tin at high stannic concentration, when there is negligible effect due to hydrogen peroxide produced, may be summarized by the relationship:

$$\frac{d}{dt}\left[Sn^{++++}\right] = k_{O_2}\left[Sn^{++++}\right]^{1/2}\left[P_{O_2}\right]^{1/2}\frac{A^{1/2}}{V}(rpm)^{0.92}\, e^{-\frac{4700}{RT}}$$

for the conditions $\left[Sn^{++++}\right] > 2.0 \text{ X } 10^{-4}$ mol/l.

$T = 293 - 318^{\circ}K$

$A = 0.91 - 7.32$ sq. cm.

$V = 400 - 500$ ml.

$P_{O_2} = 0 - 1.0$ atm.

rpm. 11,000

Experimental evidence showed that this equation is independent of surface condition of the sample. The integrated form of the equation

$$k_{O_2} = \frac{2\left[Sn^{++++}\right]^{1/2}}{t}\ \frac{V}{A^{1/2}}\ \frac{1}{(P_{O_2})^{1/2}}\ \frac{1}{(rpm.)^{0.92}}\ e^{\frac{4700}{RT}}$$

has been used for the determination of k_{O_2} to give a mean value of $9.16 \text{ X } 10^{-2}$ with an average deviation of ± 5% as shown in Table 10.

TABLE 10

Evaluation of Velocity Constant (2nd Stage Oxygen Dissolution)

$\frac{d}{dt}\left[Sn^{++++}\right]^{1/2}$ $(mol/l.)^{1/2}min.^{-1}$	rpm	T °C	A sq cm	V ml	P_{O_2} atm	k_{O_2}
1.48×10^{-4}	11,000	25	3.66	500	0.21	8.85×10^{-2}
1.85		35				8.75
2.10		40				8.75
2.50		45				9.30
1.70	13,500	25	3.66	500	0.21	8.75
1.86		30				8.60
2.16		35				8.85
2.50		40				9.00
2.85		45				9.12
2.06	15,500	25	3.66	500	0.21	8.75
2.42		30				9.30
2.66		35				9.12
2.88		40				8.60
3.10		45				8.40
2.50	11,000	30	3.66	500	0.50	8.75
3.61					1.00	8.85
1.79					0.21	9.62
0.89	11,000	30	0.91	500	0.21	9.65
1.25			1.83			9.50
1.79			3.66			9.62
2.22			5.49			9.75
2.50			7.32			9.54
0.83			0.91	550		9.60
2.06			5.49			9.95
1.55			1.83	400		9.45
2.10			3.66			9.02
2.20			7.32	600		10.00

mean value of k = 9.16×10^{-2}

The empirical rate equation for the dissolution of tin becomes,

$$\frac{d}{dt}\left[Sn^{++++}\right] = 9.16 \text{ X } 10^{-2} \left[Sn^{++++}\right]^{1/2} \frac{A^{1/2}}{V} (P_{O_2})^{1/2} (rpm.)^{0.92} e^{-\frac{4700}{RT}}$$

CHAPTER IV

CONCLUSIONS

There seems little doubt that no similarity exists between the mechanism describing the homogeneous oxidation of stannous tin and that describing the heterogeneous dissolution of the metal.

Corrosion rates are independent of hydrochloric acid concentration while the oxidation rates depend on the 3/2 power of acid concentration over the range 0.75-2.0 M HCl. Additions of ammonium chloride increase the homogeneous oxidation rate but inhibit the dissolution process slightly. The linear dependence of oxidation rate on oxygen pressure suggests reaction by molecular oxygen whereas dependence of the corrosion rate on the square root of oxygen pressure is indicative of a surface reaction involving dissociation of oxygen molecules. The low activation energy of 4.7 Kcal/gm mol for the heterogeneous process infers diffusional control. Further support for physical control is provided by the dependence on rotational speed.

For dissolution periods up to 4 hours and oxygenated hydrochloric acid solution (0.15-4.0 N) the dissolution rate is half-order with respect to dissolved tin in solution, zero-order in acid concentration, half-order with respect to surface area and partial pressure of oxygen and is inversely proportional to the volume of corroding solution.

The change in rate of the half-order reaction is due to the formation and decomposition of an intermediate peroxide. For corrosion periods less than 40 minutes, the dissolution rate is equal to the sum of the oxygen-dissolution and peroxide-dissolution rates.

The most reasonable controlling step in the dissolution of tin is the diffusion of stannic ions from the interface to the bulk of the solution.

A film formation was noted and was shown to be deposited β-tin.

Copper[25,48,49], titanium[88] and tin all show evidence of autocatalytic dissolution in aerated solutions. On the basis of the information now available and it is possible to generalize that autocatalytic rates should be expected with all metals capable of existing in two or more oxidation states in aqueous solution by virtue of an equilibrium of the type

$$M^{o} + xM^{a+} \rightleftharpoons y\,M^{b+}$$

where $a > b$, and $xa = yb$

established at the metal-solution interface.

APPENDIX I

Polarographic Determination of Tin Concentrations

A Sargent model XV polarograph was employed for the analysis of tin solutions. The general theory and procedures have been reviewed by Lingane.[53,54,55]

Analar Grade tin bar was dissolved in 1 M HCl to make up a stock 2 X 10^{-3} M stannic chloride solution. Standard stannic solutions were prepared by diluting aliquot samples of the stock solution with 1M HCl. The dropping mercury electrode calibration curve (Figure 30) was made for a supporting electrolyte of 1 M HCl and 4 M NH_4Cl containing 0.5% gelatin as maximum suppressor.

The polarographic cell containing the sample solution and the reference Calomel cell were immersed in a constant temperature bath at 25°C. Before each polarographic reading the sample solution was flushed with nitrogen for approximately 10 minutes.[81] For high tin concentrations, solutions were diluted and a corresponding amount of gelatin and NH_4Cl were added.

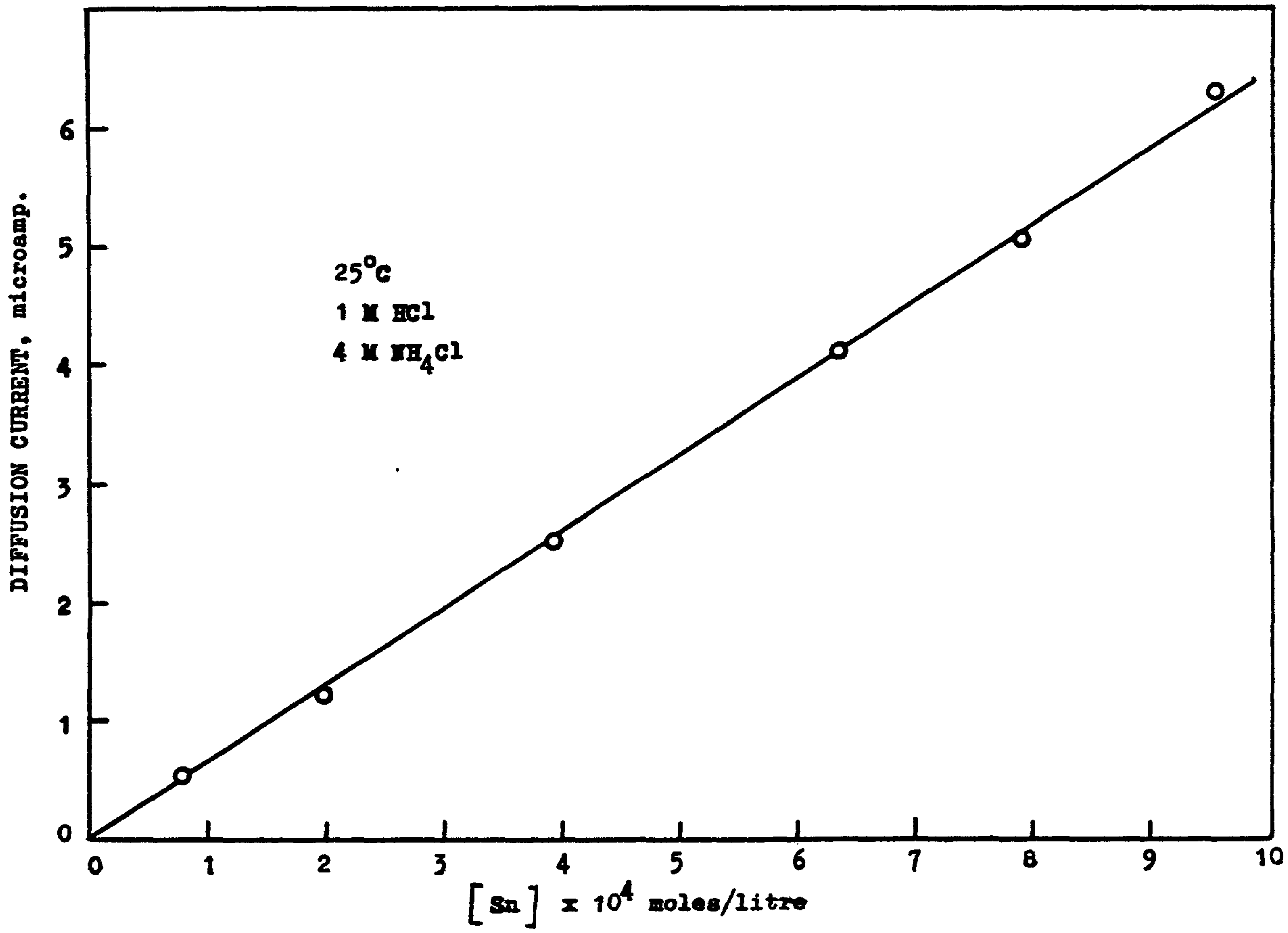

FIGURE 30 CALIBRATION CURVE

APPENDIX II

Detection of H_2O_2 by Schales Reagent

The Schales reagent[93] used for the detection of hydrogen peroxide was prepared by boiling 2 gms of phenolphthalein, 20 gms of sodium hydroxide, and 10 gms of zinc dust in 100 ml. of redistilled water for 2 hours. The resulting solution had a clear straw color. After cooling, it was filtered through glass wool and stored in the dark over zinc granules in a well stoppered container.

The detection of hydrogen peroxide was accomplished by adding 10 drops of the reagent followed by 10 drops of 10^{-2} M copper sulfate to 10 ml. of corrosion solution. A faint pink tinge indicated the presence of hydrogen peroxide. With this reagent, it is possible to detect hydrogen peroxide at levels as low as 10^{-6} M.

APPENDIX III

Polarographic Determination of Hydrogen Peroxide

The polarographic determination of hydrogen peroxide has been reviewed by Giguere and Jaillet[22], Kolthoff and Miller[46] and Pellequer.[68] The dropping mercury electrode calibration curve was prepared for a supporting electrolyte consisting of 0.1 M HCl and 1 M sodium acetate. Standard hydrogen peroxide solutions were prepared from a stock solution previously standardized with potassium permanganate.

The cathodic reactions involve the reduction of O_2 to H_2O_2 at a half-wave potential of -0.1 v vs S.C.E. and H_2O_2 to H_2O at -0.9 v. It is necessary to substract the oxygen concentration of hydrogen peroxide measured by the second wave.

APPENDIX IV

Colorimetric Determination of Stannous Chloride Concentrations

A Bausch and Lomb Spectronic 20 colorimeter was used for the determination of stannous chloride concentrations. The general theory and procedures for various systems have been reviewed by Snell and Snell.[75]

Stannous chloride is oxidized by potassium permanganate in acidic media according to

$$5SnCl_2 + 2KMnO_4 + 12HCl \longrightarrow 5SnCl_4 + 2MnO + 2KCl + 6H_2O$$

Changes in permanganate color provided an indication of the amount of permanganate reduced or stannous chloride oxidized.

Solutions of permanganate were standardized with sodium oxalate ($Na_2C_2O_4$). The calibration curve was made at a wave length of 525 mμ with a blank of distilled water. Samples of the solution from the reaction vessel were mixed thoroughly with the appropriate standardized $KMnO_4$ solution before a colorimetric reading was taken.

APPENDIX V

TIN DISSOLUTION

Variation of Rotational Speed and Temperature

1,000 rpm.
500 ml 1M HCl
3.66 sq. cm.
air

Run 1 - 25°C.		Run 2 - 35°C.		Run 3 - 15°C.	
Time (min.)	$[Sn^{++++}]$ mol/1.	Time (min.)	$[Sn^{++++}]$ mol/1.	Time (min.)	$[Sn^{++++}]$ mol/1.
0		0		0	
20	0.35 X 10^{-4}	15	0.2 X 10^{-4}	20	0.30 X 10^{-4}
40	0.65	30	0.5	40	0.75
60	1.05	45	0.75	60	1.05
80	1.45	60	0.95	90	1.60
100	1.65	80	1.25	120	2.07
120	2.10	100	1.50	150	2.75
140	2.30	120	1.85	180	3.20
160	2.80	140	2.20		
180	3.20	160	2.60		
200	3.55	180	2.95		

Variation of Rotational Speed and Temperature

3,000 rpm.
500 ml. 1M HCl
3.66 sq. cm.
air

Run 4 - 25°C.

Time (min.)	$[Sn^{++++}]$ mol/l.
10	0.1×10^{-4}
30	
55	0.65
70	0.90
90	1.20
110	1.60
130	2.00

Run 5 - 35°C.

Time (min.)	$[Sn^{++++}]$ mol/l.
15	0.35×10^{-4}
30	0.75
50	1.30
70	1.75
95	2.30
120	2.95

Run 6 - 45°C.

Time (min.)	$[Sn^{++++}]$ mol/l.
20	0.5×10^{-4}
42	1.20
60	1.60
80	2.40
100	3.00
120	3.55
140	4.40

Run 7 - 40°C.

Time (min.)	$[Sn^{++++}]$ mol/l.
15	0.35×10^{-4}
30	0.65
50	1.15
70	1.65
90	2.10
110	2.65
130	3.15

Run 8 - 30°C.

15	0.25×10^{-4}
30	0.75
50	1.20
70	1.70
90	2.10
110	2.70
130	3.20
150	3.85

Run 9 - 20°C.

20	0.45×10^{-4}
40	1.00
60	1.40
80	1.90
100	2.35
120	2.85
140	3.35
160	3.85

Variation of Rotational Speed and Temperature

5,000 rpm.
500 ml. 1M HCl
3.66 sq. cm.
Air

Run 10 - 20°C.

Time (min.)	$[Sn^{++++}]$ mol./l.
20	0.50×10^{-4}
40	1.05
60	1.60
80	2.25
100	2.60
120	3.80
140	4.30
160	4.90

Run 11 - 25°C.

Time (min.)	$[Sn^{++++}]$ mol./l.
20	0.50×10^{-4}
40	0.80
60	1.30
80	1.75
100	2.40
120	3.05
140	3.70

Run 12 - 30°C.

Time (min.)	$[Sn^{++++}]$ mol./l.
20	0.30×10^{-4}
40	1.25
60	1.85
80	2.60
100	3.35
120	4.10
140	4.85

Run 13 - 35°C.

Time (min.)	$[Sn^{++++}]$ mol./l.
20	0.75×10^{-4}
40	1.60
60	2.30
80	3.40
100	4.30
120	5.30
140	6.10

Run 14 - 40°C.

20	0.75×10^{-4}
40	1.60
60	2.50
80	3.30
100	4.10
120	5.25
140	6.25

Run 15 - 45°C.

20	0.75×10^{-4}
40	2.10
60	3.05
80	4.00
100	5.30
120	6.50
140	8.10

Variation of Rotational Speed and Temperature

7,500 rpm.
500 ml. 1M HCl
3.66 sq. cm.
Air

Run 16 - 40°C.		Run 17 - 35°C.		Run 18 - 25°C.		Run 19 - 20°C.	
Time (min.)	$[Sn^{++++}]$ mol./l.	Time (min.)	$[Sn^{++++}]$ mol./l.	Time (min.)	$[Sn^{++++}]$ mol./l.	Time (min.)	$[Sn^{++++}]$ mol./l.
20	0.80×10^{-4}	20	1.20×10^{-4}	20	0.90×10^{-4}	20	0.80×10^{-4}
40	1.60	40	2.50	40	1.80	40	1.70
60	2.45	60	3.80	60	2.65	60	2.25
80	3.65	80	5.05	80	3.60	80	3.65
100	4.95	100	6.40	100	4.65	100	4.70
120	7.10	120	7.85	120	5.55	120	5.60
140	8.60	140	9.20	140	6.75	140	6.60

Variation of Rotational Speed and Temperature

11,000 rpm.
500 ml. 1M HCl
3.66 sq. cm.
Air

Run 20 - 25°C.

Time (min.)	$[Sn^{++++}]$ mol./l.
15	0.75×10^{-4}
30	1.50
45	2.50
60	3.55
75	4.45
90	5.60
105	6.75
120	8.05

Run 21 - 35°C.

Time (min.)	$[Sn^{++++}]$ mol./l.
15	0.75×10^{-4}
30	1.95
45	2.70
60	3.75
75	4.95
90	6.20
105	7.55
120	9.25

Run 22 - 45°C.

Time (min.)	$[Sn^{++++}]$ mol./l.
15	1.35×10^{-4}
30	3.00
45	4.75
60	6.70
75	8.70
90	11.00
105	14.00

Run 23 - 30°C.

Time (min.)	$[Sn^{++++}]$ mol./l.
15	0.90×10^{-4}
30	1.85
45	2.70
60	4.20
75	5.40
90	6.55
105	7.95

Run 24 - 40°C.

15	1.10×10^{-4}
30	2.35
45	3.70
60	5.10
75	6.60
90	8.10
105	9.80

Variation of Rotational Speed and Temperature

13,500 rpm.
500 ml. 1M HCl
3.66 sq. cm.
Air

Run 25 - 25°C.		Run 26 - 35°C.		Run 27 - 45°C.		Run 28 - 30°C.	
Time (min.)	$[Sn^{++++}]$ mol/l.	Time (min.)	$[Sn^{++++}]$ mol/l.	Time (min.)	$[Sn^{++++}]$ mol/l.	Time (min.)	$[Sn^{++++}]$ mol/l.
15	1.25×10^{-4}	15	1.30×10^{-4}	15	1.60×10^{-4}	20	1.40×10^{-4}
30	2.60	30	2.85	30	3.00	30	2.15
45	4.10	45	4.50	45	4.75	45	3.40
60	5.60	60	6.30	60	6.70	60	4.70
75	7.10	75	7.85	75	8.70	75	6.05
90	8.75	90	9.90			90	7.30
105	10.30	105	11.50			105	8.60

Variation of Rotational Speed and Temperature

15,500 rpm.
500 ml. 1M HCl
3.66 sq. cm.
Air

Run 29 - 25°C.

Time (min.)	$[Sn^{++++}]$ mol/1.
15	1.30×10^{-4}
30	2.70
45	4.25
60	5.70
75	7.15
90	8.85
100	9.90

Run 30 - 35°C.

Time (min.)	$[Sn^{++++}]$ mol/1.
15	1.35×10^{-4}
30	2.95
45	4.75
60	6.60
75	8.80
90	11.20

Run 31 - 30°C.

Time (min.)	$[Sn^{++++}]$ mol/1.
15	1.85×10^{-4}
30	2.80
45	4.45
60	6.35
75	8.10
90	10.20
105	12.20

Run 32 - 45°C.

Time (min.)	$[Sn^{++++}]$ mol/1.
15	1.75×10^{-4}
30	3.65
45	5.95
60	8.50
75	11.10
90	13.50

Run 33 - 40°C.

15	1.35×10^{-4}
30	2.85
45	4.55
60	6.70
75	8.75
90	11.80

Variation of Rotational Speed and Temperature

11,400 rpm.
500 ml. 1M HCl
3.66 sq.cm.
Air

Run 34 - 5°C.

Time (min.)	$[Sn^{++++}]$ mol/1.
15	0.65 X 10^{-4}
30	1.35
45	2.15
60	2.90
75	3.80
90	4.75
105	5.70
120	6.85
135	7.90
150	8.75

Run 35 - 20°C.

Time (min.)	$[Sn^{++++}]$ mol/1.
10	0.55 X 10^{-4}
15	0.75
20	1.05
25	1.30
30	1.65
35	2.00
40	2.50
45	2.85
50	3.30
55	3.70
60	4.00
65	4.40
70	4.80

Run 36 - 25°C.

Time (min.)	$[Sn^{++++}]$ mol/1.
15	0.50 X 10^{-4}
30	1.70
45	2.85
60	4.50
75	6.00
90	7.65
105	9.40
120	10.80
135	12.20
150	15.20
165	16.60
180	17.70

Run 37 - 25°C.

Time (min.)	$[Sn^{++++}]$ mol/1.
10	0.45 X 10^{-4}
15	0.70
20	1.00
25	1.30
30	1.60
35	2.00
40	2.40
45	2.70
50	3.10
55	3.50
60	3.90
65	4.30
70	4.55

Run 38 - 24°C.

Time (min.)	$[Sn^{++++}]$ mol/1.
15	1.35 X 10^{-4}
30	2.85
45	4.00
60	5.50
75	6.65
90	7.95
105	9.40
120	10.20
135	11.70
150	13.40
165	15.30
180	16.60
195	19.40

Run 39 - 25°C.

Time (min.)	$[Sn^{++++}]$ mol/1.
10	0.8 X 10^{-4}
20	1.4
30	2.1
40	2.9
50	4.1
60	4.7
70	5.6
89	6.6
90	8.0
100	9.0
110	10.1
120	11.0

Run 40 - 25°C.

Time (min.)	$[Sn^{++++}]$ mol/1.
15	0.95 X 10^{-4}
30	2.45
45	3.90
60	5.25
75	6.65
90	8.10
105	9.80
120	11.50
135	13.50
150	14.50

Run 41 - 30°C.

Time (min.)	$[Sn^{++++}]$ mol/1.
10	0.65 X 10^{-4}
15	0.95
25	1.95
30	2.20
35	2.70
40	3.15
45	3.54
50	4.00
55	4.45
60	4.90
65	5.40
70	5.90

Variation of Rotational Speed and Temperature

11,400 rpm.
500 ml 1M HCl
3.66 sq. cm.
Air

Run 42 - 35°C.

Time (min.)	$[\text{Sn}^{++++}]$ mol/1.
10	0.65 X 10^{-4}
15	1.00
20	1.50
25	1.85
30	2.40
35	2.95
40	2.30
45	3.70
50	4.25
55	4.90
60	5.35
65	5.80
70	6.60

Run 43 - 40°C.

Time (min.)	$[\text{Sn}^{++++}]$ mol/1.
10	0.65 X 10^{-4}
15	1.00
20	1.35
25	1.80
30	2.30
35	2.70
40	3.30
45	3.80
50	4.30
55	4.80
60	5.30
65	5.70
70	6.25

Run 44 - 40°C.

Time (min.)	$[\text{Sn}^{++++}]$ mol/1.
10	0.85 X 10^{-4}
15	1.15
20	1.40
25	2.00
30	2.45
35	2.80
40	3.35
45	3.90
50	4.65
55	5.35
60	5.95
70	7.25

Run 45 - 40°C.

Time (min.)	$[\text{Sn}^{++++}]$ mol/1.
15	0.90 X 10^{-4}
30	2.00
45	3.30
60	5.10
75	6.80
90	8.6-
105	9.70
120	12.40
135	14.50
150	15.20
165	18.80

Run 46 - 45°C.

10	0.70 X 10^{-4}
15	1.10
20	1.60
25	2.10
30	2.50
35	3.05
40	3.55
45	4.15
50	4.65
55	5.35
60	6.10
65	6.60
70	7.35

Run 47 - 15°C.

10	0.50 X 10^{-4}
15	0.75
25	1.30
30	1.60
35	2.00
40	2.20
45	2.50
50	2.85
55	3.15
60	3.55
65	3.85
70	4.00

Run 48 - 10°C.

10	0.55 X 10^{-4}
15	0.80
20	1.00
25	1.30
30	1.65
35	1.85
40	2.25
45	2.75
50	3.15
60	4.00
65	4.15

Run 49 - 6°C.

10	0.60 X 10^{-4}
15	0.75
20	1.10
25	1.20
30	1.35
35	1.80
40	2.05
45	2.30
50	2.50
55	2.70
60	2.90
70	3.75

Variation of Rotational Speed and Temperature

11,400 rpm.
500 ml. 1M HCl
3.66 sq. cm.
Air

Run 50 - 50°C.

Time (min.)	$[Sn^{++++}]$ mol/1.
10	0.85×10^{-4}
15	1.25
20	1.70
25	2.30
30	2.75
35	3.30
40	4.05
45	4.40
50	5.15
55	5.90
60	6.50
70	8.15

Run 51 - 50°C.

Time (min.)	$[Sn^{++++}]$ mol/1.
15	1.30×10^{-4}
30	3.00
45	4.90
60	7.00
75	9.40
90	12.10
105	15.10
120	18.10

Effect of Surface Condition

11,500 rpm.
500 ml. 1M HCl
Air
25°C

Run 52 Surface Cleaned Every Hour		Run 53 Surface Cleaned Every 45 Min.		Run 54 Surface Cleaned Every 30 Min.		Run 55 Surface Cleaned Every 15 Min.	
Time (min.)	$[Sn^{++++}]$ mol./l.	Time (min)	$[Sn^{++++}]$ mol./l.	Time (min.)	$[Sn^{++++}]$ mol./l.	Time (min.)	$[Sn^{++++}]$ mol./l.
15		15	1.05 X 10^{-4}	15	0.8 X 10^{-4}	15	1.0 X 10^{-4}
25	1.45 X 10^{-4}	30	2.30	30	2.05	30	1.9
40	1.95	45	3.95	45	3.45	45	2.8
55	2.20	55	4.95	60	4.60	60	3.7
70	3.85	70	6.65	75	5.60	75	4.75
85	4.75	85	7.90	90	6.80	90	5.95
100	5.45	95	8.95	105	8.35	105	7.10
115	6.25	110	9.90	120	8.60	120	8.60
130	7.40	125	11.80	135	9.90	135	9.80
145	7.85	135	12.30	150	11.50	150	10.20
		150	14.20			165	11.60
		165	15.70			180	13.70
		175	17.90			195	14.60
		190	18.60			210	16.70

Effect of Surface Condition

11,500 rpm.
500 ml 1M HCl
25°C.
Air

Run 56		Run 57		Run 58		Run 59	
No Cleaning of Surf.		Initial Shiny Surf.		Initial Surf. Film		Initial Surf. Film	
Time (min.)	$[Sn^{++++}]$ mol/1.	Time (min.)	$[Sn^{++++}]$ mol/1.	Time (min.)	$[Sn^{++++}]$ mol/1.	Time (min)	$[Sn^{++++}]$ mol/1.
15	0.95 X 10^{-4}	15	0.5 X 10^{-4}	15	1.35 X 10^{-4}	15	0.9 X 10^{-4}
30	2.45	30	1.7	30	2.85	30	2.1
45	3.90	45	2.85	45	4.00	45	3.6
60	5.25	60	4.50	60	5.50	60	4.8
75	6.65	75	6.00	75	6.65	75	6.5
90	8.10	90	7.65	90	7.95	90	7.8
105	9.80	105	9.40	105	9.40	105	9.6
120	11.50	120	10.80	120	10.20	120	10.9
135	13.50	135	12.20	135	11.70	135	12.5
150	14.50	150	15.20	150	13.40	150	15.7
		165	16.60	165	15.30	165	16.3
		180	17.70	180	16.60		
				195	19.40		

Effect of Surface Condition

11,500 rpm.
500 ml 2M HCl
$25^{\circ}C$.
Air

Run 60
Initial Surf. Film

Time (min)	$[Sn^{++++}]$ mol/l.
15	1.0×10^{-4}
30	2.1
45	3.1
60	4.6
75	6.0
90	7.4
105	9.0
120	10.6
135	13.7
150	14.4
165	16.9

Effect of Surface Condition

11,400 rpm.
500 ml. 1M HCl
3.66 sq. cm.
25°C.
Air

5 samples in series, change every 30 minutes

Run 61
All new samples

Time (min.)	$[Sn^{++++}]$ mol/1.
15	0.7 X 10^{-4}
30	1.5
40	2.2
50	2.8
60	3.5
70	4.0
80	4.6
90	5.3
110	6.3
120	7.4
130	7.6
140	8.6
150	9.5

Run 62
Re-run samples of Run 61

Time (min.)	$[Sn^{++++}]$ mol/1.
15	1.0 X 10^{-4}
30	2.0
40	2.8
50	3.7
60	4.6
70	5.4
80	6.4
90	7.3
100	8.5
110	9.1
120	9.9
130	10.8
140	12.1
150	12.9

Run 63
Re-run samples of Run 62

Time (min.)	$[Sn^{++++}]$ mol/1.
0	0.90 X 10^{-4}
15	1.9
30	2.7
40	3.2
45	4.9
70	5.3
80	5.5
90	7.5
100	8.1
110	10.3
135	11.6
150	

Run 64
All new samples

Time (min.)	$[Sn^{++++}]$ mol/1.
0	
15	0.8 X 10^{-4}
30	1.6
40	2 4
50	2.9
60	3.7
70	4.4
80	5.0
90	5.9
100	6.4
110	7.4
120	8.1
135	9.2
150	10.4

Effect of Surface Condition

11,400 rpm.
500 ml. 1M HCl
25°C.
Air

Run 65 - 7.32 cm^2.

Time (min.)	$[Sn^{++++}]$ mol/1.
15	1.35 X 10^{-4}
30	3.30
45	5.30
60	8.10
75	10.40
90	13.10
105	16.20

20 microninch A.A.

Run 66
Re-run sample of Run 65

Time (min.)	$[Sn^{++++}]$ mol/1.
15	2.50 X 10^{-4}
30	5.30
45	8.05
60	10.50
75	13.20
90	15.50
105	19.20

55-65 microninch A.A.

Run 67 - 5.49 cm^2

Time (min.)	$[Sn^{++++}]$ mol/1.
15	1.25 X 10^{-4}
30	2.50
45	3.90
60	5.50
75	7.15
90	9.05
105	10.90

20 microninch A.A.

Run 68
Re-run sample of Run 67

Time (min.)	$[Sn^{++++}]$ mol/1.
15	1.45 X 10^{-4}
30	2.95
45	4.55
60	6.30
75	8.10
90	10.00
105	11.50

55-65 microninch A.A.

Run 69 - 1.83 cm^2.

15	0.4 X 10^{-4}
30	0.90
45	1.45
60	1.95
75	2.45
90	3.00
105	3.60
120	4.35

20 microinch A.A.

Run 70
Re-run sample of Run 69

15	0.5 X 10^{-4}
30	1.10
45	1.60
60	2.30
75	3.00
90	3.55
105	4.35
120	5.05

55-60 microinch A.A.

Effect of Hydrogen Peroxide

11,400 rpm.
500 ml. 1M HCl
3.66 sq.cm.
25°C.
Air

Run 71
Addition of 1 ml.
1.2 X 10^{-1} M H_2O_2 at
end of 30 min. and
every 10 min. after

Time (min.)	$[Sn^{++++}]$ mol/l.
10	0.7 X 10^{-4}
20	1.4
30	2.2
40	3.0
50	4.3
60	5.4
70	6.8
80	8.8
90	10.0

Run 72
Addition of 1 ml.
1.2 X 10^{-1} M H_2O_2 at
end of 30 min. and
every 10 min. after

Time (min.)	$[Sn^{++++}]$ mol/l.
10	1.0 X 10^{-4}
20	1.4
30	2.1
40	3.2
50	4.1
60	5.4
70	6.1
80	8.3
90	9.6
100	11.0

Run 73
Addition of 1 ml.
1.2 X 10^{-1} M H_2O_2 every
10 min. from beginning

Time (min.)	$[Sn^{++++}]$ mol/l.
10	0.7 X 10^{-4}
20	1.5
30	2.6
40	3.9
50	5.4
60	6.9
70	7.7
80	10.1
90	12.1
100	13.8
110	15.5
120	17.3

Run 74
Addition of 5 ml.
.2 X 10^{-1} M H_2O_2 at
end of 30 min.

Time (min.)	$[Sn^{++++}]$ mol/l.
10	0.6 X 10^{-4}
20	1.3
30	2.2
40	3.7
50	4.9
60	6.2
70	7.7
80	9.0
90	10.4
100	11.6
110	13.2
120	15.1

Effect of Hydrogen Peroxide

11,400 rpm.
500 ml. 1M HCl
3.66 sq. cm.
25°C.
Air

Run 75
Addition of 1 ml.
1.2 X 10^{-1} M H_2O_2 at
end of every 30 min.

Time (min.)	$[Sn^{++++}]$ mol/1.
10	0.7 X 10^{-4}
20	1.5
30	1.9
40	2.5
50	3.6
60	4.5
70	5.6
89	6.7
90	7.6
100	8.8
110	10.0
120	11.1

Run 76
Addition of 1/2 ml.
1.2 X 10^{-1} M H_2O_2 at
end of 30 min.

Time (min.)	$[Sn^{++++}]$ mol/1.
10	0.5 X 10^{-4}
20	1.1
30	1.9
40	2.6
50	3.6
60	4.6
70	5.8
80	7.1
90	8.5
100	9.6

Effect of HCl Concentration

11,400 rpm.
500 ml. HCl
3.66 sq. cm.
25°C.
Air

Run 77 - 2.05M HCl		Run 78 - 2.03M HCl		Run 79 - 2.05M HCl		Run 80 - 0.499M HCl	
Time (min.)	$[Sn^{++++}]$ mol/l.	Time (min.)	$[Sn^{++++}]$ mol/l.	Time (min.)	$[Sn^{++++}]$ mol/l.	Time (min.)	$[Sn^{++++}]$ mol/l.
15	0.90×10^{-4}	10	0.60×10^{-4}	15	1.00×10^{-4}	10	0.70×10^{-4}
30	1.80	15	1.00	30	2.10	15	1.10
45	2.70	20	1.30	45	3.10	20	1.40
60	3.90	25	1.70	60	4.60	25	1.90
75	5.00	30	2.20	75	6.00	30	2.30
90	6.20	35	2.50	90	7.40	35	2.70
105	7.30	40	3.10	105	9.00	40	3.30
120	8.90	45	3.40	120	10.60	45	4.00
135	10.40	50	3.70	135	13.70	50	4.30
150	11.80	55	4.60	150	14.40	55	4.90
165	13.20	60	4.70	165	16.90	60	5.20
180	14.90	70	5.50			70	6.40
195	16.30						

Effect of HCl Concentration

11,400 rpm.
500 ml. HCl
3.66 sq. cm.
25°C.
Air

Run 81 - 0.250M HCl		Run 82 - 0.146M HCl		Run 83 - 2.875M HCl		Run 84 - 2.875M HCl	
Time (min.)	$[Sn^{++++}]$ mol/l.	Time (min.)	$[Sn^{++++}]$ mol/l.	Time (min.)	$[Sn^{++++}]$ mol/l.	Time (min.)	$[Sn^{++++}]$ mol/l.
10	0.60×10^{-4}	10	0.60×10^{-4}	10	0.67×10^{-4}	10	0.45×10^{-4}
20	1.10	20	1.00	15	0.95	15	0.90
30	2.00	30	2.20	20	1.02	20	1.05
40	2.70	40	3.20	25	1.22	25	1.50
50	3.50	50	4.00	30	1.50	30	2.25
60	4.30	60	4.90	40	1.64	40	2.70
65	4.70	70	6.00	45	1.73	45	3.00
		80	7.10	50	1.73	50	3.00
		90	8.30	60	2.09	60	4.35
		100	8.90	70	2.26	70	5.10
		110	10.30	80	2.48	80	6.15
		120	11.40	90		90	6.75

Effect of HCl Concentration

11,400 rpm.
500 ml. HCl
3.66 sq. cm.
25°C.
Air

Run 85 - 4.03M HCl

Time (min.)	$[Sn^{++++}]$ mol./l.
10	0.40×10^{-4}
20	1.00
30	1.40
40	2.40
50	3.40
60	4.00
70	5.00
80	6.00
90	7.00
100	7.80
110	9.20
120	10.00

Run 86 - 1M HCl

Time (min.)	$[Sn^{++++}]$ mol./l.
10	0.80×10^{-4}
20	1.40
30	2.10
40	2.90
50	4.10
60	4.70
70	5.60
80	6.60
90	8.00
100	9.00
110	10.10
120	11.00

Run 87 - 1M HCl

Time (min.)	$[Sn^{++++}]$ mol./l.
10	0.45×10^{-4}
15	0.70
20	1.00
25	1.30
30	1.60
35	2.00
40	2.40
45	2.70
50	3.10
55	3.50
60	3.90
65	4.30
70	4.55

Run 88 - 1.014M HCl

Time (min.)	$[Sn^{++++}]$ mol./l.
15	0.90×10^{-4}
30	1.85
45	2.70
60	4.20
75	5.40
90	6.55
105	7.95

Effect of HCl Concentration

11,400 rpm.
500 ml. HCl
3.66 sq. cm.
25°C.
Air

Run 89 - 0.802M HCl

Time (min.)	$\left[Sn^{++++}\right]$ mol/1.
15	1.00×10^{-4}
30	2.10
45	3.20
60	4.25
75	5.55
90	7.20
105	8.85

Run 90 - 0.546M HCl

Time (min.)	$\left[Sn^{++++}\right]$ mol/1.
15	1.15×10^{-4}
30	2.45
45	3.65
60	5.20
75	6.65
90	8.05
105	10.20

Run 91 - 0.401M HCl

Time (min.)	$\left[Sn^{++++}\right]$ mol/1.
15	1.00×10^{-4}
30	2.35
45	3.05
60	4.95
75	6.40
90	7.85
105	9.30
120	10.90

Run 92 - 0.323M HCl

Time (min.)	$\left[Sn^{++++}\right]$ mol/1.
15	1.00×10^{-4}
30	2.20
45	3.40
60	4.20
75	6.00
90	7.60
105	8.70
120	10.20

Run 93 - 0.101M HCl

15	1.10×10^{-4}
30	2.40
45	3.50
60	4.80
75	6.00
90	6.80
105	8.50

Effect of Initial Stannic Concentration

11,400 rpm.
500 ml. 1M air-saturated HCl
3.66 sq.cm.

Run 94 - 25°C.

Time (min.)	$[Sn^{++++}]$ mol/l.
0	0.75×10^{-4}
15	1.40
30	2.10
45	3.40
60	4.60
75	6.00
90	8.00
105	9.70
120	11.70
135	13.20
150	15.10

Run 95 - 25°C.

Time (min.)	$[Sn^{++++}]$ mol/l.
0	4.10×10^{-4}
15	5.00
30	6.30
45	7.30
60	8.60
75	10.10
90	11.60
105	13.10
120	14.40
135	15.90
150	17.74

Run 96 - 25°C.

Time (min)	$[Sn^{++++}]$ mol/l.
0	8.10×10^{-4}
15	9.60
30	10.80
45	12.70
60	14.40
75	16.30
90	17.7

Run 97 - 25°C.

Time (min)	$[Sn^{++++}]$ mol/l.
0	10.10×10^{-4}
15	11.80
30	13.50
45	15.60
60	17.50
75	19.70

Run 98 - 25°C.

0	5.70×10^{-4}
10	5.85
20	6.20
35	6.75
50	7.65
65	8.20
80	8.70
100	9.20
120	10.00

Run 99 - 31°C.

0	6.35×10^{-4}
10	6.50
20	6.90
30	7.30
40	7.70
50	8.00
60	8.20
80	9.30
100	9.90
120	11.10

Run 100 - 26°C.

0	1.05×10^{-4}
10	1.40
20	1.75
30	2.05
50	2.75
70	3.40
90	4.10
110	4.90

Run 101 - 26°C.

0	3.55×10^{-4}
15	4.00
30	4.50
45	5.10
60	5.55
75	6.00
90	6.70
105	7.10

Variation of Oxygen Concentration

11,000 rpm.
500 ml. 1M HCl
3.66 sq. cm.
30°C.

Run 102 - P_{O_2} = 1.0 atm.		Run 103 - P_{O_2} = 0.5 atm.		Run 104 - P_{O_2} = 0.21 atm.		Run 105 - P_{O_2} = 0 atm.	
Time (min.)	$[Sn^{++++}]$ mol/1.	Time (min.)	$[Sn^{++++}]$ mol/1.	Time (min.)	$[Sn^{++++}]$ mol/1.	Time (min.)	$[Sn^{++++}]$ mol/1.
0		0		0		0	
15	3.20×10^{-4}	15	1.10×10^{-4}	15	0.90×10^{-4}	15	0.35×10^{-4}
30	6.30	30	2.35	30	1.85	30	0.75
45	10.30	45	3.70	45	2.70	45	1.30
60	14.20	60	5.45	60	4.20	60	1.85
75	18.80	75	7.25	75	5.40	75	1.90
90	23.60	90	8.70	90	6.55	90	2.05
		105	12.00	105	7.95	105	2.15
						120	2.55
						135	3.00

Variation of A/V Ratio

11,000 rpm.
1M HCl
30°C.
Air

Run 106 - $\frac{3.66\ \text{cm}^2}{500\ \text{ml.}}$

Time (min.)	$[\text{Sn}^{++++}]$ mol/1.
15	0.90×10^{-4}
30	1.85
45	2.70
60	4.20
75	5.40
90	6.55
105	7.95

Run 107 - $\frac{3.66\ \text{cm}^2}{400\ \text{ml.}}$

Time (min.)	$[\text{Sn}^{++++}]$ mol/1.
15	1.10×10^{-4}
30	2.05
45	3.30
60	4.65
75	6.00
90	7.40
105	9.15

Run 108 - $\frac{1.83\ \text{cm}^2}{400\ \text{ml.}}$

Time (min.)	$[\text{Sn}^{++++}]$ mol/1.
15	0.50×10^{-4}
30	1.10
45	1.70
60	2.35
75	3.05
90	3.85
105	4.50

Run 109 - $\frac{7.32\ \text{cm}^2}{600\ \text{ml.}}$

Time (min.)	$[\text{Sn}^{++++}]$ mol/1.
15	1.70×10^{-4}
30	3.70
45	5.35
60	7.65
75	9.60
90	12.10
105	14.90

Run 110 - $\frac{5.49\ \text{cm}^2}{550\ \text{ml.}}$

15	1.40×10^{-4}
30	2.85
45	4.35
60	6.05
75	7.55
90	9.40
105	10.90

Run 111 - $\frac{0.91\ \text{cm}^2}{500\ \text{ml.}}$

15	0.10×10^{-4}
30	0.35
45	0.55
60	0.80
75	1.10
90	1.35
105	1.65
120	2.05
135	2.30

Run 112 - $\frac{0.91\ \text{cm}^2}{550\ \text{ml.}}$

15	0.25×10^{-4}
30	0.50
45	0.80
60	1.15
75	1.45
90	1.75
105	2.05
120	2.40

Run 113 - $\frac{1.83\ \text{cm}^2}{500\ \text{ml.}}$

15	0.50×10^{-4}
30	1.10
45	1.60
60	2.30
75	3.00
90	3.55
105	4.35
120	5.05

Variation of A/V Ratio

11,000 rpm.
1M HCl
30°C.
Air

Run 114 - $\frac{5.49\ cm.^2}{500\ ml.}$		Run 115 - $\frac{7.32\ cm.^2}{500\ ml.}$	
Time (min.)	$[Sn^{++++}]$ mol/1.	Time (min.)	$[Sn^{++++}]$ mol/1.
15	1.45×10^{-4}	15	2.50×10^{-4}
30	2.95	30	5.30
45	4.55	45	8.05
60	6.30	60	10.50
75	8.10	75	13.20
90	10.00	90	15.50
105	11.50	105	19.20

Effect of Ammonium Chloride

11,000 rpm.
500 ml 0.1M HCl
3.66 sq.cm.
30°C.
Air

Run 116 - 0.1M NH_4Cl		Run 117 - 0.4M NH_4Cl		Run 118 - 0.8M NH_4Cl		Run 119 - 1.0M NH_4Cl	
Time (min.)	$[Sn^{++++}]$ mol/1.	Time (min.)	$[Sn^{++++}]$ mol/1.	Time (min.)	$[Sn^{++++}]$ mol/1.	Time (min.)	$[Sn^{++++}]$ mol/1.
15	1.00 X 10^{-4}	15	0.90 X 10^{-4}	15	0.90 X 10^{-4}	15	0.80 X 10^{-4}
30	2.60	30	2.00	30	1.41	30	1.81
45	3.50	45	3.10	45	1.82	45	2.70
60	4.60	60	4.40	60	2.05	60	4.00
75	6.60	75	5.60	75	2.30	75	5.20
90	7.10	90	6.80	90	2.59	90	6.10
105	8.50	105	7.90	105	2.79	105	7.30
120	9.80	120	9.10	120	3.00	120	9.10

Dissolution by Hydrogen Evolution

5,000 rpm.
500 ml. 1M HCl
3.66 sq. cm.
26°C.
N_2

Run 120

Time (min.)	$[Sn^{++++}]$ mol/l.
20	0.075×10^{-4}
60	0.15
80	0.40
100	0.55
120	0.75
140	0.80
160	1.00
180	1.25
200	1.60
220	2.00

Dissolution by Hydrogen Evolution

11,400 rpm.
500 ml.
25°C.

Run 121 - 0.495M HCl, 3.66 sq. cm.

Time (min.)	$[Sn^{++++}]$ mol/l.
10	0.09×10^{-4}
20	0.15
30	0.22
40	0.24
50	0.36
60	0.46
70	0.50
80	0.52
90	0.62
100	0.73
110	0.80
120	0.90

Run 122 - 1.01M HCl, 3.66 sq. cm.

Time (min.)	$[Sn^{++++}]$ mol/l.
10	0.10×10^{-4}
20	0.20
30	0.24
40	0.30
50	0.35
60	0.42
70	0.55
80	0.62
90	0.68
100	0.79
110	0.86
120	0.93

Run 123 - 2.12M HCl, 3.66 sq. cm.

Time (min.)	$[Sn^{++++}]$ mol/l.
10	0.15×10^{-4}
20	0.20
30	0.30
40	0.35
50	0.40
60	0.60
70	0.60
80	0.70
90	0.70
100	0.80
110	0.90
120	0.95

Run 124 - 2.80M HCl, 3.66 sq. cm.

Time (min.)	$[Sn^{++++}]$ mol/l.
10	0.15×10^{-4}
20	0.20
30	0.25
40	0.31
50	0.40
60	0.46
70	0.54
80	0.67
90	0.75
100	0.80
110	0.86
120	0.94

Run 125 - 1M HCl, 7.32 sq. cm.

Time (min.)	$[Sn^{++++}]$ mol/l.
10	0.15×10^{-4}
20	0.20
30	0.32
40	0.45
50	0.56
60	0.62
70	0.75
80	0.85
90	0.99
100	1.02

Run 126 - 1M HCl, 1.83 sq. cm.

Time (min.)	$[Sn^{++++}]$ mol/l.
10	0.10×10^{-4}
20	0.15
30	0.20
40	0.25
50	0.30
60	0.34
70	0.46
80	0.46
90	0.55
100	0.62

Run 127 - 1M HCl, 3.66 sq. cm.

Time (min.)	$[Sn^{++++}]$ mol/l.
15	0.05×10^{-4}
30	0.15
45	0.35
60	0.42
75	0.60
90	0.75
105	0.90
120	1.05
135	1.20
150	1.45
165	1.65
180	1.85

Dissolution by Hydrogen Evolution

11,400 rpm.
500 ml. 1M HCl
3.66 sq. cm.

Run 128 - 30°C.		Run 129 - 40°C.		Run 130 - 20°C.	
Time (min.)	$[Sn^{++++}]$ mol/l.	Time (min.)	$[Sn^{++++}]$ mol/l.	Time (min.)	$[Sn^{++++}]$ mol/l.
10	0.15×10^{-4}	10	0.15×10^{-4}	10	0.10×10^{-4}
20		20	0.20	20	0.15
30	0.31	30	0.35	30	0.20
40	0.45	40	0.50	40	0.20
50	0.60	50	0.60	50	0.30
60	0.70	60		60	0.40
70	0.75	70	0.85	70	0.45
80	0.95	80	1.00	80	0.50
90	1.00	90	1.10	90	0.55
100	1.10	100	1.20	100	0.70
110	1.10	110	1.25	110	0.75
120	1.25	120	1.35	120	0.85

APPENDIX VI

HOMOGENEOUS OXIDATION

Effect of Temperature
Solution: 0.9934M HCl

Run 1 26°C.		Run 2 35.5°C.		Run 3 36°C.		Run 4 27°C.	
Time (min.)	$[SnCl_2]$ mol/l.	Time (min.)	$[SnCl_2]$ mol/l.	Time (min.)	$[SnCl_2]$ mol/l.	Time (min.)	$[SnCl_2]$ mol/l.
0	4.81×10^{-3}	0	5.62×10^{-3}	0	6.52×10^{-3}	0	7.94×10^{-3}
5	4.13	5	5.44	10	4.96	10	7.25
10	3.81	10	4.87	20	3.90	20	6.18
15	3.63	15	4.44	30	2.49	30	5.05
20	2.88	20	3.75	40	1.90	40	3.94
25	2.88	25	3.19	50	0.79	50	3.00
30	2.50	30	2.38	60	0.29	60	2.32
40	2.00	40	1.93	70	0.23	70	1.82
50	1.31	50	0.75	80	0.10	80	1.20
60	0.69	60	0.375			90	0.825
						100	0.575

Effect of Temperature
Solution: 0.9934N HCl

Run 5 0°C.		Run 6 2.75°C.		Run 7 34.5°C.		Run 8 35°C.	
Time (min.)	$[SnCl_2]$ mol/l.	Time (min.)	$[SnCl_2]$ mol/l.	Time (min.)	$[SnCl_2]$ mol/l.	Time (min.)	$[SnCl_2]$ mol/l.
0	6.37×10^{-3}	0		0		0	
10	5.62	5	5.63×10^{-3}	5	5.88×10^{-3}	5	5.8×10^{-3}
20	5.37	10	4.94	10	5.2	10	5.05
30	5.00	15	4.25	15	4.87	15	4.37
40	4.87	25	3.38	20	3.94	20	3.19
50	4.62	35	2.63	30	2.88	30	2.62
60	4.37	45	2.12	40	1.69	40	1.81
70	4.25	55	1.50	50	1.00	50	1.06
80	4.25	65	0.94	60	0.625	60	0.56
90	3.94	75	0.69	70	0.313	70	0.38
		85	0.375	80	0.313	80	0.38

Effect of Temperature
Solution: 0.9934N HCl

Run 9 40°C.		Run 10 20°C.		Run 11 15°C.		Run 12 25°C.	
Time (min.)	$[SnCl_2]$ mol/l.	Time (min.)	$[SnCl_2]$ mol/l.	Time (min.)	$[SnCl_2]$ mol/l.	Time (min.)	$[SnCl_2]$ mol/l.
0		0		0		0	
5	8.2×10^{-3}	5	8.12×10^{-3}	10	7.87×10^{-3}	5	15.4×10^{-3}
10	7.3	10	8.00	20	7.32	10	14.4
15	7.0	15	7.87	30	6.70	15	13.9
20	5.8	20	7.75	40	6.05	20	13.2
30	3.81	25	7.30	50	5.55	25	11.9
40	2.62	30	6.80	60	4.87	35	10.4
50	1.31	35	6.45	70	4.50	45	9.1
60	0.75	40		80	3.94	55	7.1
70	0.19	50	5.5	90	3.38	65	6.2
80	0.19	60	4.7	100	3.00	75	5.12
		70	4.0	110	2.63	85	4.12
		80	3.38	120	2.32	95	3.38
		90	2.81	130	2.32		
		100	2.37				

Effect of Temperature
Solution: 0.9934N HCl

Run 13 25°C.		Run 14 30°C.		Run 15 20°C.		Run 16 35°C.	
Time (min.)	$[SnCl_2]$ mol/l.	Time (min.)	$[SnCl_2]$ mol/l.	Time (min.)	$[SnCl_2]$ mol/l.	Time (min.)	$[SnCl_2]$ mol/l.
5	3.06×10^{-3}	5	3.56×10^{-3}	5	4.31×10^{-3}	5	3.50×10^{-3}
10	2.81	10	3.44	10	3.94	10	2.81
15	2.28	15	3.00	15	3.75	15	2.31
20	2.10	20	2.63	20	3.38	20	1.88
25	1.63	25	2.19	25	3.13	25	1.31
30	1.50	30	1.88	30	2.81	30	1.00
35	0.94	35	1.44	35	2.63	35	0.78
40	1.06	40	1.19	40	2.38	40	0.69
45	1.06	45	1.06	45	2.19	45	0.56
50	0.81	50	0.88	50	2.06	50	0.44
55	0.56	55	0.75	55	1.88	55	0.38
60	0.50	60	0.63	60	1.75	60	0.19
65	0.44	65	0.44	65	1.50	65	0.28
70	0.31	70	0.31	70	1.38	70	0.19
75	0.29	75	0.13	75	1.25	75	0.13
80	0.19	80	0.29	80	1.13	80	0.19
85		85	0.29	85	1.06		
90		90	0.13	90	1.00		
				95	0.81		
				100	0.81		
				105	0.75		
				110	0.69		
				115	0.63		

Effect of Temperature
Solution: 0.9934N HCl

Run 17 40°C.		Run 18 25°C.		Run 19 10°C.	
Time (min.)	$[SnCl_2]$ mol/1.	Time (min.)	$[SnCl_2]$ mol/1.	Time (min.)	$[SnCl_2]$ mol/1.
5	4.10×10^{-3}	5	3.13×10^{-3}	5	4.13×10^{-3}
10	3.92	10	2.94	10	3.94
15	3.35	15	2.50	15	3.69
20	2.29	20	2.13	20	3.56
25		25	1.94	25	3.38
30	1.41	30	1.56	30	3.31
35	1.06	35	1.25	35	3.06
40	0.79	40	1.13	40	3.00
45	0.60	45	1.06	45	2.94
50	0.50	50	0.94	50	2.69
55	0.41	55	0.75	55	2.50
60	0.41	60	0.63	60	2.31
65	0.10	65	0.56	65	2.31
70	0.29	70	0.31	70	2.00
75	0.35	75	0.31	75	2.06
80	0.41	80	0.31	80	1.75
85	0.35	85	0.19	85	
90	0.29	90	0.19	90	1.75
				95	1.69
				100	

Effect of Oxygen Concentration
Solution: 1.004M HCl
Temperature: 25°C.

Run 20 50% Oxygen 50% Nitrogen		Run 21 75% Oxygen 25% Nitrogen		Run 22 33.3% Oxygen 66.6% Nitrogen		Run 23 66.6% Oxygen 33.3% Nitrogen	
Time (min.)	$[SnCl_2]$ mol/1.	Time (min.)	$[SnCl_2]$ mol/1.	Time (min.)	$[SnCl_2]$ mol/1.	Time (min.)	$[SnCl_2]$ mol/1.
0		0		0		0	
10	4.85×10^{-3}	5	7.5×10^{-3}	5	10.7×10^{-3}	5	6.75×10^{-3}
20	2.25	9	5.3	10	9.45	10	4.25
25	1.44	15	2.75	15	8.70	15	1.75
30	0.81	25	1.44	20	6.95	20	0.875
35	0.50	25	0.75	25	6.45	25	0.25
40	0.31	30	0.56	30	5.70	30	0
45	0.31	35	0.50	35	4.68	35	0
		40	0.50	40	4.00	40	
		45		45	3.25		
				50	2.81		
				60	1.75		
				70	1.25		
				80	0.75		

Effect of Oxygen Concentration
Solution: 1.004M HCl
Temperature: 25°C.

Run 24
75% Oxygen
25% Nitrogen

Time (min.)	$[SnCl_2]$ mol/1.
0	
5	5.62 X 10^{-3}
10	3.62
15	2.25
20	1.00
25	0.50
30	
35	

Run 25
66.6% Oxygen
33.3% Nitrogen

Time (min.)	$[SnCl_2]$ mol/1.
0	
5	
10	7.75 X 10^{-3}
15	5.30
20	3.88
25	2.25
30	1.37
35	0.75
40	0.44
45	0.44

Run 26
50% Oxygen
50% Nitrogen

Time (min.)	$[SnCl_2]$ mol/1.
0	
5	8.0 X 10^{-3}
10	7.2
15	5.7
20	4.06
25	3.12
30	1.94
35	1.44
40	

Run 27
14.5% Oxygen
85.5% Nitrogen

Time (min.)	$[SnCl_2]$ mol/1.
0	
5	
10	11.7 X 10^{-3}
20	11.2
30	10.8
40	10.1
50	9.5
60	9.05
70	8.50
80	8.05
90	7.35
100	6.88
110	6.12

Effect of Oxygen Concentration
Solution: 1.004M HCl
Temperature: 25°C.

Run 28		Run 29		Run 30		Run 31	
40% Oxygen 60% Nitrogen		50% Oxygen 50% Nitrogen		60% Oxygen 40% Nitrogen		12.9% Oxygen 87.1% Nitrogen	
Time (min.)	$[SnCl_2]$ mol/1.	Time (min.)	$[SnCl_2]$ mol/1.	Time (min.)	$[SnCl_2]$ mol/1.	Time (min.)	$[SnCl_2]$ mol/1.
10	7.75×10^{-3}	10	7.7×10^{-3}	5	10.8×10^{-3}	10	11.6×10^{-3}
20	5.7	15	6.2	10	8.8	15	11.5
30	3.5	20	4.7	15	6.37	20	11.2
35	2.81	25	3.4	20	4.25	25	11.0
40	2.38	30	2.25	25	2.62	30	10.5
45	1.94	35	1.63	30	1.50	35	10.2
50	1.56	40	1.06	35	0.88	40	9.95
55	1.00	45	0.69	40	0.50	45	9.75
						50	9.30
						55	
						60	8.62
						70	8.12
						80	7.5
						90	6.8
						100	6.4
						110	5.8

Effect of Initial $SnCl_4$ Concentration
Solution: 1N HCl
Temperature: 25°C.

Run 32

Time (min.)	$[SnCl_2]$ mol/1.
5	9.45×10^{-3}
10	8.8
15	8.25
20	7.47
25	6.75
30	6.45
35	5.90
40	5.25
45	4.68
50	4.37
55	4.12
60	3.56
65	3.19
70	2.62
75	2.31
80	2.19
85	1.75
90	1.56

Surface Area Effect
Solution: 0.9838N HCl
Temperature: 25°C.

Run 33

Time (min.)	$[SnCl_2]$ mol/l.
10	5.87×10^{-3}
15	5.45
20	5.00
25	4.56
30	4.19
35	3.75
40	3.38
45	3.00
50	2.50
55	2.25
60	1.75
65	1.50
70	1.19
75	1.19

Surface area is increased by immersing tefflon strips inside reaction vessel (contact area increased 3-4 times.)

Effect of Hydrochloric Acid Concentration
Temperature: 25°C.
Aeration: Air

Run 34 0.4973N HCl		Run 35 0.7357N HCl		Run 36 0.2498N HCl		Run 37 0.1009N HCl	
Time (min.)	$[SnCl_2]$ mol/l.	Time (min.)	$[SnCl_2]$ mol/l.	Time (min.)	$[SnCl_2]$ mol/l.	Time (min.)	$[SnCl_2]$ mol/l.
10	7.85×10^{-3}	15	6.7×10^{-3}	10	7.55×10^{-3}	10	7.7×10^{-3}
20	7.70	28	5.87	20	7.30	20	7.7
30	7.30	45	4.87	30	7.25	30	7.55
40	6.80	55	4.37	40	7.20	40	7.07
50	6.50	65	3.69	50	7.00	50	6.20
60	6.05	75	3.19	60	6.70	60	5.50
70	5.44	85	2.62	70	6.36	70	4.62
80	5.50	95	2.31	80	6.12	80	4.00
90	4.87	105	1.81	90	6.00	90	3.69
100	4.87	115	1.63	100	5.70	100	3.19
110	4.25	125	1.56	110	5.55	110	2.62
120	3.88	135		120	4.94	120	2.25
130	3.56			130	5.10	130	2.12
				140	4.80		
				150	4.62		

Effect of Hydrochloric Acid Concentration
Temperature: 25°C.
Aeration: Air

Run 38 1.4685N HCl		Run 39 1.6675N HCl		Run 40 2.1926N HCl	
Time (min.)	$[SnCl_2]$ mol/l.	Time (min.)	$[SnCl_2]$ mol/l.	Time (min.)	$[SnCl_2]$ mol/l.
10	7.70×10^{-3}	10		10	
15	6.80	15		20	
20	6.05	20		25	
25	5.45	25		30	
30	4.44	30		35	
35	3.56	35	7.55×10^{-3}	40	
40	3.00	40	6.70	45	7.63×10^{-3}
50	2.00	45	5.30	50	6.56
60	1.25	50	4.56	55	5.20
65	0.98	55	3.56	60	3.87
		60	3.00	65	2.88
		65	2.25	70	2.16
		70	1.70	75	1.25
		80	0.69	80	0.63
		85	0.69		

Effect of Hydrogen Ion
Temperature: 25°C.
Aeration: Air

Run 41
0.5M H_2SO_4
1M NH_4Cl

Time (min.)	$[SnCl_2]$ mol/1.
5	7.82 X 10^{-3}
10	7.68
15	7.30
20	6.75
25	6.06
30	5.94
35	5.56
40	5.12
45	4.81
50	4.56
55	4.18
60	3.87
65	3.69
70	3.31
75	3.12
80	2.94
85	2.31
90	2.31

Run 42
0.75N H_2SO_4
1M NH_4Cl

Time (min.)	$[SnCl_2]$ mol/1.
5	10.25 X 10^{-3}
10	9.32
15	8.43
20	7.75
25	7.56
30	7.32
35	7.06
40	6.43
45	6.31
55	5.44
60	5.37
65	4.87
70	4.57
75	4.21
80	3.69
85	3.69

Run 43
1.0N H_2SO_4
1.0M NH_4Cl

Time (min.)	$[SnCl_2]$ mol/1.
10	7.94 X 10^{-3}
15	7.18
20	6.62
25	6.06
30	5.50
35	5.43
40	5.06
45	4.63
50	4.42
55	3.94
60	3.56
65	3.19

Run 44
1.5N H_2SO_4
1M NH_4Cl

Time (min.)	$[SnCl_2]$ mol/1.
5	10.37 X 10^{-3}
10	9.70
15	8.88
20	8.49
25	7.44
30	7.37
35	6.75
40	6.44
45	6.06
50	5.56
55	5.00
60	4.81
65	4.37
70	3.81
75	3.69
80	3.37
90	2.94

Effect of Hydrogen Ion
Temperature: 25°C.
Aeration: Air

Run 45
2N H_2SO_4
1M NH_4Cl

Time (min.)	$[SnCl_2]$ mol/1.
10	11.1×10^{-3}
15	10.6
20	10.3
25	9.37
30	8.75
35	8.12
40	7.62
45	7.06
50	6.50
55	6.00
60	5.62
65	5.20
70	4.38

Effect of Chloride Ion
Temperature: 25°C.
Aeration: Air

Run 46 1N HCl 0.5M KCl		Run 47 1N HCl 1M KCl		Run 48 1N HCl 1.5M KCl		Run 49 1N HCl 2.0M KCl	
Time (min.)	$[SnCl_2]$ mol/1.	Time (min.)	$[SnCl_2]$ mol/1.	Time (min.)	$[SnCl_2]$ mol/1.	Time (min.)	$[SnCl_2]$ mol/1.
5	11.75 X 10^{-3}	5	10.0 X 10^{-3}	5	10.1 X 10^{-3}	5	10.38 X 10^{-3}
10	10.8	10	8.8	10	8.75	10	10.36
15	10.2	15	8.0	15	7.75	15	8.13
20	8.7	20	6.94	20	6.69	20	7.32
25	8.05	25	6.8	25	5.62	25	6.13
30	7.0	30	5.5	30	5.06	30	5.33
35	6.37	35	4.25	35	4.31	35	5.15
40	4.81	40	4.13	40	3.88	40	4.25
45	4.37	45	3.12	45	2.75	45	3.44
50	3.69	50	2.69	50	2.31	50	2.81
55	3.09	55	1.50	55	1.87	55	2.38
60	3.06	60	0.81	60	1.56	60	1.81
65	2.50	65		65	1.25	65	1.38
70	2.31	70		70	0.88	70	1.19

Effect of Chloride Ion
Temperature: 25°C.
Aeration: Air

Run 50 0.75M KCl 1N HCl		Run 51 1.00N HCl 0.25M KCl		Run 52 1N HCl 1.0M NH_4Cl		Run 53 1N HCl 2.0M NH_4Cl	
Time (min.)	$[SnCl_2]$ mol/l.	Time (min.)	$[SnCl_2]$ mol/l.	Time (min.)	$[SnCl_2]$ mol/l.	Time (min.)	$[SnCl_2]$ mol/l.
5	9.82×10^{-3}	5		5	7.1×10^{-3}	5	7.95×10^{-3}
10	8.75	10		10	6.41	10	6.50
15	7.88	15	7.44×10^{-3}	15	5.50	15	5.12
20	6.88	20	6.94	20	4.44	20	4.30
25	6.32	25	6.06	25	3.75	25	2.94
30	5.44	30	5.37	30	3.06	30	2.38
35	4.88	35	4.75	35	2.44	35	1.37
40	4.06	40	4.25	40	2.00	40	0.94
45	3.50	45	3.62	45	1.19	45	0.56
50	2.69	50	3.18	50	1.06	50	0.56
55	2.44	55	3.00	55	0.69	55	0.44
60	2.06	60	2.50	60	0.38	60	0.44
65	1.31	65	2.12	65	0.38		
70	1.00	70	1.81				

Ef Chloride Ion
ure: $25^{\circ}C$.
: Air

Run 54
1N HCl
1.5M NH_4Cl

Time (min.)	[Sn mol/
5	8.8 X
10	7.37
15	5.75
20	5.15
25	3.62
30	2.81
35	2.19
40	1.44
45	1.00
50	0.50

Run 55
1N HCl
0.5M NH_4Cl

Time (min.)	[S mo
5	9.2
10	8.5
15	7.7
20	6.62
25	5.72
30	5.05
35	4.50
40	3.75
45	3.25
50	2.62
55	2.38
60	1.81
65	1.31
70	1.19

Run 56
1N HCl
0.25M NH_4Cl

Time (min.)	$[SnCl_2]$ mol/1.
5	8.25×10^{-3}
10	7.20
15	6.75
20	6.00
25	5.25
30	5.25
35	4.00
40	3.25
45	3.00
50	2.44
55	2.13
60	1.56
65	1.38

Run 57
1N HCl
2.5M NH_4Cl

Time (min.)	$[SnCl_2]$ mol/1.
5	9.0×10^{-3}
10	7.55
15	6.05
20	4.70
25	3.69
30	2.62
35	1.63
40	1.19
45	0.88
50	0.88

Effect of Chloride Ion
Temperature: 25°C.
Aeration: Air

Run 58
1N HCl
1.25M NH_4Cl

Time (min.)	$[SnCl_2]$ mol/1.
5	8.75×10^{-3}
10	7.45
15	6.20
20	5.30
25	4.20
30	3.25
35	2.75
40	2.19
45	1.37
50	1.06
55	0.88
60	0.75

BIBLIOGRAPHY

1. Abramova, T.M., I.I. Gankina, and A.S. Fomenko. Doklady Akad, Nauk S.S.S.R. 129, 820 (1959).
2. Ammar, I.A., and S. Riad. J. Electrochem. Soc., 106, 926 (1959).
3. Baskerville, C., and R. Stevenson. J. Am. Chem. Soc., 33, 1104 (1911).
4. Bailey, K.C. Sci. Proc. R. Soc. Dub. 21, 153 (1935).
5. Berzelius, J.J. Ann. Chim. Phys. 87, 50 (1813).
6. Berzelius, J.J. Ann. Chim. Phys. 5, 149 (1817).
7. Bekier, E., and A. Basinski. J. Chim. Phys. 27, 256 (1930).
8. Berg, T.G. Corrosion 16, 198t (1960).
9. Britton, S.C., and D.G. Michael. J. Appl. Chem. 7, 349 (1957).
10. Bircumshaw, L.L., and A.C. Riddiford. Quarterly Reviews 6, 157 (1952).
11. Bumbulis, J., and W.F. Graydon. J. Electrochem. Soc., 109, 1130 (1962).
12. Churchill, J.R. Trans. Electrochem. Soc., 76, 341 (1939).
13. Cher, M., and N. Davidson. J. Am. Chem. Soc., 77, 793 (1955).
14. Campbell, W.E., and U.B. Thomas. Trans. Electrochem. Soc., 76, 303 (1939).
15. Clark, R.E. Analyst, 61, 242 (1936).
16. Clark, R.E. Analyst, 62, 661 (1937).
17. Dawden, D.A., and P.W. Reynolds. Disc Faraday Soc., 8, 184 (1950).
18. Dhar, N.R. J. Asiatic Soc. Bengal, 17, 130 (1921).
19. Ditte, A. Ann. Chim. Phys. 19, 68 (1891).
20. Evans, M.G., J.T. Baxendale, and G.S. Park. Trans. Faraday Soc., 42, 155 (1946).
21. Filson, G.W., and J.H. Walton J. Phys. Chem., 36, 740 (1932).
22. Giguere, P.A., and J.B. Jaillet Can. J. of Res. B26, 767 (1948).

23. George, P. J. Chem. Soc. (London), 4349 (1954).

24. Garett, A.B., and R.R. Cooper. J. Phys. Coll. Chem. 54, 437 (1950).

25. Gnyp, A.W. Ph.D. Thesis, Toronto, 1958.

26. Hill, G.R. J. Electrochem. Soc., 100, 345 (1953).

27. Haber, F., and J. Weiss. Proc. Roy. Soc., A147, 332 (1934).

28. Haring, R.C., and J.H. Walton. J. Phys. Chem., 37, 133 (1933).

29. Haring, R.C., and J.H. Walton. J. Phys. Chem., 37, 375 (1933).

30. Haring, R.C., and J.H. Walton. J. Phys. Chem., 38, 153 (1934).

31. Hagymas, G., and M. Quintin. Compt. Rend., 7, 256 (1963).

32. Hagymas, G., and M. Quintin. J. Chim. Phys. et Phy Chim. Biol., 61, 541 (1964).

33. Hole, A.J., and H.S. Foster. J. Soc. Chem. Ind., 34, 464 (1915).

34. Henry, T. Trans. Roy. Soc. (London), 135, 367 (1845).

35. Ireland, J. Metallurgia, 31, 75 (1944).

36. Johnson, R.S., and H.J. McDonald. J. Am. Chem. Soc., 72, 666 (1950).

37. Khitrov, V.A., and V.I. Shatalova. Tsvetn. Metal, 35, 95 (1962).

38. Khitrov, V.A., I.S. Smolyaninov, V.I. Shatalova, and Y.I. Sadavskaya. Zh. Fiz. Khim., 36, 1058 (1962).

39. Kramer, J. Z. Physik, 125, 739 (1949).

40. Kramer, J. Z. Physik, 128, 538 (1950).

41. Kramer, J. Z. Physik, 129, 34 (1951).

42. King, C.V., and M. Schack. J. Am. Chem. Soc., 57, 1212 (1935).

43. King, C.V., and M.M. Bravernan. J. Am. Chem. Soc., 54, 1744 (1932).

44. Kerr, R. J. Soc. Chem. Ind. 65, 101 (1946).

45. Kerr, R. J. Soc. Chem. Ind. 66, 5 (1947).

46. Kolthoff, I.M., and C.S. Miller. J. Am. Chem. Soc. 63, 1013 (1941).

47. Louw, J.D., and S.M. Naude. Phys. Rev., 76, 571 (1949).

48. Lu. B.C-Y., and W.F. Graydon. J. Am. Chem. Soc., 77, 6136 (1955).

49. Lu, B.C-Y., and W.F. Graydon. Can. J. Chem. 32, 153 (1954).

50. Larsen, E.C., and J.H. Walton. J. Phys. Chem., 44, 70 (1940).

51. Lamb, A.B., and L.W. Elder. J. Am. Chem. Soc., 53, 147 (1931).

52. Lochman, S.J., and F.C. Tompkin. Trans. Faraday Soc., 40, 130 (1944).

53. Lingane, J.J. J. Am. Chem. Soc., 67, 919 (1945).

54. Lingane, J.J. Chem. Rev., 29, 1-35 (1941).

55. Lingane, J.J. Ind. Eng. Chem. Anal. Ed., 18, 429 (1946).

56. McIntosh, D.M. J. Phys. Chem., 6, 15 (1902).

57. Mackenzie, H.A.E., and F.C. Tompkins. Trans. Faraday Soc., 38, 465 (1942).

58. Milas, N.A. Chem. Rev., 10, 295 (1932).

59. Miyamoto, S. Bull Chem. Soc. Japan, 2, 74 (1927).

60. Miyamoto, S. Bull Chem. Soc. Japan, 2 259 (1927).

61. Miyamoto, S. Bull Chem. Soc. Japan, 4, 48 (1929).

62. Naumann, A. Ber. 37, 336 (1905).

63. Pound, J.R. J. Phys. Chem. 43, 955 (1939).

64. Pound, J.R. J. Phys. Chem. 43, 969 (1939).

65. Posner, A.M. Trans. Faraday Soc., 49, 382 (1953).

66. Phillips, S.L. Anal. Chem. 32, 1062 (1960).

67. Phillips, S.L., and E. Morgan. Anal. Chem. 33, 1192 (1961).

68. Pellequer, H. Compt. Rend., 225, 116 (1947).

69. Reichert, S.A., M.C. Neight, and H.W. [illegible], [illegible], 194 (1939).

70. Richardson, G.M. Am. Chem. J., 14, 91 (1892).

71. Russell, A.S. J. Chem. Soc. (London), 497 (1926).

72. Seidell, A. "Solubilities of Inorganic and Metal Organic Compounds" D. Van Nostrand Co. Inc., N.Y. (1940).

73. Schales, O. Ber., 71B, 447 (1938).

74. Shah, S.N., and D.E. Davies, Electrochim. Acta., 8, 663 (1963).

75. Snell, F.D., and C.T. Snell. "Colorimetric Methods of Analysis", D. Van Nostrand Co. Inc., New York, 3rd ed. (1954).

76. Stafford, N. Mikrochem. Acta., 2, 306 (1937).

77. Stone, J. Ind. Eng. Chem. Anal. Ed. 13, 791 (1941).

78. Thomas, J.G.N. Trans. Faraday Soc., 57, 1603 (1961).

79. Vaubel, W. Ber. 57B, 515 (1924).

80. Whitman, W.G., and R.P. Russell, J. Ind. Eng. Chem. 17, 34B (1925).

81. Willard, H.H., L.L. Merritt, and J.A. Dean, "Instrumental Method of Analysis", D. Van Nostrand Co. Inc., New York (1953).

82. Weeks, J.R., and G.R. Hill, J. Electrochem. Soc., 103, 203 (1956).

83. Wiegel, B. Z. Physik Chem. 143A, 81 (1929).

84. Wade, K., A. Hidejiro, K. Kalsunori, and N. Toshiro. Boshoku Gijutsu, 11, 49 (1962).

85. Weiss, J. Trans. Faraday Soc., 31, 1547 (1935).

86. Weiss, J. Symposium, Sur Transferts Electronique en Solution et Aux Electrodes (Paris, 1951).

87. Young, S.W. J. Am. Chem. Soc., 23, 21 (1901).

88. Bodner, J.J. Unpublished work.

89. Lui, A.W.K. Unpublished work.

VITA AUCTORIS

1936	Born in Hong Kong.
1957	Completed high school education in St. Joseph's College, Hong Kong.
1961	Received the Degree of Bachelor of Science in Chemical Engineering from Queen's University, Kingston, Ontario.
1962	Received the degree of Master of Applied Science in Chemical Engineering from the Assumption University of Windsor, Windsor Ontario.
1964	A candidate for the Degree of Doctor of Philosophy in Chemical Engineering at the University of Windsor.